INFORMATION TO USERS

This manuscript has been reproduced from the microfilm master. UMI films the text directly from the original or copy submitted. Thus, some thesis and dissertation copies are in typewriter face, while others may be from any type of computer printer.

The quality of this reproduction is dependent upon the quality of the copy submitted. Broken or indistinct print, colored or poor quality illustrations and photographs, print bleedthrough, substandard margins, and improper alignment can adversely affect reproduction.

In the unlikely event that the author did not send UMI a complete manuscript and there are missing pages, these will be noted. Also, if unauthorized copyright material had to be removed, a note will indicate the deletion.

Oversize materials (e.g., maps, drawings, charts) are reproduced by sectioning the original, beginning at the upper left-hand corner and continuing from left to right in equal sections with small overlaps.

ProQuest Information and Learning
300 North Zeeb Road, Ann Arbor, MI 48106-1346 USA
800-521-0600

UMI®

ULTRASONIC MONITORING OF DIE-CASTING PROCESS USING CLAD BUFFER ROD SENSOR

Jean-François Moisan

Department of Electrical Engineering
McGill University
Montreal, Quebec, Canada
August 2001

A thesis submitted to the Faculty of Graduate Studies and Research in partial fulfillment of the requirements of the degree of M. Eng.

© Jean-François Moisan
2001

National Library of Canada
Bibliothèque nationale du Canada

Acquisitions and Bibliographic Services
Acquisitions et services bibliographiques

395 Wellington Street
Ottawa ON K1A 0N4
Canada

395, rue Wellington
Ottawa ON K1A 0N4
Canada

Your file Votre référence

Our file Notre référence

The author has granted a non-exclusive licence allowing the National Library of Canada to reproduce, loan, distribute or sell copies of this thesis in microform, paper or electronic formats.

L'auteur a accordé une licence non exclusive permettant à la Bibliothèque nationale du Canada de reproduire, prêter, distribuer ou vendre des copies de cette thèse sous la forme de microfiche/film, de reproduction sur papier ou sur format électronique.

The author retains ownership of the copyright in this thesis. Neither the thesis nor substantial extracts from it may be printed or otherwise reproduced without the author's permission.

L'auteur conserve la propriété du droit d'auteur qui protège cette thèse. Ni la thèse ni des extraits substantiels de celle-ci ne doivent être imprimés ou autrement reproduits sans son autorisation.

0-612-75278-X

Canada

Abstract

In-line monitoring of die-casting of aluminum (A356, A357, 86S), magnesium (AZ91) and a metal matrix composite (Gra-Ni® 6S:3G) will be monitored using the reflection coefficient obtained by using an ultrasonic technique, the pulse/echo. For each of the materials enumerated above, the average temperature of the mold through its thickness, the end of filling of the part, the solidification of the part in the cavity of the mold, the gap and/or the detachment of the part, the sound velocity and the attenuation of the material will be measured by this ultrasonic technique during the process.

For the materials the melt temperature will not exceed 600°C because the casting is made at the semi-solid state, between the solidus and liquidus, of the materials. A novel high performance buffer rod with a cooling system is integrated into the die. Therefore, ultrasonic measurements can be carried out with high signal-to-noise ratio at elevated temperatures.

Résumé

Nous avons étudié, au moyen du coefficient de réflexion obtenu par le mode réflexion, la caractérisation en-ligne du moulage sous pression de l'aluminium (A356, A357, 86S), du magnésium (AZ91) et du matériaux composite à matrice métallique (Gra-Ni® 6S:3G). Pour chacun des matériaux énumérés ci-dessus nous avons mesuré, par cette technique ultrasonore, la température moyenne du moule sur son épaisseur, la fin de l'arrivée du métal fondu, la solidification de la pièce dans la cavité du moule, le développement de l'interstice et/ou du décollement de la pièce, ainsi que la vélocité des ondes ultrasonores et de son atténuation.

Pour ce qui est des matériaux fondus, la température ne dépasse pas les 600°C parce que le moulage se fait à l'état semi-solide, c'est-à-dire entre le point liquidus et solidus des métaux. Nous avons inséré dans le moule une ligne à délai novatrice à haute performance avec un système de refroidissement. Se faisant, nous obtenons les mesures ultrasonores avec un excellent rapport signal-sur-bruit, et ce, malgré les températures élevées.

Acknowledgments

I would like to thank my parents, my sister and my friends for their love, support and encouragement throughout my years of study.

I also want to thank my supervisor , Dr. C.K. Jen. Without his help, guidance and caring, this work would not have been possible. Through his dedicated efforts I have learned a lot, not only about the ultrasound technique, but also about research in general.

Many thanks to Mr. Harold Hébert for his implementation of original data acquisition and signal processing programs and his teaching of the conceptual process in designing the clad buffer rod. Thanks also to Mr. Tzu-Fang Chen who helped me in the manipulation of the equipment during the acquisition of data and in processing some of the results. I would like also to acknowledge the contribution of Mr. Zhigang Sun for his implementation of a Matlab program for the calculation of the attenuation and sound velocity.

The work of Mr. Daniel Simard in polishing and etching the samples for taking micrograph pictures was also greatly appreciated. Without his help, I would still be working on those magnesium samples. Thanks also to Mr. Chang-Qing Zheng and Mr. Normand Nardini for the operation and maintenance of the die-casting machine and to Mr. Alexandre Beaulieu for his encouragement and his work during the casting experiments.

Finally, the financial support from the Natural Science and Engineering Research Council of Canada (NSERC) and the National Research Council of Canada (NRC), and especially its Industrial Materials Institute (IMI) of Boucherville where all the experiments were carried out, is gratefully acknowledged.

Table of Contents

List of Figures

List of Tables

Chapter 1: Introduction

1.1 Background

Increasing industrial demand for high-quality products and production efficiencies have resulted in the need for improved process monitoring and control [1-4]. Light weight metal die-casting and injection molding have been commonly used as mass production methods. So far, most industrial efforts have been oriented mainly towards machine control and new processes; little attention has been paid to use the cast part properties inside the cavity for process control. For example, it is common for metal die casters and injection molders to use temperature, pressure and position sensors to control piston injection without direct reference to the properties of the cast parts. The evaluation of the part is usually performed after it has been ejected from the die or mold.

To improve the process, numerical models are used for computer simulations to reduce the cost of the design of the part and to optimize the process [5,6]. Even a virtual die concept has been mentioned recently. It could simulate the entire product process virtually by computer without going through any real processing [7]. Although these computer simulations are used extensively for analysis and optimization of process parameters, input data are often derived from simplified assumptions in order to facilitate problem solving and reduce computation time. Therefore, *in situ* monitoring with sensors may provide a practical understanding of the process and a crucial validation of the models derived [8-12]. These sensing [13,14] can also help to determine the source of errors and to improve the mathematical models [8,9,15]. For example, the information from the feedback of a cavity sensor may be used to control the system, allow direct supervision of the process and ensure constant quality of the finished part [16,17]. Furthermore, different advanced control strategies such as close loop, statistics and knowledge based expert system may now be integrated into the production [17-21].

Process control is also a desired tool to reduce production cost and improve product quality. Since light weight metal die-casting and injection molding are difficult to maintain in a steady state due to the fast metallic solidification process, complex control strategies are needed [17-21]. In order to improve the quality of the cast or molded part and to verify the assumptions, process parameters such as die or mold and melt temperature, cavity and hydraulic pressure, shear stress and flow front advancement have been monitored and used to control the casting and molding processes [22]. However, the available sensors used are limited to conventional pressure, temperature, heat flux and flow detector measurements and have shortcomings such as slow response, unsteadiness and non-repeatability. In addition, these sensors are used for machine control only and not for process control which requires the information of the part properties inside the cavity. As a result, there is a significant need for the development of cost effective sensors for in-line measurements and for machine and process control [19,21,23].

In this thesis, one of the objective is to use a new high performance clad buffer rod consisting of a steel core and stainless steel cladding to perform in-line ultrasonic monitoring. We hope that this new sensor will be able, in time, to solve some of the problems mentioned above for conventional available sensors and increase the overall knowledge of the process by performing process control.

1.2 Die-casting

The processes of metal die-casting and injection molding are similar. Both of them have feeding materials that are heated, melt and injected into a die or mold which has the desired shape. Thereafter, the part is cooled and solidified inside the cavity of the die or mold until it is ejected out and a new cycle begins.

One can consider the die-casting process as consisting of three stages: (1) the filling stage during which the material is injected into the cavity of the die; (2) the intensification stage where additional material is forced into the cavity under high pressure. The pressure is applied until the gate is frozen to compensate the shrinkage due to the continuous cooling of the process; and (3) the solidification stage during which the part is cooled until the state of solidification is almost completed. Once these three stages are completed, the part is ejected and the production cycle restarts.

At the filling stage, flow front advancement and flow front velocity are important information. The flow front advancement indicates when the cavity of the die is completely filled. The information retrieved on the position of the flow can be used to control the plunger speed for a smooth transition between the filling and the intensification stage. This smooth transition could reduce or avoid the flashing or die damage due to high impact. Since the viscosity of the material depends on the local flow rate, the measurement and control of the flow front velocity may give a consistent material behavior throughout the filling phase. In addition, the flow front velocity which can be related to cold shut or air entrapment (porosity) has an important effect on the quality. The pressure and temperature sensors can detect the flow front arrival, but all pressure sensors have a threshold value below which little readings can be obtained and temperature sensors have a delayed response. Therefore, the measured flow front arrival may be overestimated. The advantages of in-line ultrasonic monitoring have been demonstrated for the arrival and advancement of the molten metal flow front for a conventional liquid metal die-casting process [24].

During the intensification stage, the gate freezing time is considered an important element since no more material can be added into the cavity and further application of holding pressure is a waste of energy from the apparatus. Upon further cooling during the solidification phase, when the part begins to shrink from the wall, an air gap is formed between the wall of the die and the part. This gap development produces a significant change in the heat transfer behavior between the part and the die. The effects of this gap formation on injection molding of polymers have been well documented [25,26]; the same is true for die-casting [24,27,28]. However, up to now, little efforts have been devoted to its monitoring during die-casting. This formation of air increases the thermal contact resistance between the part and the cavity wall and reduces the heat transfer efficiency resulting in a long process cycle. Furthermore, the time needed for the gap to develop, as well as its location, can result in a difference in the temperature uniformity in the thickness direction which induces residual stresses and warpage of the part. Ultrasonic technique was used previously to monitor the gap development during injection molding and die-casting [29]. Nishiwaki, and al. demonstrated the principle of identifying both detachments from moving (referred to in this thesis as mobile) and stationary (referred to in this thesis as in-mobile) molds using ultrasonic techniques [30].

During the solidification part, it is desirable to use the part properties as input parameters for process control in order to achieve a high control on the quality part [22]. Furthermore, the understanding of the solidification is crucial. For instance, the temperature and pressure during the solidification stage must be investigated as they determine part quality characteristics such as weight, density distribution, shrinkage and warpage. How does the cast part undergo this stage is essential to the die and cooling line design and ejection time prediction. Moreover, part properties such as density and elastic constants change rapidly during solidification as the material transforms itself from liquid to solid state.

The study in this thesis concentrates on a new die-casting process which becomes more and more important in the market today. Its potential was first recognized in the early 1970's but, today, its place in the market is beginning to grow [31,32]. This new forming processing technique is called Semi-Solid (SS) forming. The main differences between this technique and the die-casting process, at the machine level, are the conception of the die and the feeding material.

The fabrication of a die is not simple. Engineers commonly use computer simulations to answer their questions [5,6] and reduce the cost of its development. For now, only the hands-on experience of conventional liquid metal die-casting mixed with the knowledge of the properties and behaviors of SS materials are used for the die design. It is generally accepted that SS needs larger volume for the sprue, the runner and the gate compared to die-casting [33]. The rest of the die design relies on the same design rules as those used in the conventional liquid metal die-casting.

The microstructure of the feed alloy for the SS die-casting is composed of spheroidal particles of solid surrounded by a liquid phase of a lower melting point, rather than the interlocking tree-like dendrites of conventional cast alloy. It is the microstructure that gives the material its thixotropic properties; when sheared the material flows, but when allowed to stand it does not move; we can say it is like butter. In general, this thixotropic material gives a high integrity and low part porosity because that material is injected into the die in a laminar flow during SS die-casting compared to a turbulent flow for conventional case. This difference in the flow is due to the material injected at a solid fraction of around 50 % during SS die-casting compared to 0 % for conventional one. The 50 % of solid fraction implies another important fact, that is, the feedstock of the SS processing is at a temperature between the liquidus and solidus [34].

Figure 1-1 shows the temperature range of thixoforming process for aluminum. In conventional liquid metal die-casting, the material is cast at a temperature above the liquidus.

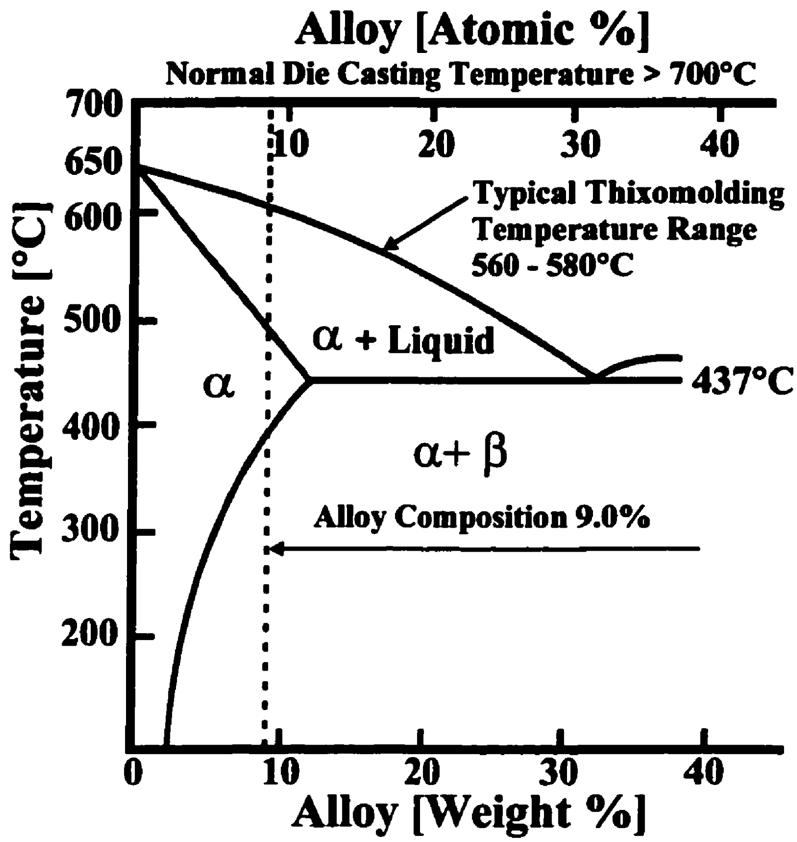

Figure 1-1: Phase diagram of aluminum and temperature range of SS casting processes.

1.3 Semi-solid die-casting or Thixoforming

The Semi-Solid (SS) die-casting processes or thixoforming may be divided in three categories: rheocasting (or rheomolding) [35], thixocasting [36,37] and thixomolding [38].

Rheocasting is a process to produce a thixotropic material by electro-mechanically or eletro-magnetically stirring during the solidification of the molten metal. Thereafter, this new material is injected into the die-casting machine at the desired temperature, between the liquidus and solidus. Typically the material is injected with around 50 % or less of solid fraction. A near net shape part is then retrieved from the process. This process is also called "slurry-on-demands". It is coming from the fact that the feedstock is created just before an injection into the die; and the quantity of materials needed to make the piece can be changed easily if we do not take into account the limit of the mold.

After the thixocast material is cooled down to the room temperature and then it is cut at the desired length. Normally, the material is in the form of a cylinder and it is called billet. Then, it is heated to its SS state (between liquidus and solidus) and injected into the die cavity and produces a thixocast part [36,37]. This is called thixocasting process which is used for the investigation of this entire thesis.

With respect to thixomolding [38], it begins with small pellets of the desired thixotropic material, which are at the room temperature. These pellets are fed into a feed hopper which is similar to the one used for polymer extrusion, heated and, simultaneously, shear forces are applied by a single or twin screws. This provides the thixotropic properties of the material. Then, like the other two methods, it is injected into the die or mold in its SS state.

There are advantages to use thixoforming processes compared to conventional liquid metal die-casting. Because the feedstock is only heated to a temperature between the liquidus and solidus, it is an energy efficient process which can be easily automated and controlled to achieve repeatable parts. The production rates are similar, or even better, to conventional liquid metal high pressure die-casting. The smooth filling, which implies a laminar flow, of the die with little air entrapment and low shrinkage porosity produces the parts with a high integrity [34-46]. Furthermore, low processing temperatures reduce the thermal shock of the die, extend the die life and allow the processing of high melting point alloys (such as toll steels) that are difficult to form by other means [44-46]. It may also allow the use of soft and economical die materials due to reduced mechanical stresses acting on the die during filling and the use of low alloy processing temperature. A fine and uniform microstructure provides enhanced component properties. Weight savings may also be achieved through the optimization of the part design.

However, at present, there are also drawbacks in SS processes such as the high cost of raw material due to complex procedures, limited quantity of production and low number of suppliers. Furthermore, because of the lack of available process experience and design rules, considerable research effort and expenses are required to implement a viable manufacturing process and die development compared to conventional liquid metal forming technologies [34].

The relatively high price of suitable feedstock for thixoforming processes is perceived as the major barrier to its commercial growth in production. As these processes are related to volume of raw material production, the price will not fall until demand increases significantly. This is the reason why researchers have increased their efforts on the rheocasting process in the last few years with the hope to reduce the cost of raw material and increase the number of thixocast produced [34].

Recently one method is used with the intention to reduce the price of feedstock. It is the application of materials with dendritic microstructures as feedstock with the same billet form of the thixocasting process. The material is heated in the same way as the thixocast; but, at the end of the heating process, there is one more step: soaking. The soaking allows the nucleation of small spheroidal microstructures that behave as thixotropic material. This technique removes the need to produce the thixocast billet which is difficult and expensive to make [37,39,40,42,47].

1.4 Sensors

As mentioned in the previous section, the development of process control requires the development of cost effective sensors for the in-line measurements of metal die-casting, injection molding and thixoforming processes.

One of the most important parameters throughout the process is the temperature since it determines the final properties of the product such as residual stresses and warpage. Its measurement is difficult, especially in the thickness direction. The insertion of thermocouples into the metal at different depths cannot be done like in polymers [48,49] to give the temperature profile of the pieces because of the corrosive nature of molten metals. This invasive nature of the thermocouples in the die also introduces problems such as heat conduction through thermocouples and melt flow alteration [50,51]. Infrared (IR) temperature sensors provide a fast response (10 ms) and is a non-invasive measurement [52,53]; but this technique must have a direct vision to the part. Furthermore, its calibration is difficult [54] and needs a black corpse to be effective which is difficult in casting metals because of the reflective nature of the surface of the part. Errors can also be induced in the IR signatures from the surroundings such as the mold walls. In addition, Bur and al. have demonstrated the capacity of determining mold filling, the start of solidification, crystallinity, part detachment and part shrinkage using the optical technique [55,56]. However, the polymer or the material need to be transparent and the approach is not applicable for metals. Even the mold wall must be modified to accommodate a transparent sapphire window for the transmission of light into the transparent polymer.

The pressure is another important parameter. It can help to determine the flow front arrival and the internal pressure of the cavity. The flow front is determined with the variation of the pressure at the location of the sensor. For the internal pressure, it gives valuable information on the internal forces acting on the die. This information can lead to improvements in the die design, but there is a limit to the pressure sensor; it has a threshold value below which no reliable reading can be obtained. Therefore, the measured flow front arrival is overestimated. Furthermore, the pressure sensor measures the force acting on the sensor's membrane which includes the viscous forces but not the bulk pressure in the material. To protect the pressure sensor from high temperature in metal die-casting, injection molding and SS forming processes, the sensors can be installed behind an ejector pin; but it puts another limit on the sensor's capacities. Because of the non-steady contact and the non-straightness of the ejection pins, the reading of the pressure sensor is not steady and repeatable. Thus, often they do not fulfill the requirements of fast process and repeatable monitoring.

Altogether, many essential process parameters can be monitored throughout the metal die-casting, injection molding and thixoforming processes such as the flow front advancement, the velocity, the gap development caused by shrinkage of the part, the pressure and temperature. However, there is no single sensor that can provide all the above information. In previous works, it has been shown qualitatively that ultrasonic sensors can be used to obtain more information than any single sensor mentioned above. Furthermore, the ultrasonic sensors are non-invasive and non-destructive [10]. In addition, in-line ultrasonic monitoring measurements of industrial processes are often performed at high temperatures which are about 250 to 350 °C for aluminum die-casting and thixocasting. Non-contact ultrasonic methods such as laser ultrasound [57,58] and electromagnetic acoustic transducers (EMATs) [59,60] are possible approaches. Laser ultrasonic systems can provide advantages such as fast scanning and probing materials of complex shapes but are generally bulky and have a high cost. Laser safety is also a concern. The signals produced by EMATs have much poorer qualities in frequency bandwidth and signal-to-noise-ratio (SNR) than those generated by piezoelectric ultrasonic transducers (UTs). There is a strong need to find a broadband ultrasonic transducers of high efficiency for measurements at high temperatures.

The desired broadband piezoelectric contacts UTs together with a coupling medium and should work well at high temperature. The operating range in frequencies of the UT can vary from 1 to 10 MHz. Such high temperature UTs are commercially supplied by several companies: Etalon (Lizton, Indiana), Ultran (Boalsburg, PA), Ishikawajima Inspection and Instrumentation Co. LTD (IIICL, Tokyo, Japan), RTD (German), etc.... However, the price of these UTs is expensive and there is no tolerable solution for choosing the ultrasonic couplant used with the steel walls of the die at high temperature and for a long period of time. In general, the ultrasonic couplant is a type of grease for which the ultrasonic coupling coefficient changes significantly as the temperature varies. Furthermore, except for the IIICL UTs for which the details of the UT designs were given [61], the broad bandwidth is provided by a method using an epoxy backing [58] that is not adapted for thermal cycling. Since there is a difference between the thermal expansion coefficient of the electrode material for the piezoelectric crystal of the UT and the epoxy, a major problem can occur. The epoxy and the electrode can disband during repeated thermal cycling. When this occurs the bandwidth is no longer sufficient for ultrasonic monitoring of our processing. Furthermore, the UTs from IIICL also require a high temperature couplant.

1.4.1 Buffer Rod and Ultrasonic Sensor

The ability of the ultrasound to interrogate non-invasively, non-destructively and rapidly the regions of the mold and cast part is desirable for a modern molding process control. Such a control should not disturb normal processing conditions, although ultrasonic techniques have been used for the improvement of material processes for some time due to recent advances in transducer materials, sensing techniques, microprocessors and digital signal processing. It allows the data to be obtained and analyzed rapidly, reliably and economically [62-67]. These progresses make ultrasound an attractive tool for in-line process monitoring.

One way to bypass the problems enumerated above for the monitoring processes at high temperature is to insert a metallic ultrasonic waveguide (buffer rod) between the UT and the part to be monitored. One end of the buffer rod is water cooled down to 50 °C or lower and the other end is touching the material in the cavity of the die. This method allows the use of commercially high performance UTs and couplants. The ultrasonic waves are generated by the UT, transmitted through the buffer rod and then into the processing part. The reflected ultrasonic waves return to the same UT through the same but reversed path. The application and properties of the buffer rod for ultrasonic monitoring of conventional liquid metal die-casting and metal injection molding have been reported [62-67]. It is the objective of this study to use a new and high performance clad buffer rod consisting of a steel core and stainless steel cladding to perform in-line ultrasonic monitoring of thixocast processes. The energy of the ultrasonic waves are guided in the core of this clad buffer rod. Such high performance clad metallic buffer rod has the following advantages: high signal to spurious ultrasonic noise ratio due to the significant reduction of the trailing echoes, high signal amplitude due to proper wave guidance, suitability for reflection and transmission measurement geometries, high temperatures, no cross talk between adjacent buffer rods since the ultrasonic energy is concentrated in the core and no loss during immersion in molten metals [68,69].

1.4.2 Laser-Ultrasonic Technique

In the die cavity the cast part undergoes a high pressure and a high temperature which affect the ultrasonic properties such as the velocity and attenuation in the part. In order to compare these ultrasonic properties in materials with different microstructures such as thixotropic, dendritic or other different compositions, a non-contact non-destructive non-invasive laser ultrasonic technique [66] with a Gleeble thermal simulator is used. In previous works [70,71], it was used to measure the ultrasonic longitudinal and shear wave velocities (or Young's and shear moduli) of ceramic samples up to 1800 °C. In this method, a high power pulsed laser is used to generate ultrasound on one side of the heated sample and another laser coupled to an optical interferometer is used to detect the ultrasonic wave at the opposite side. Samples are taken from billets of different microstructures and compositions.

1.5 Thesis Content

The focus of this thesis is to use the high performance clad steel buffer rod sensors to perform in-line ultrasonic monitoring of thixocasting process only and to obtain an improved understanding of this process, such as the part microstructures, pressure release, temperature, end of filling, etc… . Although, this sensor can be used to monitor the rheocasting and thixomolding processes mentioned before. Chapter 2 describes the clad steel buffer rod sensor developed for the purpose of in-line ultrasonic monitoring of thixocasting (SS die-casting). The shape and the differences between this new sensor and the old design will be the main study of this chapter. The position of the sensor in the die and its ultrasonic properties such as signal-to-noise-ratio (SNR) will be illustrated.

In chapter 3, the ultrasonic techniques used to obtain the results of the in-line ultrasonic monitoring of thixocasting will be presented. First, the reflection mode will be introduced. It is important to indicate at this stage of the thesis that all the ultrasonic experiments performed have been done using the reflection mode except when mentioned otherwise. Its propagation in two media will be presented. Then the reflection (or transmission) coefficient variation will be used to monitor the flow front arrival and the gap development during the die-casting process. It will be demonstrated how the signals are selected for the calculation of the velocity and the total loss in the cast part. Thereafter, the solidification will be explained by using the time delays of the ultrasonic echoes traveling in the cast parts. Finally, the results of the ultrasonic pulse-echo measurements to derive the average temperature of the die will be explained.

In chapter 4, the ultrasonic velocity and attenuation in the aluminum alloys A356, A357, 86S purchase from Ormet (Hannibal, OH), Gra-Ni® 6S:3G made by INCO Limited (Ontario, Canada) and magnesium alloy AZ91 made by Performag (Montreal, Canada) will be evaluated using a laser ultrasonic technique together with a Gleeble thermal simulator. Samples are taken from the billet form of the above mentioned aluminum and magnesium alloys. These measurements provide the ultrasonic velocity and attenuation data at the elevated temperature but at the atmosphere pressure. The data obtained may be used as a basis for the comparison with those obtained for the cast part inside the cavity under high pressure. However, the Gleeble thermal simulator and the SS casting are different in a way that the thixocasting is a procedure of solidification (liquid to solid) while the Gleeble thermal simulator is a procedure of "liquefaction" (solid to liquid). In previous works [72-74], it has been demonstrated that the difference of procedure can be important in polymers and metals.

Investigations of in-line ultrasonic monitoring of the SS casting will be presented in chapter 5. The flow front, the gap development and the solidification will be monitored by using longitudinal ultrasonic wave in the parts described in the preceding chapter. For each monitoring, all the parameters of the machine will be indicated: this includes the hydraulic pressure and injection velocity, the cavity pressure, the temperature of the mold, the time of the cycle and the temperature of the mold at different locations near the cavity. Then, with digital signal processing, the ultrasonic velocity and attenuation of the material and the temperature will be shown. All these results will be repeated for four different kinds of semi-solid materials: the aluminum alloy A356 and A357, the Gra-Ni® 6S:3G and magnesium alloy AZ91 made by Performag and CANMET (Ottawa, Canada).

The summary of the thesis and the conclusions from all the experiments done in this work will be in the final chapter of the text. Furthermore, potential improvements and future work to be undertaken will be presented at the same time.

Chapter 2: The Clad Buffer Rod Probe and the Data Acquisition System

For in-line monitoring of thixocast process clad buffer rods (CBRs) probe with a high signal-to-noise ratio (SNR) can be inserted into the die made for the thixocast process. As mentioned in the introduction they can be operated in the pulse/echo reflection mode and only one side access of the die is required. In [24], three zirconium (Zr) CBRs consisting of a Zr core and a stainless steel cladding to monitor liquid aluminum (Al) alloy high pressure die-casting. The molten Al alloy is directly poured into the shot sleeve, followed by metal injection into the gate and the die cavity (by means of the plunger (piston)). The flow front, gap formation due to part shrinkage, contact time of the part with the die wall, temperature variations in the die and the time delay variations in the solidifying Al alloy part were observed.

In the present investigation, a steel CBR probe, which consists of a steel core and a stainless steel cladding, is used. The clad steel rod not only has thermal characteristics closer to those of the steel die compared to what was reported for the clad Zr rod in [24], but it also has higher ultrasonic performance which will be demonstrated later on in the text and figures. Because the steel CBR provides ultrasonic signals with a high signal-to-noise ratio, data on velocity and attenuation in the part, which could not be obtained in [24], can be used to build up an improved understanding of the die-casting process. For instance, the variation of the ultrasonic velocity in the cast part can be related to its change of the average temperature while the attenuation in the cast part may also reveal its microstructure. Furthermore, in this investigation, pressure and temperature sensors throughout the die were installed and in [24] none of them were inserted.

2.1 Ultrasonic wave propagation path

In all experiments ultrasound is generated by the longitudinal wave UT, propagated through the core of the CBR probe and reaches its probing end. Ultrasound is then transmitted into the viscous semi-solid melt being injected in the die cavity and is reflected by the other side of the cavity surface and returned back to the UT via the same path. The clad buffer rod ensures good ultrasonic guidance [24,63,75,69]. All ultrasonic signals were acquired with a PC based data acquisition system. The A/D board was a GAGE CS12100 card (Gage Applied Science Inc., Montreal) with 8 Mega-bytes on board memory. Figure 2-1 represents a typical signal and nomenclature acquired from experiments. The first echo represents the longitudinal ultrasonic wave reflected from the probing end of the CBR and it is denoted as L^1. We can see that L^1 has a time delay of about 35 μs; and the echoes L^2, L^3, L^4, etc… having time delays of multiples of about 35 μs represent the 2nd, 3rd, 4th, etc... round trip ones as seen in Figure 2-1. The echoes between those of L^1 and L^2 or L^2 and L^3 are the signals in the cast part that are reflected back from the back wall of the die. They are called L^1_2, L^1_4, L^2_2, L^2_4, L^3_2, etc… The subscript is a multiple of two because the echoes traveling in the cast part traverse the thickness twice before they reach the UT. Figure 2-2 is a brief representation of the reflected and transmitted wave.

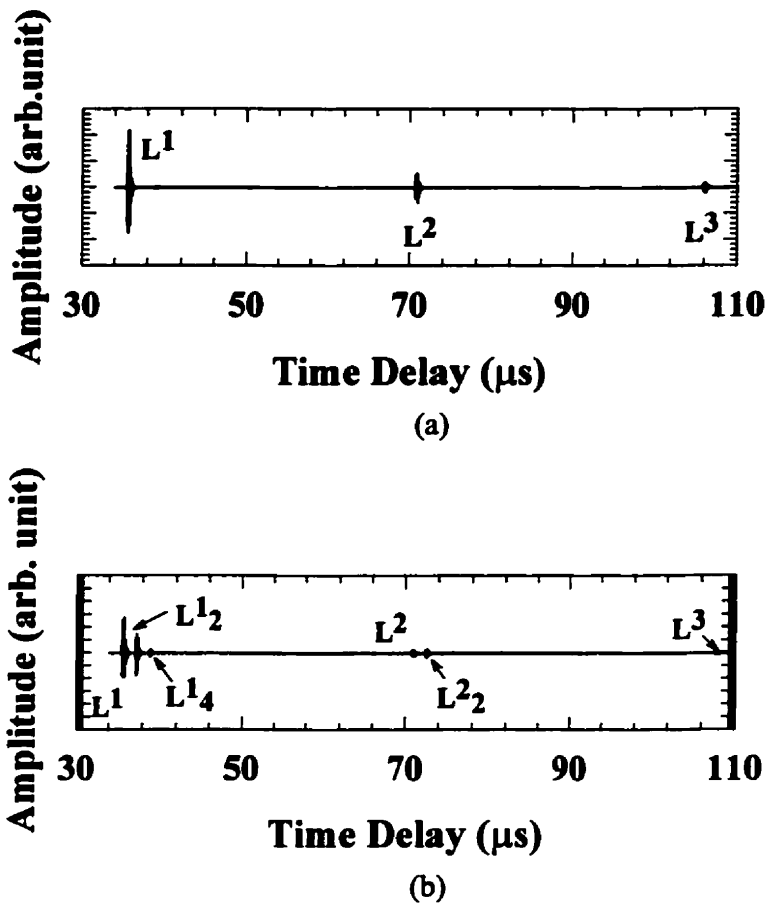

Figure 2-1: Echoes reflected from the probing end of the CBR (a) without and (b) with cast part.

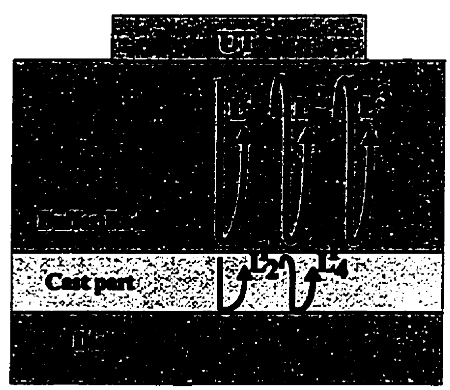

Figure 2-2: Representation of the transmitted and reflected echoes in the CBR and cast part.

2.2 Steel Clad Buffer Rod

As mentioned above, a steel CBR consisting of a steel core and a stainless steel cladding fabricated by a thermal spray technique is used in all experiments. The core of this steel CBR has a tapered cylindrical shape,γ as we can see in Appendix A. The use of a taper has been demonstrated to be effective to reduce unwanted spurious echoes [75]. For the current CBR, the tapering angle, θ, is about 2° (see Figure 2-3). Our measurement results show that this CBR has always a SNR of more than 30 dB [69] even at 250 °C. By comparison, using the same UT and pulser/receiver, the Zr CBR exhibited about 20 dB at room temperature because of the large trailing echo right after L^1. In Figure 2-4, we can see the improvement in the signal of the steel CBR as compared with the old Zr CBR at room temperature. In addition, liquid Al alloy in the die cavity "wets" the steel CBR better than the Zr CBR and thus more ultrasonic energy is transmitted into the Al alloy when the steel CBR is used. The increase of the SNR can improve the analysis of the signals. It also implies that, if one can see the signal better (better SNR i.e. smaller trailing echoes) near L^1, one can impose a shorter acquisition time per frame (explained in later sections).

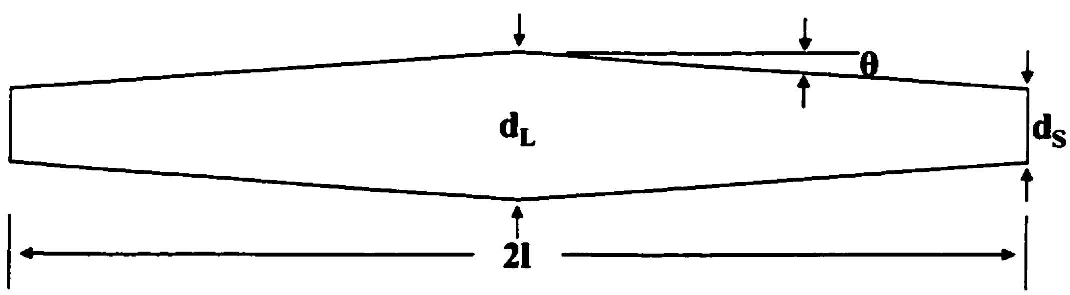

Figure 2-3: Schematic of the steel CBR double taper shape.

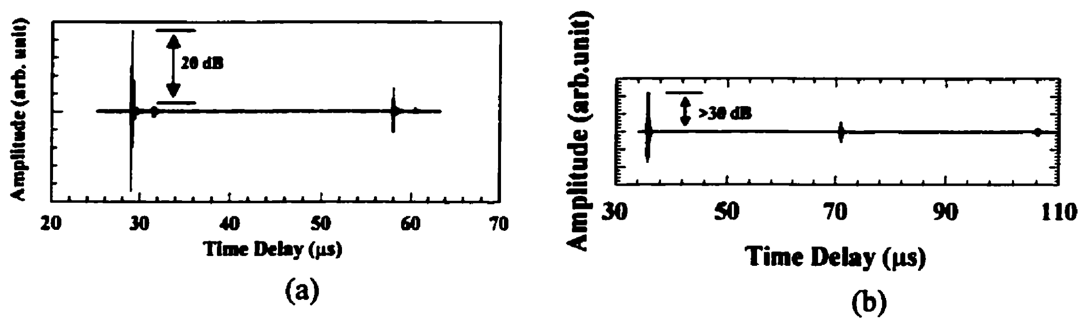

Figure 2-4: Signal of (a) the Zr CBR at room temperature and (b) the new steel CBR at 250°C.

A schematic of the steel CBR is presented in Figure 2-3 and the dimensions are as follows: the biggest diameter (d_L) is 11.684 mm (0.46"), the smallest one (d_S) is 7.518mm (0.296") and the length (2l) is 103.68 mm (4.082"). By comparison, the Zr CBR had a uniform diameter of 6.35 mm and a length of 69.9 mm. We can see an actual representation of the new and old design in Figure 2-5 (a) and (b), respectively. This steel CBR consists of a fine grain steel core with a 1.016 mm (0.04") thick thermal sprayed stainless steel cladding. However, since the rod geometry and thermal sprayed cladding described above are complex, the exact theoretical investigation of the ultrasonic wave propagation characteristics has not yet been carried out. Furhtermore, no investigation was perfomed to identify the relevant modes. The approximated analysis using a finite difference method was demonstrated in [76].

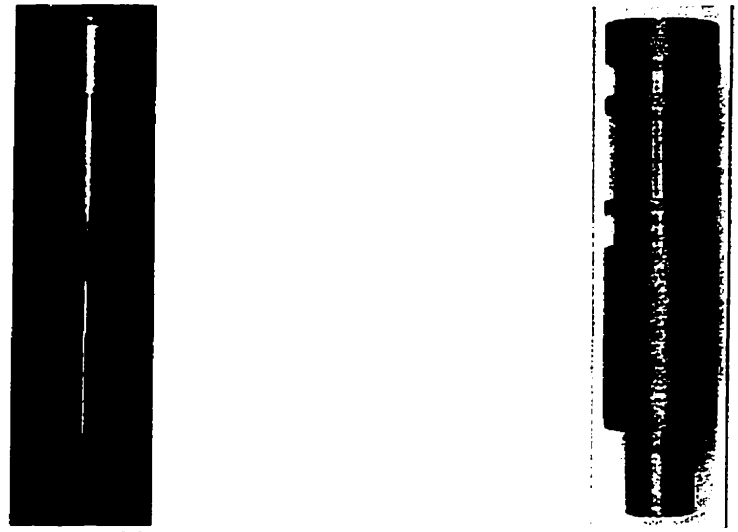

(a) (b)

Figure 2-5: Picture of (a) the steel CBR and (b) the Zr CBR.

The new steel CBR has a shape and dimensions which are different from those of Zr CBRs as shown in Figure 2-6 and reported in [24]. But, this new CBR design is based on the same design of those presented in [62-67]; the only change in the new CBR is the stainless steel cladding which has been ameliorated due to improvement in the thermal spraying technique. The Appendix A provides all the drawings and all the steps required to produce the new CBR. First, Appendix A presents the three steps required for producing a CBR. Firstly, one needs to machine, in this case the steel core into its tapered shape. Secondly, the stainless steel cladding needs to be fabricated onto the tapered core by the arc spray. Finally, two tubes of stainless steel are added by press fitting and weld together over the arc sprayed rod. Those two tubes are an added layer to protect the cladding and they also permit the machining of the CBR into the desired shapes such as thread. Appendix A also shows the details of the machining of the two stainless steel tubes. Then the cooling element is added by silver brazing on the machined two tubes of stainless steel. Furthermore, we can see the holder of the transducer, which has the attachment for the quick connection for the cooling system (air or water pipes), and the holder of the CBR in the die. Finally, an overview of the final assembly is shown. Furthermore, a picture of all components, except the holder of the die-casting machine, of the CBR is shown in Figure 2-7.

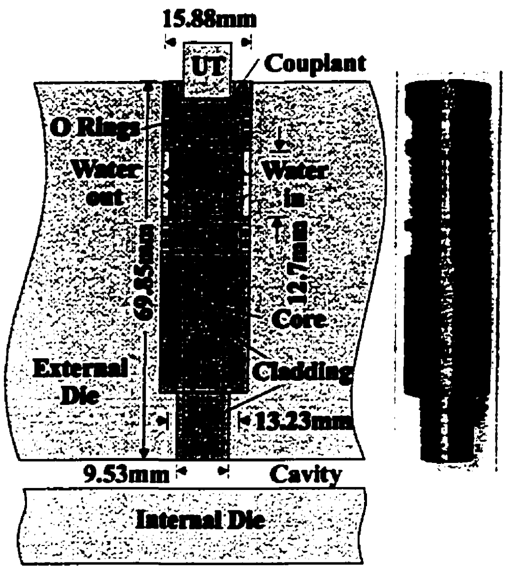

Figure 2-6: Dimensions of the Zr CBR used in previous works [24].

Figure 2-7: All the components needed to assemble a CBR.

As with the old Zr CBR, a commercially available broadband and high performance UT is attached to the cooling end of each buffer rod with the use of a viscous couplant and pressure. The UT end is cooled below 50 °C by water during the casting. To prevent thermal damage to the UT, the new design of the CBR must be verified. To undertake this verification, we did experiments that put a blank transducer rather than a real one in the CBR setup. In the middle of the blank, a hole was drilled for the installation of a thermocouple of 1.6 mm (1/16") as seen in Figure 2-8. Then the CBR was inserted into the die. Thereafter, it was heated up to 250°C and maintained at that level for two hours. The reading of the thermocouple never surpassed 30°C, which is well below the maximum of 50°C that a commercial UT can sustain. It is expected that during a casting of a piece, the temperature does not increase significantly. It is noted that the die is kept open for a few minutes after the casting that helps to dissipate the heat; but the die is closed a few minutes before the casting to let the surfaces of the die take back its initial value (250°C). In addition, the flow rate of the water cooling system is equal to 350 ml/min and the increase in the temperature of the water during the test is 1.5 °C, going from 20 to 21.5 °C. This small increase of temperature provides no threat to damage the UT thermally. In the same experiment, the CBR was tested for leaking and some was found at the connection of the cooling body and the general purpose cap (see Figure 2-7). The design was improved, based on this experiment, by adding a cork ring at connection of the two elements and some silicon grease at the connection of the UT.

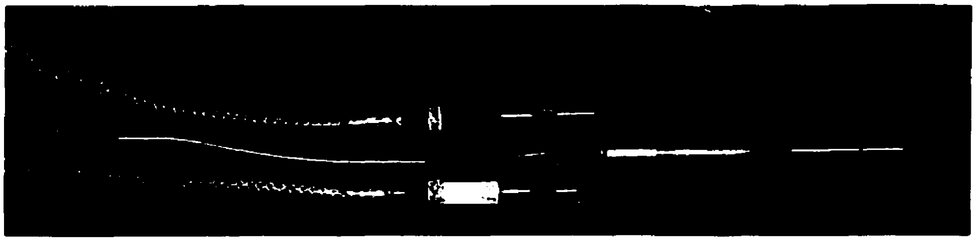

Figure 2-8: Steel CBR together with a thermocouple inserted at the UT's place.

Another important consideration in the installation of the CBR is its position in the die because a proper location can help to focus on certain phenomena such as the solidification or the end of filling. There are in total six positions for us to install the CBR as shown in Figure 2-9. Each of them is for the monitoring of certain characteristics of the die-casting process. For example, those at position 3 and 4 can help determine the beginning of the solidification of the metal. For the thesis, we have decided that the main focus would be on the completion of the filling and the solidification of the part; therefore, the CBR was installed at the present position (position 2, shown in Figure 2-9). In addition, this position of the CBR allows a contact with the molten metal at a lower temperature than the one near the gate; this further protects the UT. At this point, it is important to mention that numerous discussion have been made concerning the installation and the position of the CBRs into the brand new die with dimensions (40 cm by 50 cm by 60 cm). These CBRs should not disturb the desired thermal distribution and cooling channels of the die.

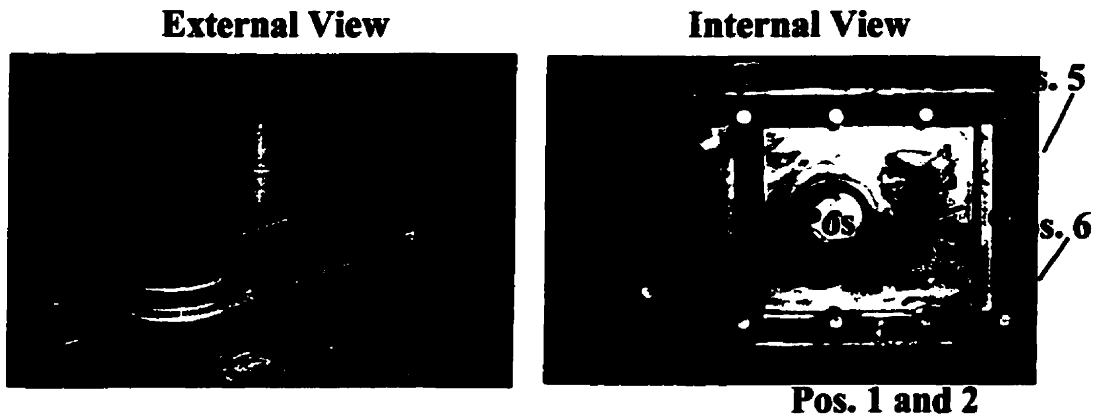

Figure 2-9: Representation of the six positions where the CBR can be inserted.

2.3 Acquisition System: electrical and software

There are two data acquisition techniques developed and used in this research. The first has a slow acquisition speed but lasts for a long period of time and its repetition rate depends on the computer speed. The second one is a fast acquisition method, at high repetition rate, but lasts for a small period of time due to the limitation of the on board memory (8 Mega-bytes in our case). Each system uses the software LabView®, a Graphic programming software. All programs made are called Virtual Instruments (VIs). Those VIs are simple, easy to be implemented and uses a friendly graphic interface. In this section, the two methods will be explained in details, including their advantages and disadvantages. We will call the fast acquisition, multiple recording because it is the approach used in the description of the Gage card, our acquisition board. For the slow acquisition method, we will call it serial recording.

The hardware of the data acquisition system is composed of a digitizer CompuScope 12100 (Gage Applied Science Inc., Montreal, Canada), a 12 bits card. The sampling rate is up to 100 Mega-Point per Second (MPS) for one channel mode and up to 50 MPS for a two channel mode. Furthermore, two pulsers/receivers were used: model 5072PR (Panametric) or PR35 (JSR). Low pass filters are used to filter out the DC components. A 7856 oscilloscope (Tektronix) was used to monitor, in real time, the signals because, when the acquisition starts, the VI program freezes the first signal and the evolution of the echoes can not be seen from computer monitor. The computer is a Pentium III with a CPU of 550 MHz and with 384 MB of RAM. In addition, when we were in a multiple recording mode, we used a digital delay/pulse generator, model DG 535 (Stanford Research Systems Inc., Sunnyvale, California, USA), which provides a precise repetition rate and delay. Figure 2-10 (a) and (b) represents the schematic representation (block diagram) of the set-up used, respectively, of the serial acquisition and the multiple recording which has the time delay generator as an addition to the system.

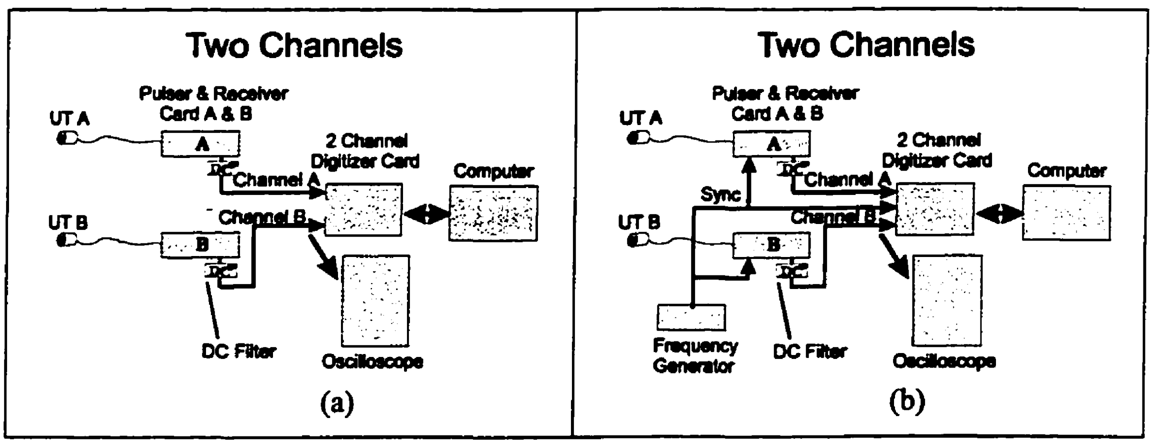

Figure 2-10: Schematic representation of the two approach used: (a) the serial recording, (b) the multiple recording.

The software used are divided for two acquisition approaches as well: the multiple and serial recording. Basically, they have the same interface for the selection of the trigger level, sensibility level, channel used, delay, width, etc... . The main difference is in the way they acquire the data. Their similitude makes the distinction between them difficult. This is the reason why the emphasis for their description is based on their differences. Both software use the same format for the acquired file; to recognize this format the extension file name "*.ser" is used. It consists of a multitude of shots taken from the real time ultrasonic signal, at different moments in time, in a single file. As an example, for a repetition rate of 400 Hz and for a sinusoidal wave that we acquired for 60 seconds. Then the file consists of 24 000 frames following each other of a sine wave. This format has the advantages that it can be easily visualized using the VIs that have been developed for this purpose.

2.3.1 Serial recording

For the serial recording VI, the signal is acquired directly from the Gage card to the computer. A representation of the front panel of the VI is shown in Figure 2-11. Depending on the computer speed, the time for the data file taken from the Gage card and then transferred to the computer can vary. For each frame, in repetition rates, the data transfer speed is between 65 and 5 Hz; this means that it is not constant for each frame. Figure 2-12 shows an example of this variation of time for one casting piece. This lack of stability in this acquisition will only have one repercussion, that is, the number of points in the resulting data. Furthermore, some phenomena such as the fast solidification from liquid to solid state, which takes a time less than several ms, and the filling, which takes about 40 ms, will be difficult to monitor due to the slow acquisition rate (<65 Hz) in the serial acquisition mode.

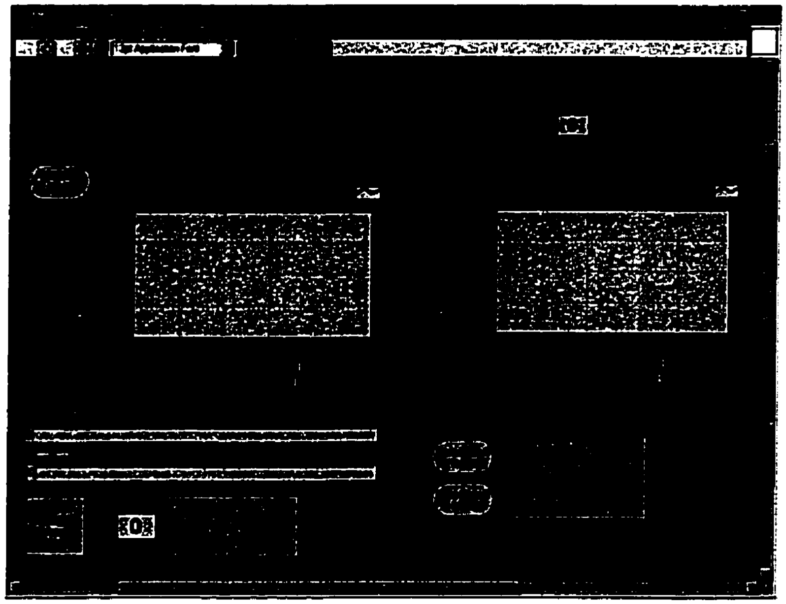

Figure 2-11: Front panel of the VI doing the serial recording.

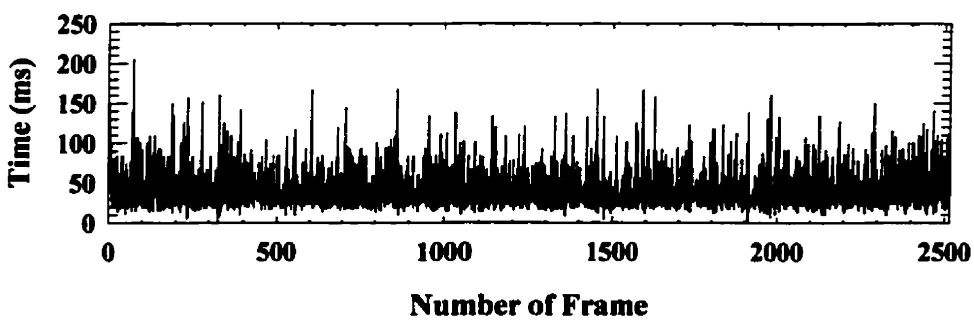

Figure 2-12: Repetition rate for each frame taken during the serial recording.

However, one of the advantages of the serial acquisition is that the acquisition time can be infinite. The limit of total recording time depends on the memory available in the hard disk drive of the computer where this VI is installed. As an example, for 100 seconds of acquisition, which is enormous considering that the full cycle of SS process is about 20 to 30 seconds in our case, the data file occupies about 100 MB of disk space. In addition, this recording is fast enough to see the different stages of solidification, flow front, filling completion, temperature change, etc..., that will be explained in the following chapter. This approach also allows the user to start the acquisition before the die-casting process begins because of the large computer memory. This is useful in our case because there is no need to synchronize our acquisition system with the die-casting machine.

At this moment there is no synchronization between the ultrasonic and die-casting control systems because of the safety and IMI's insurance policy that does not permit us, at present time, to install a switch which can trigger the machine and the ultrasonic system simultaneously. Therefore, this VI can bypass this problem by manually starting the data acquisition just before the injection of the material starts.

2.3.2 Multiple recording

The multiple recording was developed to acquire as fast as possible many signals in a short period of time. As mentioned before, the time frame is limited by our current on board 8 Mega-bytes. However, the on board memory can be increased up to 1 Giga-bytes (told by Gage specification booklet). A representation of the front panel of this approach is shown in Figure 2-13. It uses a function integrated in the Gage card that is called multiple recording. With this function the card can store the signals in the on board memory. When the memory is full, the acquisition is stopped and the transfer of the signals begins from the on board memory to the hard drive of the computer. After the on board memory has been cleaned, the system is ready to acquire more data. But for now, the data transfer takes 26 seconds and the die-casting cycle is about 20-30 seconds. Therefore, it does not permit us to make another recording during the same cast cycle. The multiple recording VI allows high repetition rates. With the help of the digital delay/pulse generator mentioned above, our system can reach a repetition rate as high as 3000 Hz. The fastest recording time for a data set of 7500 bytes can be 3 ms. Therefore, this software allows us to see the details of certain phenomena such as the initial solidification that could not be seen with the serial recording.

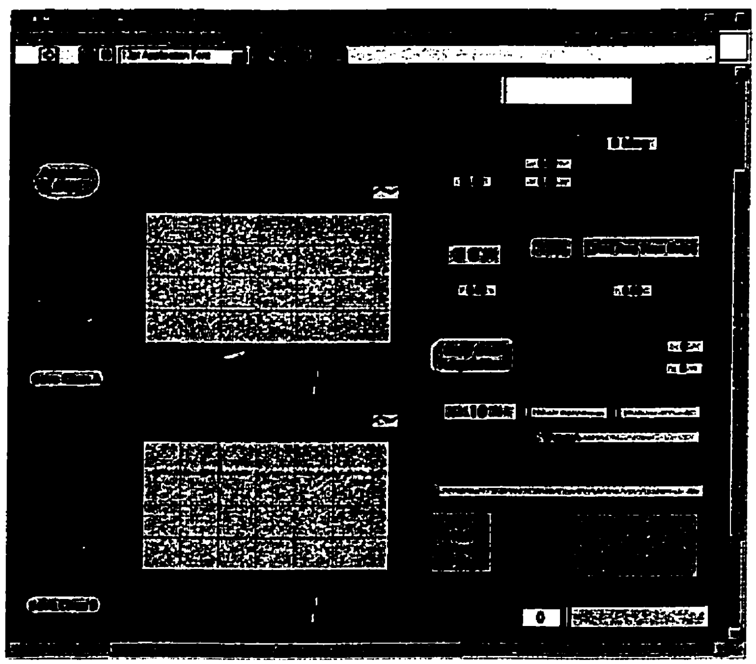

Figure 2-13: Front panel of the VI doing the multiple recording.

Again, the limitation of the multiple recording method is the maximum time duration of acquisition. We can only acquire for a short period of time with this system as shown on Table 2-1. This is a disadvantage because we can not monitor the entire cast cycle. With this system, only a part of the process may be focused. An ideal system would include the synchronization switch mentioned above, that synchronizes the ultrasonic and die-casting systems and where we could adjust the delay between the start of the injection of the machine and the acquiring system or, simply, add more on board memory to the card.

Table 2-1: Time of acquisition for specific repetition rates in function of acquisition time per frame for a 8 Mega-bytes in board memory at a sampling rate of 100 MPS.

Repetition Rates(Hz)	Acquisition time per frame		
	7μs (second)	42μs (second)	120μs (second)
30	---	---	23.4
100	---	20.4	6.9
150	---	13.6	4.6
300	36	6.8	2.3
500	21.6	---	---
1000	10.8	---	---
2000	5.4	---	---
4000	2.7	---	---
5000	2.1	---	---

Now, with the new Gage driver, we can achieve faster acquisition time than the ones described in Table 2-1. The new driver permits to flush the memory (save to the hard disk drive) at the same time that the on board memory of the Gage card is saving information coming from the acquisition.

2.4 Summary

In this chapter, the new design of the steel Clad Buffer Rod (CBR) which can sustain high temperature was introduced. This new steel CBR have a SNR more than 30 dB at 250°C compared to 20 dB at room temperature for the Zirconium (Zr) CBR. The new design has a double tapered cylindrical shape of 2° and the maximum diameter is of 11.684 mm and its length is 103.68 mm. The old Zr CBR as uniform diameter of 6.35 mm and a length of 69.9 mm. This steel CBR is composed of fine grain steel for the core and a steel cladding made by plasma spray. Furthermore, a water cooling system is added to the CBR to be able to use commercially available ultrasonic transducer (UT) which cannot sustain temperature higher than 50 °C. In fact, the cooling system keeps the UT at a temperature lower than 22 °C during the semi-solid die-casting simulation of the process. The CBR is used in conjunction with an acquisition system recording the signals. The acquisition board is GAGE CS12100 with 8 Mega-bytes on board memory. The system can have a repetition rate of up to 3000 Hz at a sampling rate of 100 MHz. It has a limited acquisition time because the data need to be stored in the on board memory which is 8 Mega-bytes. But, a repetition rate, around 50 Hz is used, we can acquire for hundreds of seconds, which is much longer than the die cast cycle time of about 20 seconds, due to the fact that the signal is stored directly to the hard disk drive of the computer.

Chapter 3: Ultrasonic Techniques and Theories

3.1 Introduction

Ultrasound has been and is still used in the industry due to its non-destructive nature, high accuracy, fast response and low cost. It plays an important role in the characterization of material and in-line process monitoring. The ultrasonic measurements make use of ultrasonic waves generated by ultrasonic transducer (UT), transmitted into a certain medium, traversed inside the material and received by the same or another UT. The received ultrasonic waves carry the information of the properties of the material. The ultrasonic results of properties can be obtained using the wave amplitude or the transit time of the ultrasonic waves propagating inside the medium. The measured ultrasonic velocity and attenuation in the medium can be correlated to material properties such as Poisson ratio, density, viscosity, grain size, temperature, pressure, Young's and shear moduli, etc... [77].

This section is divided in two parts. The first part is devoted to the techniques of the reflection and transmission modes and the second one will be on the theories for the calculations of the reflection and transmission coefficients, temperature, velocity, attenuation, solidification, flow front advance and gap development.

3.2 Ultrasonic Techniques- Reflection and transmission mode

There are many techniques used in ultrasonic measurements. The commonly used techniques are the reflection and transmission modes. In the reflection mode, the signal is transmitted and received by the same UT A, as shown in Figure 3-1 (a). For the reflection mode, a part of the energy is reflected at the BR-cast part interface and received by the same UT A; another part of the energy is transmitted into the cast part, then reflected at the cast part-mobile die interface, goes through, once more, the cast part-BR interface and is received by the UT A via the BR. In the transmission mode, the signal is transmitted by UT A and received by UT B Figure 3-1 (b). In Figure 3-1 (b), the ultrasonic waves generated by UT A propagate though the clad buffer rod (BR) and impinge on the BR-cast part interface. A part of the energy is transmitted into the cast part, reaches the cast part-mobile die interface and is received by the UT B.

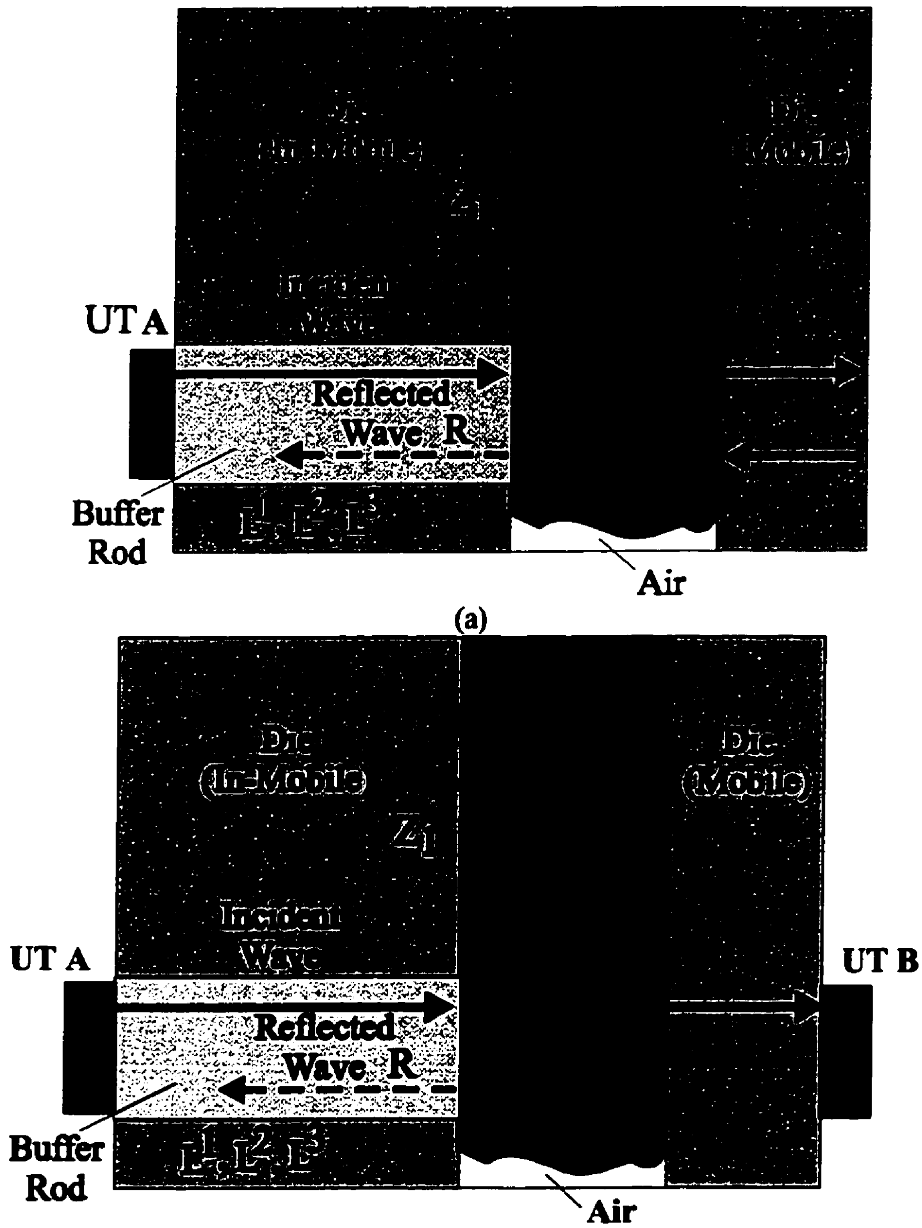

(b)

Figure 3-1: (a) Reflection and (b) transmission of ultrasonic waves at the interfaces.

For certain in-line ultrasonic monitoring of industrial material processes, it is not practical to use the transmission method because it would require a two-side access for two UTs at a specific location of the die or mold. The reflection mode is preferred in some situations because only one side access is required. However, one disadvantage in this approach is that it suffers from a higher loss of energy. This is due to the fact that the ultrasonic waves travel a round trip in the part instead of single trip as in the transmission mode; therefore, it has twice the signal loss the transmission mode. Proper signal processing algorithm, UT and coupling, etc..., may enhance the signal-to-noise ratio (SNR) and the need to have high energy in the signal. The signal strength and SNR of the clad buffer rod probe used in this research are sufficient to perform the monitoring because of its properties described in the previous chapter and in references [75,69]. In this thesis only the reflection mode is used for ultrasonic measurement.

Looking at different in-line or on-line monitoring possibilities in the market [78-82], we have found that the ultrasonic approach may be ahead of other options because of its capacity to provide a fast response as well as sub-surface information. In this research, the reflection coefficient, the attenuation coefficient and the time delay in the cast material are used for the process analysis. We can determine (1) the ultrasonic velocity; (2) temperature; and (3) attenuation coefficient in the cast part; as well as (4) the flow front; (5) gap development at the die-cast part interface (die-cast part and cast part-die), and (6) solidification of the cast part.

3.3 Reflection and Transmission Coefficient

When ultrasonic waves impinge on the boundary of two different media, a part of the energy is transmitted from the first medium into the second medium and the rest of the energy will be reflected back by the boundary, as shown in Figure 3-2. The energy reflected back is used for the calculation of the reflection coefficient and the transmitted energy is used for the calculation of the transmission coefficient.

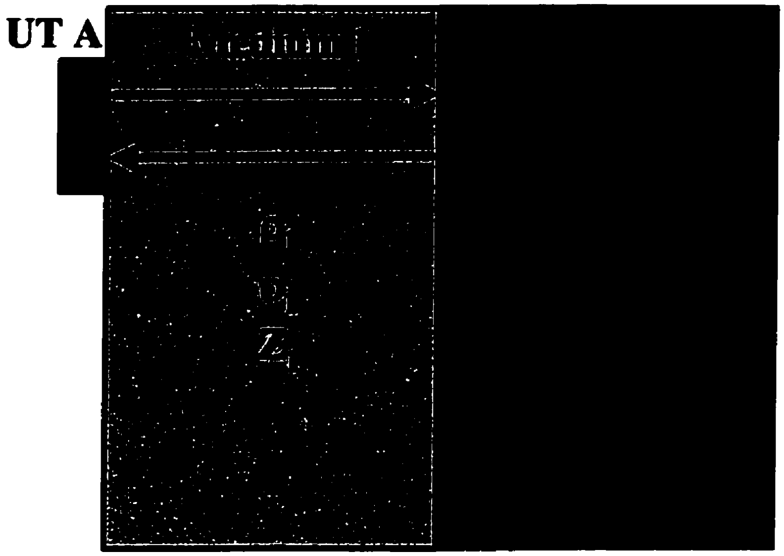

Figure 3-2: Reflection of ultrasonic waves at the interface of two medium.

In the literature, it is well understood that, for plane waves at an interface between two infinite media, the reflection and transmission coefficients, abbreviated as R and T respectively are represented in their mathematical forms by the following equations [83]:

Reflection coefficient:

$$R = \frac{Z_1 - Z_2}{Z_1 + Z_2},$$ **Equation 3-1**

Transmission coefficient:

$$T = 2\frac{Z_2}{Z_1 + Z_2} = 1 - R,$$ **Equation 3-2**

where the subscript represents the first and the second medium and Z the acoustical impedance of the medium (Figure 3-2). The acoustic impedance, Z, is defined as the product of the density, ρ, of the medium and by the sound velocity (wave velocity), υ, of the same medium.

These two equations are practical when evaluating the impedance matching of two media and provide a simple way to determine the type of delay line (such as steel or polymer) to be used for particular application. As an example, if an ultrasonic delay line made of steel with a Z_{steel}=45.63 Kg/m^{2}s*10^6 (1020 steel) is used to test a piece of aluminum in water (Z_{water}=1.48 Kg/m^{2}s*10^6), a reflection coefficient of 0.94 is obtained at the steel-water interface. It means that the most of the energy of the wave is reflected back to the UT and little ultrasonic wave energy is transmitted into the water or, consequently, to the piece of aluminum. Sometimes though, this small amount of energy may be sufficient for certain measurements. As another example, if we use molten aluminum (Z_{Al}=17.06 Kg/m^{2}s*10^6) to replace water, the reflection coefficient at the steel-molten aluminum interface, reduces to 0.456. It means, that nearly 54% of the ultrasonic wave energy is transmitted into the molten aluminum. Therefore, the choice of delay line material is crucial.

3.4 Velocity

For in-line ultrasonic monitoring of die-casting processes, several parameters are of interest. They are the velocity in the BR and the velocity in the cast part.

3.4.1 Velocity in the BR

This velocity can be derived from the $\frac{2*l_{BR}}{td_{BR}}$, where l_{BR} is the length of the BR and td_{BR} is the time delay between echoes L^1 and L^2 or L^2 and L^3.

3.4.2 Velocity in the cast part

The velocity in the cast part, υ_{part}, can be obtained from $\frac{2 * h_{part}}{td_{part}}$, where h_{part} is the thickness of the cast part and td_{part} is the time delay between echoes L^1 and L^1_2 or that between L^2 and L^2_2.

3.5 Attenuation in the cast part

Let $A_0(f)$ be the Fourier transform (FT) of the incident ultrasonic wave impinging on the BR-cast part interface (probe-cast part), $S_0(f)$ the FT of the echo signal, L^1, reflected back to UT A from the BR-cast part, $S_2(f)$ and $S_4(f)$ the FT's of the echo signals, L_2 and L_4, which have gone through respectively once and twice the round trip between the BR-cast part and the cast part-mobile die interfaces before returning back to the UT A. Assuming that probing end of the buffer rod is parallel to the internal wall of the mold facing the probe and given that the diameter of the active area of the probing end was about 12 mm (0.47"), which was much larger than the part thickness of 4.7752 mm, we consider that it is quite reasonable to assume that the beam loss was negligible. However, we did not check experimentally to which extent this assumption holds. Under these conditions, we have:

$$S_0(f) = A_0(f)R_{12}(f) \qquad \textbf{Equation 3-3}$$

$$S_2(f) = A_0(f)T_{12}(f)R_{23}(f)T_{21}(f)e^{-2\alpha(f)h}$$
$$= A_0(f)\left[1 - R_{12}(f)^2\right]Q(f) \quad \textbf{Equation 3-4}$$

$$S_4(f) = A_0(f)T_{12}(f)R_{23}(f)R_{21}(f)R_{23}(f)T_{21}(f)e^{-4\alpha(f)h}$$
$$= -A_0(f)\left[1 - R_{12}(f)^2\right]R_{12}(f)Q(f)^2 \quad \textbf{Equation 3-5}$$

$$Q = R_{23}(f)e^{-2\alpha(f)h} \quad \textbf{Equation 3-6}$$

where $T_{12}(f)$ and $R_{12}(f)$ are respectively the transmission and reflection coefficients of the BR-cast part interface when the ultrasonic wave impinges on the interface from the probe (medium 1) to the cast part (medium 2), $T_{21}(f)$ is the transmission coefficient of the BR-cast part interface when the ultrasonic wave passes through this interface from the cast part to the probe, $R_{23}(f)$ is the reflection coefficient of the interface between the cast part and the mobile die (medium 3) when the ultrasonic wave impinges on the interface from the cast part side. In the above equations, $\alpha(f)$ represents the ultrasonic attenuation coefficient inside the cast part (molten metal), and h denotes the thickness of the cast part, i.e., the distance between the probe end of the sensor and the internal wall of the mobile die facing the probe.

Let's assume that the ultrasonic attenuation in the molten metal is small in such a way that the reflection coefficients $R_{12}(f)$ and $R_{23}(f)$ can be regarded as real numbers. Dividing Equation 3-4 by 3-3, taking the magnitudes of both sides of the resulting equation, and taking into account that $|R_{12}(f)| \leq 1$, we can solve the equation for $|R_{12}(f)|$ and obtain:

$$|R_{12}(f)| = \frac{-\left|\frac{S_2(f)}{S_0(f)Q}\right| + \left[\left|\frac{S_2(f)}{S_0(f)Q}\right|^2 + 4\right]^{1/2}}{2} \quad \textbf{Equation 3-7}$$

Dividing Equation 3-5 by 3-4, taking the magnitudes of both sides of the resulting equation, and solve the equation for Q, we obtain:

$$|Q| = \left| \frac{S_4(f)}{S_2(f)R_{12}(f)} \right| \qquad \textbf{Equation 3-8}$$

Solve Equations. 3-7 and 3-8 for $|R_{12}(f)|$ and $|Q|$, we obtain:

$$|R_{12}(f)| = \left[1 + \left| \frac{S_2(f)^2}{S_0(f)S_4(f)} \right| \right]^{-1/2} \qquad \textbf{Equation 3-9}$$

$$|Q| = \left[\left| \frac{S_4(f)}{S_2(f)} \right|^2 + \left| \frac{S_4(f)}{S_0(f)} \right| \right]^{1/2} \qquad \textbf{Equation 3-10}$$

From Equations 3-6 and 3-10, the ultrasonic attenuation coefficient can be obtained as:

$$\alpha(f) = -\frac{1}{2h} ln \left\{ \left[\left| \frac{S_4(f)}{S_2(f)} \right|^2 + \left| \frac{S_4(f)}{S_0(f)} \right| \right]^{1/2} \Big/ |R_{23}(f)| \right\} \qquad \textbf{Equation 3-11}$$

In the current study, the buffer rod and the mold are both made of steel. As a consequence, we assume:

$$|R_{23}(f)| \approx |R_{12}(f)| \qquad \textbf{Equation 3-12}$$

Taking this into account, we can substitute Equation 3-9 for $|R_{23}(f)|$ in Equation 3-10 and obtain:

$$\alpha(f) \approx -\frac{1}{4h}\ln\left\{\left[\left|\frac{S_4(f)}{S_2(f)}\right|^2 + \left|\frac{S_4(f)}{S_0(f)}\right|\right]\left[1 + \left|\frac{S_2(f)^2}{S_0(f)S_4(f)}\right|\right]\right\} \qquad \textbf{Equation 3-13}$$

Equation 3-13 is used for the calculations of the ultrasonic attenuation coefficient in the cast part (molten metal). The results shown in the figures will be the attenuation coefficient per centimeter obtained for the frequency at which $S_0(f)$ has the maximum magnitude.

3.6 Temperature

The ultrasonic velocity (time delay) in a medium (such as cast part, die or CBR) is a function of temperature. In general for a metal, the velocity decreases as temperature increases. Therefore, the velocity (time delay) variation in the cast part can be used to evaluate its temperature change. Similarly, we can use the velocity variation in the CBR to access the variation of the average temperature in the die because the CBR is embedded in the die and materials (steels) are similar.

3.7 Monitoring of flow front and the end of filling

As shown in Figure 3-1, the UT A is operated in reflection mode. Before the molten metal is injected into the mold or die, the cavity is empty and filled with air and the ultrasonic reflection coefficient(R_{12}) at the BR-cast part (air) interface is almost one (total reflection) due to the poor acoustic impedance matching between the BR steel (Z_{steel}=45.63 Kg/m^2s*10^6) and the air (Z_{air}=4.27 Kg/m^2s*10^2). At, the filling stage, the flow front advances inside the cavity and the metal replaces the air. As soon as the molten material wet the probing surface of the probe (BR), a part of ultrasonic wave energy is transmitted into the molten metal. The reflection coefficient (R_{12}) at the probe-cast part interface decreases. It means that the amplitude of the echo, L^1, reduces when the flow front arrives, as shown in Figure 3-3, indicating the arrival of the flow front at that particular location.

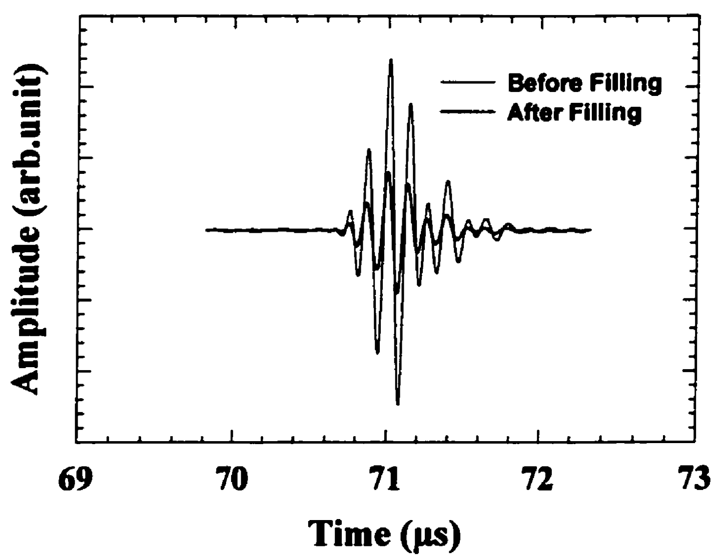

Figure 3-3: Amplitude of echo L^1 as the flow front arrives.

When we make a comparison between the polymer injection molding reported in [82] and the die-casting of aluminum (Al), presented here, we note that the reduction of the reflection coefficient as the flow front arrives is greater for Al alloy cast part because of its closer acoustic impedance matching with the steel CBR. It means that more ultrasonic energy can be transmitted into the cast part from the steel CBR. Another difference is that the filling time is much faster for the die-casting case, about 40 ms compared to a few seconds for the polymer injection molding; thus, a high speed acquisition system (multiple recording system at 500 MHz) is needed to perform those measurements to detect the filling process.

However, due to oxidation of the molten Al, an oxide layer exists between the probing end surface and the cast part. The oxide layer prevents efficient ultrasonic coupling from the CBR probe to the cast part and the reflection coefficient does not decrease at this moment. Once the pressure in the cast part has increased significantly as the part is filling the entire cavity, the high pressure will brake the oxide layer and then, the cast part "wets" the CBR probe. It means that a much more efficient coupling exists at the end of the filling and the reflection coefficient (R_{12}) reduces dramatically. Figures of this monitoring will be given in chapter 5 and will be referred to as time A.

3.8 Gap Development

It is understood in the literature [24-30] that the gap formation between the cast part and the die can be detected by ultrasound. It is important in die-casting to monitor the gap formation because the transfer of thermal energy (cooling) is mainly in the form of conduction and the gap prevents the transfer of energy in the die and makes the cooling inefficient.

As mentioned in the previous section, before the filling the ultrasonic signal is almost totally reflected back at the steel CBR-air interface (see Figure 3-1). As soon as the filling is completed, the amplitude drops as the interface changes to steel CBR-cast part boundary. The cast part cools down after the filling and then it gradually solidifies. At the beginning, the ultrasonic signal amplitude, L^1, changes slightly due to minor changes in elastic properties of the part. As the solidification progresses, the part begins to shrink in thickness and a gap is formed. After a sizable gap (>1 μm thick) is developed, the interface returns to the steel CBR-air condition and the amplitude of L^1 returns to its previous level. For more information on the gap size please see the master thesis of Mr. Cao [24].

In Figure 3-4, we can see the effect of the gap on the signals when it is created at the interface of the cast part-mobile die or at steel CBR-cast part. In the case (a), when there is no gap, the signal will be composed of the L^1, L^2, L^3 and the echoes which have passed the material (L_2, L_4, L_6). When a gap is forming on the side of the mobile die (case (b)), we can still see the same echoes as in case (a), but the amplitude of the signals (L_2, L_4, L_6) should be greater due to the fact that the energy is reflected back to the cast part at the cast part-mobile die interface and not transmitted to the mobile die as in case (a). When case (c) happens or when gaps are forming on both side of the die, we can only see the reflection of the CBR (L^1) and we cannot say at 100% if the gap is formed on the steel CBR-cast part or cast part-mobile or both interfaces. The only time that we can be sure where the gap is formed is when the gap at the cast part-mobile interface is formed before that at the steel CBR-cast part interface. If the situation is reversed, the conclusion is that a gap exists, at the steel CBR-cast part interface.

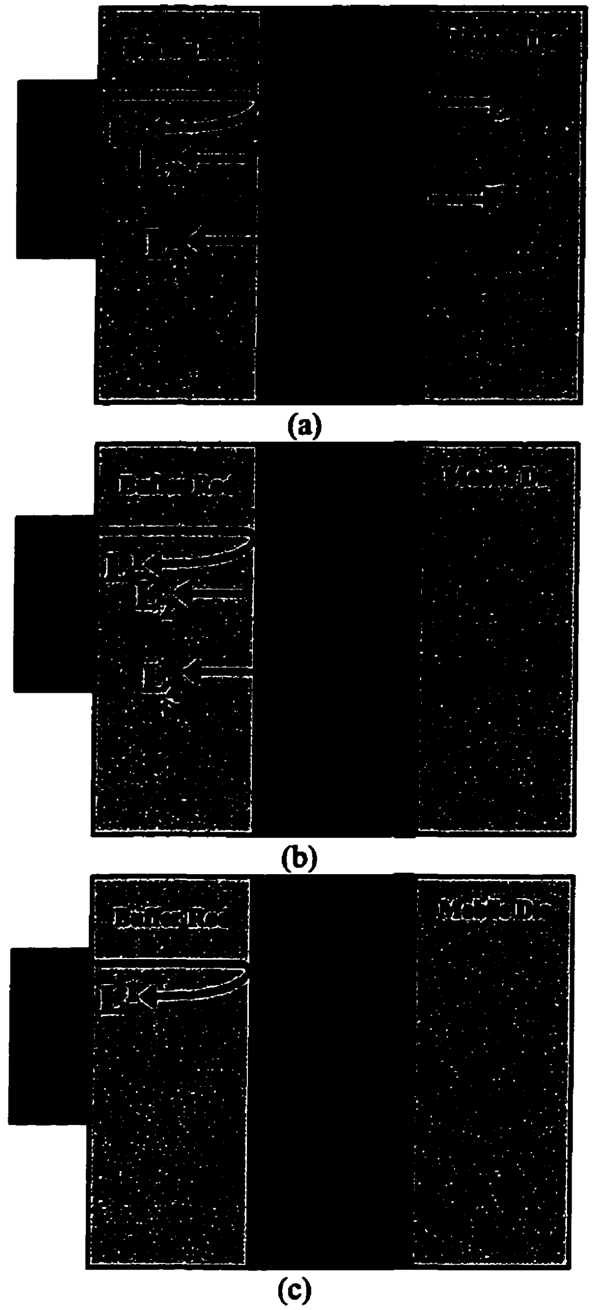

Figure 3-4: Gap formation. (a) before gap formation, (b) gap forming at the cast part-mobile die interface and (c) gap formation at both sides of the cast part.

3.9 Solidification

As soon as the molten metal is injected into the cavity, the part starts its solidification because the die is cold compared to the injected metal. During the solidification, the properties of the part change continuously and, as we know from the previous sections, the ultrasonic velocity of a specific material changes as a function of temperature. Because of this change, time delay between two echoes (L_2 and L_4) varies accordingly. This variation is the basis for the solidification detection.

3.10 Summary

In this chapter the basics of ultrasonic monitoring of the end of filling, gap development, solidification of the cast part in the die-casting process, the average temperature in the steel CBR and in the cast part, the ultrasonic velocity in the CBR and in the cast part and, finally the attenuation coefficient in the cast part were introduced. The monitoring of the end of filling and the gap development can be carried out by studying the change of amplitudes of echoes L^1 and L^2 respectively, which are the first and second round trip echoes reflected from the steel CBR-cast part interface. The ultrasonic velocity can be calculated as twice the thickness of the cast part divided by the time delay. As we know, the ultrasonic velocity is a function of temperature; thus, the temperature can be correlated with the ultrasonic velocity. The solidification in the cast part can be monitored by looking at the variation of the ultrasonic velocity in the cast part (or the time delay between echoes L_2 and L_4); the ultrasonic speed increases with the decrease of temperature of the cast part. The attenuation coefficient is the ultrasonic wave energy dissipated in each centimeter traversed by the ultrasonic wave in the cast part. It determines the limit of allowable thickness for ultrasound monitoring. Throughout this thesis the pulse-echo reflection mode is used. The reflection mode uses a single ultrasonic transducer (UT) for the transmission of ultrasonic waves as well as the reception of ultrasonic echoes bounced back from the interface of two different materials. The reflection mode is sometimes preferred because of its simplicity to install. However, particular attention must be paid to the SNR of the system.

Chapter 4: Ultrasonic Characterization of Die Casting Billets Using a Laser-Ultrasonic Technique

Laser-ultrasonic is a non-contact and non-destructive method that can be used to measure the ultrasonic properties of materials at elevated temperatures. Laser-based ultrasonic offers a great deal of advantages for material characterization over other ultrasonic techniques. For example, its acquisition can be done without contact and far from the measured target; thus, applicable in harsh industrial environments and moving surfaces. Furthermore, the laser beam does not need to be perpendicular to the inspected surface and making it possible to make accurate velocity and attenuation measurements for tubes with curved surfaces in industrial conditions. Another advantage is the possibility to have broadband generation and detection of ultrasonic waves, ease of adjustment of detection and generation ultrasonic beam sizes.

The interest in this area of laser-ultrasonic has increased considerably over the past twenty years. The most published works concern the characterization of material properties, including ultrasonic velocity, attenuation, elastic constants, texture, grain size, etc... [72]. Laser-ultrasonic, in its broad sense, involves the use of lasers for the generation or the detection of ultrasounds or both simultaneously. By doing this, it is possible to scrutinize the structures for defects and integrity as well as for characterizing materials. This is done without contact and at an offset distance in the order of a meter.

In previous works concerning elevated temperature environment [70,71], laser-ultrasonic was used to measure the ultrasonic longitudinal and shear wave velocities (or

Young's and shear moduli) of ceramic samples up to 1800 °C and to measure steel seamless tubing at 1000 °C on the production line [57,84].

In this thesis, the laser-ultrasonic method uses a high power pulsed laser to generate ultrasound on one side of the heated sample and another laser coupled to an optical interferometer is used to detect the ultrasonic wave at the opposite side as shown in Figure 4-1. In this work ultrasonic waves are generated by a pulsed Nd:YAG laser. This laser emits light pulses (infrared) at 1.064 μm with a total energy of 400 mJ and 12 ns fwhm duration and a repetition rate of about 10 Hz. Both spots for generation and detection were about 5 mm in diameter. Note that the sample can be located far away (one meter or so) from the laser source and optical components. The material properties measured in this section of the thesis are taken without pressure and can be used as references for comparison with those of the next chapter which consist of ultrasound waves taken during a high pressure die-casting process. Furthermore, here, we used a Gleeble thermal simulator to heat the samples which are made from the billets (feedstock material) used for die-casting.

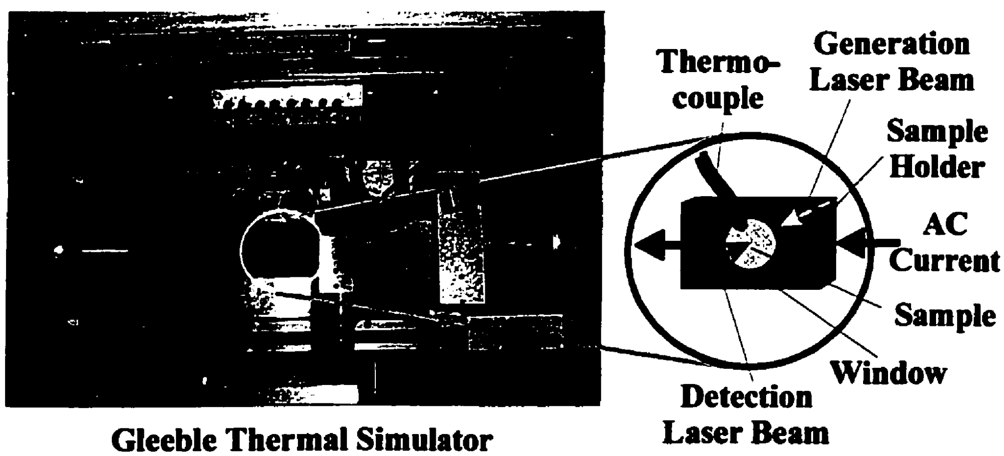

Figure 4-1: Laser ultrasonic measurement setup in the chamber of a Gleeble thermal simulator.

It is noted that during laser-ultrasonic measurements the Gleeble system provides the heating for the melting (solid to liquid) process, but during the in-line ultrasonic monitoring the thixocasting goes through a cooling and solidification (liquid to solid) process. This means that the data obtained by laser-ultrasonic method may be somewhat different from those obtained by in-line ultrasonic method given in Chapters 5.

In this chapter, six different kinds of billets were investigated: three thixotropic aluminum (Al) alloys used for SS processing (the A356, A357 and 86S) which are commercially available (ORMET, Hannibal, OH), a dendritic A356, a dendritic magnesium (Mg) alloy AZ91 and a dendritic Metal Matrix Composite (MMC) Gra-Ni® 6S:3G. They were chosen because of their availability even though in limited quantity for the Mg alloy and MMC. The Mg and the MMC billets were supplied from our collaborators, Performag (Montreal, Canada) and INCO Limited (Ontario, Canada), respectively. The Mg alloy was made by Performag and produced by solidifying conventional molten AZ91 in the sleeve of a die-casting machine creating billets. They have porosity and dendritic microstructure. Furthermore, for security reason (to prevent fire), the Mg alloy was heated in the Gleeble system with SF_6. The MMC was made by INCO Limited at their Ontario facility and was produced by gravity casting with a dendritic microstructure. To our knowledge, MMC billet is not commercially available at this moment.

4.1 Aluminum Alloys

The Al alloy samples used in this research were taken from the thixotropic A356, A357, 86S and the dendritic A356 billets. Table 4-1 shows the composition of each sample. Each sample was heated in the Gleeble thermal simulator at a rate of 60°C per minute up to 480°C, then at a rate of 10°C per minute till 535°C and finally at a rate of 1.1°C per minute until 575°C. This heating procedure was arbitrary chosen, but based on past experience with different types of samples. A thermocouple was spot welded to the sample to measure the temperature. Since the sample thickness, h, is known and the traveling time, t_d, of the ultrasonic wave into the sample can be measured, then the velocity can be obtained as $v=2h/t_d$. In those experiments, only the longitudinal wave was used and the shear wave not considered.

Table 4-1: Aluminum alloys composition.

Aluminum Alloy	Elements (% wt)								
	Al	Si	Fe	Cu	Mn	Mg	Zn	Ti	Others
A356	Balance	6.5-7.5	0.2	0.2	0.1	0.25-0.45	0.1	0.2	0.15
A357	Balance	6.5-7.5	0.2	0.2	0.1	0.4-0.7	0.1	0.2-0.4	0.15
86S	Balance	5-7.2	<1.5	1-5	---	<1	<3	---	<3

Figure 4-2 and Figure 4-3 show the measured ultrasonic velocity and total attenuation, respectively for the above mentioned four different Al alloys. The frequency chosen for the comparison is 10 MHz which is the centre frequency of the ultrasonic transducer (UT) for in-line die-casting monitoring. The sample used was about 20 mm by 25 mm and 1.3 mm thick. Ultrasonic velocity and attenuation were measured using the first and second round trip echoes traveling through the sample thickness, if we refer to the given nomenclature (L_2, L_4 echoes) mentioned in Chapter 2. It is found that the velocities and attenuations of the billets A356 and A357 have an abrupt change at around 565°C whereas those of the 86S and the dendritic alloy have a smooth variation at about

480°C and 500°C respectively. In Figure 4-2, we can also see that ultrasonic velocities in the thixotropic billets A356 and A357 are about 180 m/s higher than that of the dendritic sample, whereas the velocity in 86S is about 100 m/s higher. But for all those studied, up to around 480°C, the beginning of the curve can be considered as linear which is helpful in the interpolation of temperature.

The difference in the velocity and attenuation in different samples may be attributed to three possible causes: (1) the composition of the alloy, (2) microstructure (in our case dendritic or globular (thixocast)), and (3) porosity in the sample. If we examine the results of the thixotropic A356 and A357 samples shown in Figure 4-2 and Figure 4-3, one can see that both have a similar velocity and attenuation. The reason must be that these alloys have the same amount (7%) of silicon and their compositions are very much alike, as their microstructure, as shown in Figure 4-4. The difference between thixotropic A356 and 86S could very well be caused by the different amount of Si (1%) and Cu (3%) contents. We can also see that ultrasonic velocities in the thixotropic A356 are at least 180 m/s higher than those of the dendritic A356. This difference increases with the temperature except in the Al alloy softening range. Between 425 and 535 °C, the difference may be even more than 2000 m/s. However, the velocity difference between thixotropic 86S and dendritic A356 is less than the one between thixotropic A356 and dendritic A356, but still significant.

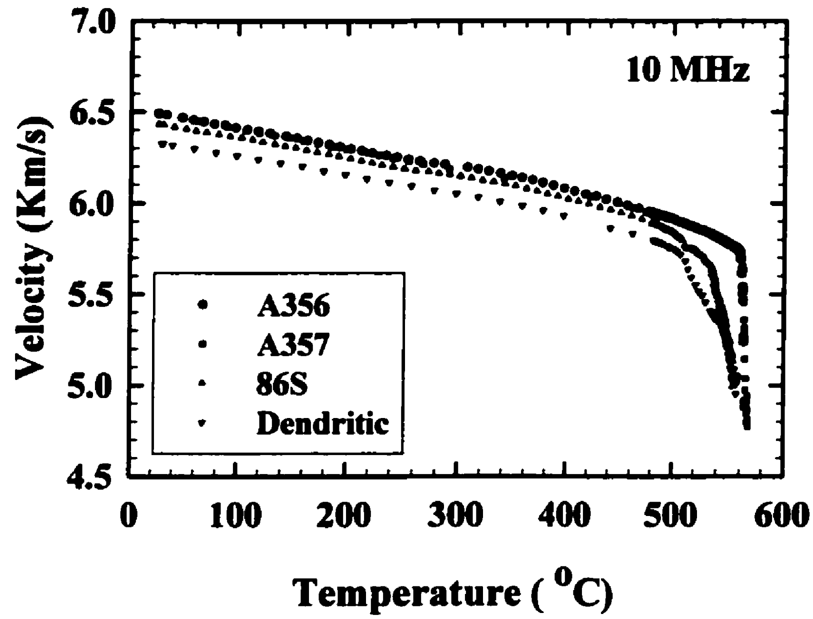

Figure 4-2: Velocity measurements of four samples of aluminum alloys at 10 MHz.

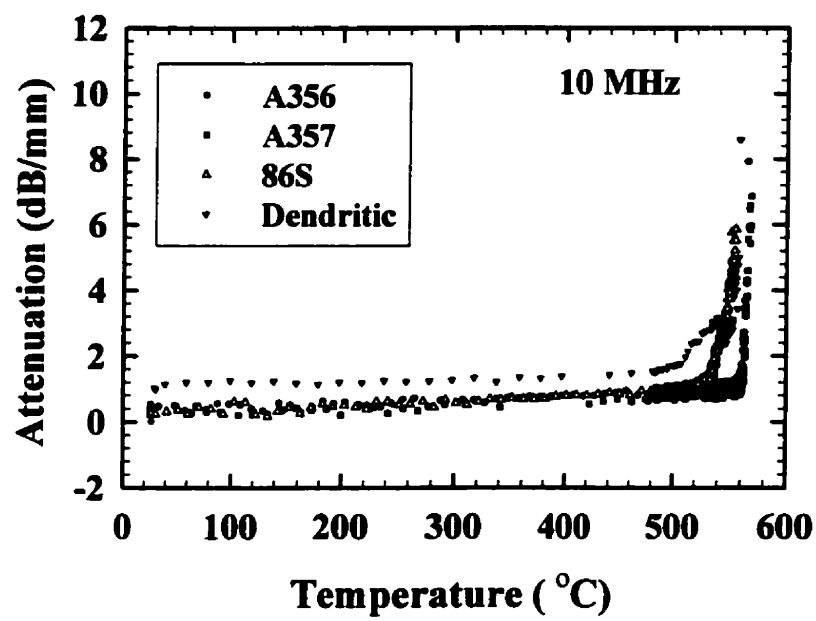

Figure 4-3: Attenuation measurements of four samples of aluminum alloys at 10 MHz.

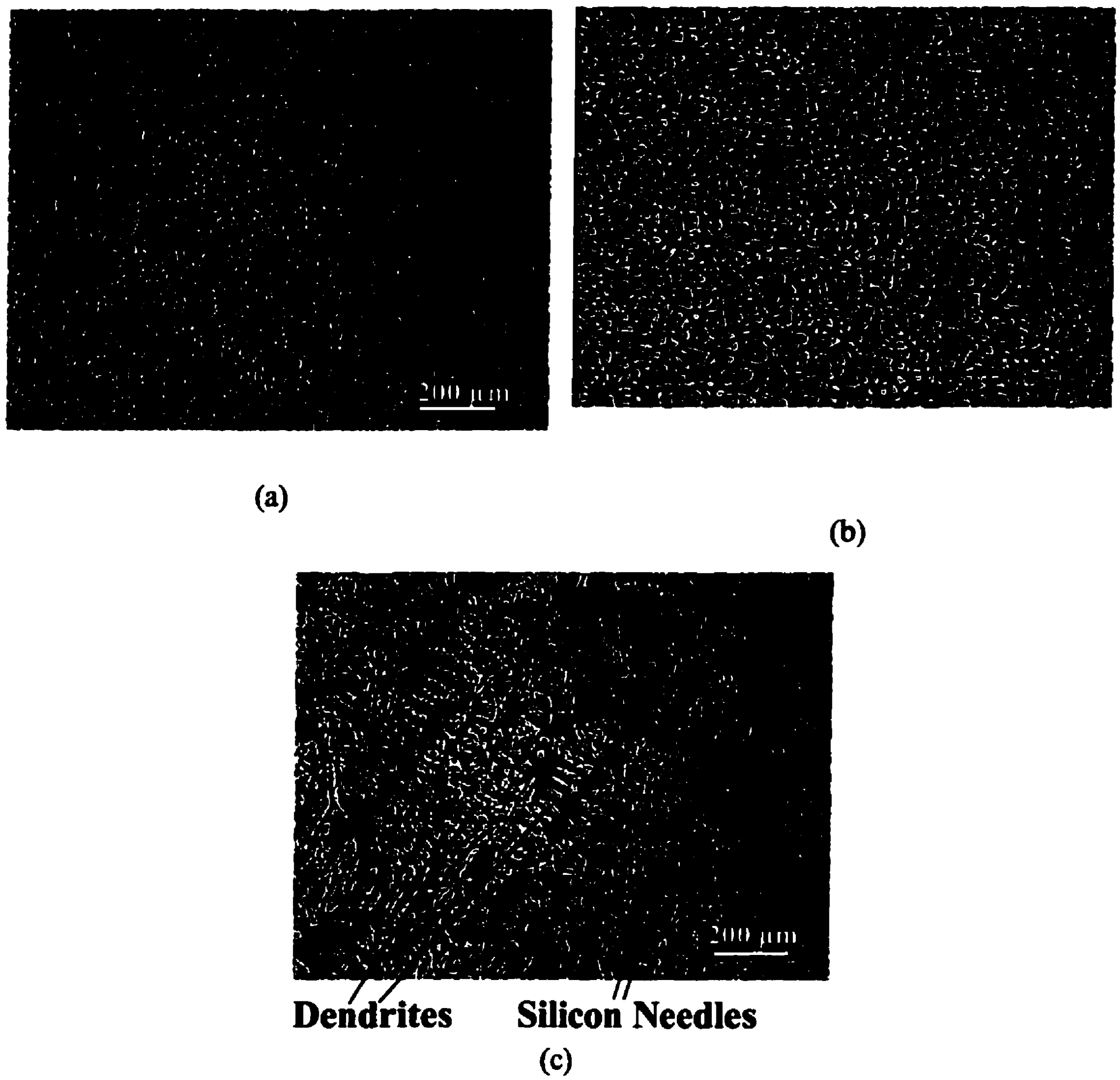

Figure 4-4: Microstructure of semi-solid cast part of: (a) A356 at 10 X, (b) A357 at 100X compared to (c) cast A356 dendritic.

Figure 4-2 shows an interesting behavior in the mushy zone, where both liquid and solid coexist; the ultrasonic longitudinal wave velocity changes abruptly and falls more than 1200 m/s within about 20 °C. This means that if one can measure the velocity accurately (±1 m/s is typical), then the temperature and the associated solid-liquid fraction information may be obtained with high precision. It is well known that the solid-liquid fraction is an important parameter for SS processing. Furthermore, this abrupt change in the velocity versus the temperature curve for thixotropic A356 and A357 implies that during the cooling stage of the SS process, the solidification front of the part in the die may be monitored because when the velocity has an abrupt change the density and, consequently, the acoustic impedance which is the product of the density and velocity, have both an abrupt variation. Such an abrupt change causes an additional reflected ultrasonic echo during the in-line ultrasonic monitoring. This phenomenon has been observed during injection molding of semi-crystalline polymers in which the velocity versus temperature curve has a similar abrupt change near the melting temperature [62]. We do not expect that the solidification front for thixotropic 86S and dendritic Al can be as easily monitored due to the smoother change near the melting point in the velocity versus temperature curve.

Figure 4-3 indicates that ultrasonic attenuations in the thixotropic billets are about 0.8 dB/mm less than that in the dendritic alloy up to 500°C. We also carried out the same laser-ultrasonic measurement for two SS cast parts; one was the A356 and the other one was the 86S. The velocities and attenuations profiles versus temperature of these samples are very similar to those of corresponding billets shown in Figure 4-2 and Figure 4-3. Therefore, ultrasonics can provide us a mean to determine whether the processed part has the desired thixotropic structure or not [66].

However, when the sample starts to soften, it is not possible with the configuration used to measure the sample thickness accurately. Therefore, we did not continue the velocity and attenuation measurements above the value of around 575°C as shown in Figure 4-2 and Figure 4-3. Furthermore, the thermocouple, which is spot weld to the sample, used to measure the temperature may detach itself when the material begins to melt. This is another reason for the measurement limit of around 575°C. A new ultrasonic sensing geometry is being considered in order to remedy such a drawback and allow us to obtain temperature readings higher than 575 °C.

4.2 Magnesium Alloy, AZ91

Tests were also made for the magnesium (Mg) alloy samples of a dendritic billet of AZ91. There were no available thixtropic AZ91 billets for the laser-ultrasonic measurement due to limited quantities although several were made by CANMET for in-line ultrasonic monitoring of SS die-casting process. All results were similar; therefore, only the result with the highest measured final temperature is shown. In this sample, the thermocouple is not spot welded but, instead, small holes are made to accommodate the Nickel-Chromium and Nickel-Aluminum wires of the K type thermocouple. The holes were made to help the thermocouple withstand higher temperature because the spot welds were melting at high temperature and no more reading could be made. The composition of the dendritic AZ91 Mg alloy is given in Table 4-2. For the Mg, because of a better understanding of the Gleeble system and its capacities with the analysis of samples (few trials), the heating procedure can be modified and shortened. Therefore, the sample was heated at a rate of 5°C per second till 400°C and, thereafter, at 1°C per second until the ultrasonic signal from the laser could not be analyzed anymore because of the high attenuation of the material at those high temperatures and/or the detachment of the thermocouple. In this case, the maximum value has been reached at a temperature of 490 °C.

Table 4-2: Composition of the magnesium alloy AZ91.

Magnesium Alloy	Elements (%wt)								
	Mg	Si	Fe	Cu	Mn	Al	Zn	Ti	Others
AZ91	Balance	0.3	---	0.1	0.13	8.1-9.3	0.4-1	---	0.31

Figure 4-5 and Figure 4-6 show the measured ultrasonic, ultrasonic velocity and total attenuation respectively for the dendritic AZ91 sample. The frequency chosen for the comparison is also 10 MHz. The sample used had a rectangular shape with the following dimensions: 31.3 mm by 105.4 mm and 6.64 mm thick. This new geometry permits the abolition of the sample holder and allows a more uniform temperature distribution and a better thickness control in the sample during the heating process. Ultrasonic velocity and attenuation were measured using the first and second round trip echoes traveling through the sample thickness, as it was done for the Al alloys samples. It is found that the velocity and attenuation of the sample have a smooth variation from 380°C up to the final value of 490°C.

In Figure 4-5, we can also see that there is a change of slope at about 440-450°C. To determine the meaning of the slope change at around 450°C, a phase diagram (DSC curves) of the material at room temperature to evaluate the phases in the AZ91 sample is needed. It allows us to establish with more precision the phases present in the sample and their temperature range. Since Mg at high temperature would burn and cause fire, the safety regulations are strict. At present, since at IMI there is no sufficient protection environment for the DSC measurement of Mg or Mg alloys such as AZ91, DSC curves were not obtained. Therefore, we decided to approximate the dendritic AZ91 as a binary material made of Al-Mg for the explanation of the Figure 4-5. In Figure 4-7, for a Al content of 9%, the liquid-solid phase of a binary Al-Mg material is between 370-500°C. So, it could explain the smooth variation of the curve at around 370° and the sudden stop of the curve at 500°C and the detachment of the thermocouple. But it cannot explain the change of the slope at 450°C. Further investigation is needed with the help of the DSC curves and micrographs to validate the velocity curve of Figure 4-5. Figure 4-5 shows the same interesting behavior of a dendritic AZ91 as those of the Al alloys except that the measured drop is about a 1000 m/s within 90 °C.

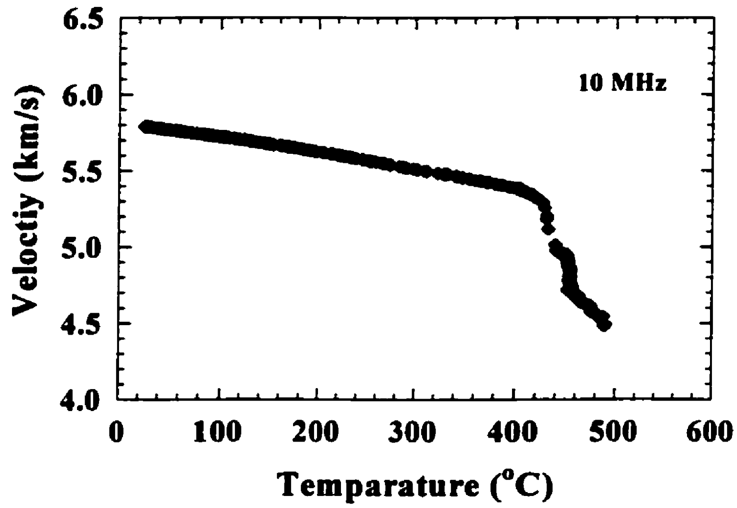

Figure 4-5: Velocity measurements of magnesium AZ91 before casting.

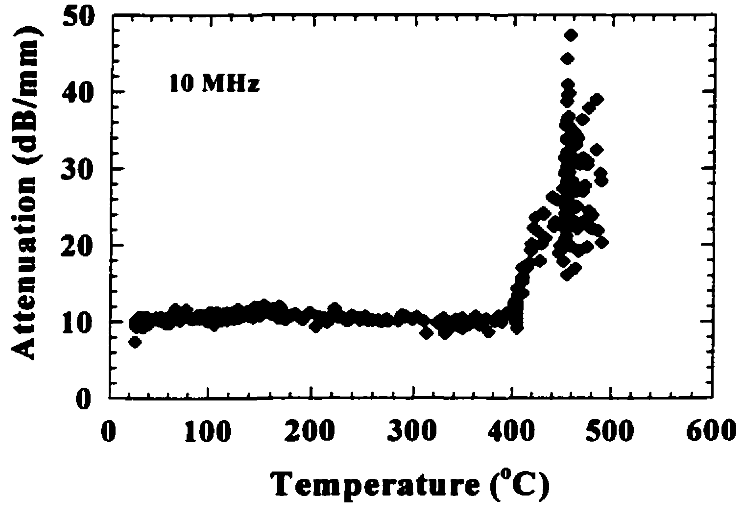

Figure 4-6: Attenuation measurements of magnesium AZ91 before casting.

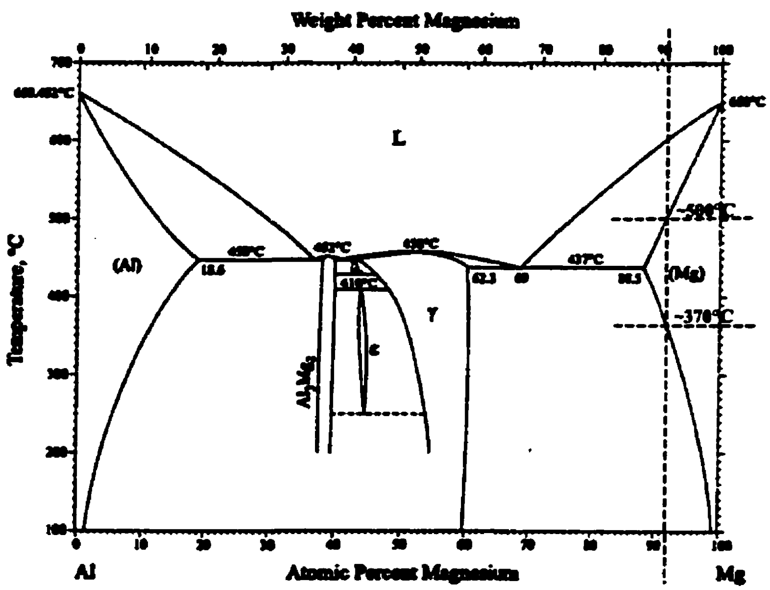

Figure 4-7: Al-Mg binary phase diagram from H. Okamoto, *J. Phase Equilibria*, Vol. 19, No. 6, pp. 598, 1998.

Figure 4-6 indicates that the ultrasonic attenuation in the Mg alloy AZ91 is higher than the Al alloys by almost 10 dB/mm up to 400°C; after this temperature, the attenuation of the Mg quickly goes up to 20dB/mm and, at a certain point, it reaches the 50dB/mm. This explains the limit in the analysis of the signal (high attenuation at high temperature). This high attenuation also reduces the ultrasonic monitoring sensitivity to detect the filling and solidification because the signal in the acquisition system could be small. This high attenuation is explainable when we look at how the samples were made. The samples were made from a magnesium billet that was produced by solidifying molten AZ91 in the sleeve of a die-casting machine. This method produces samples with high porosity and it is confirmed by the above testing method which gives high attenuation results.

At this moment, we have not been able to carry out the same measurement for a cast part of AZ91 because of the lack of availability of the Gleeble system and laser-ultrasonic system.

4.3 MMC, Gra-Ni® 6S:3G

For the dendritic MMC samples the same set-up and tests were made as those undertaken for the Al and Mg AZ91 alloy. All results were similar; therefore, like for the AZ91 magnesium alloy, only the results with the highest final temperature will be shown in this thesis. The composition of the Gra-NI® 6S:3G can be seen in Table 4-3. The sample was heated at a rate of 5°C per second till 400°C, thereafter at 2°C per second up to 500°C and finally at 1°C per second until 550°C, the temperature at which the thermocouple died. This heating procedure was established after a few trial of MMC and the thermocouples were placed in holes as mentioned in Section 4.2.

Table 4-3: Composition of the MMC Gra-Ni® 6S:3G

Aluminum Alloy	Elements (%wt)						
	Al	Si	Ni	Mg	Fe	SiC	graphite
Gra-Ni® 6S:3G	Balance	7.5	2	0.3	0.5	6	3

Figure 4-8 and Figure 4-9 show the measured ultrasonic velocity and total attenuation respectively for the MMC sample. The frequency chosen for the comparison is 10 MHz. The sample used was 15.57 mm by 117.45 mm and 2.05 mm thick. The ultrasonic velocity and attenuation are also evaluated using the first and second round trip echoes traveling through the sample thickness, as it was done for the Al and magnesium alloys samples. It was found that the velocity and attenuation of the sample have a variation different from those of the Al alloys listed in Table 4-1 and AZ91 samples. The results are more scattered than the two other alloys; this could be explained by the composition of the MMC. The presence of 6% of SiC and 3% graphite acts as scatterers in the signal that makes large differences in the results. Therefore, the general tendency of the curves should be considered and, if we do so, we can see the same general curve for the velocity as for the Al and magnesium samples. At around 550°C we can see the beginning of a drop in the velocity.

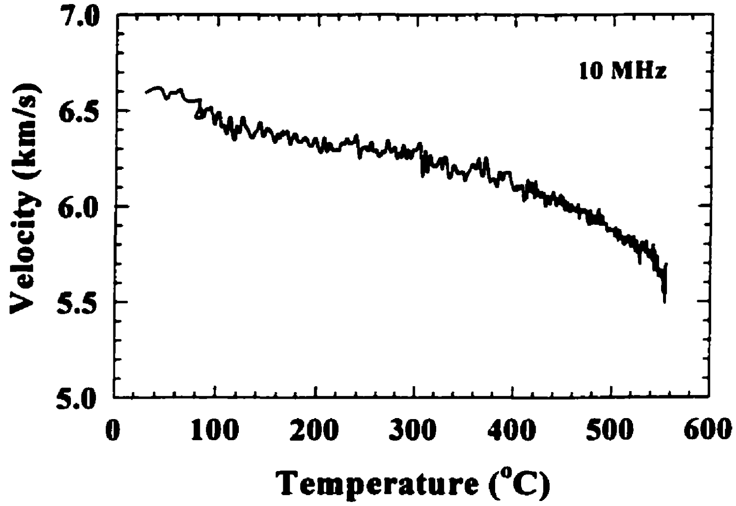

Figure 4-8: Velocity measurements of the MMC Gra-Ni® 6S:3G at 10 MHz.

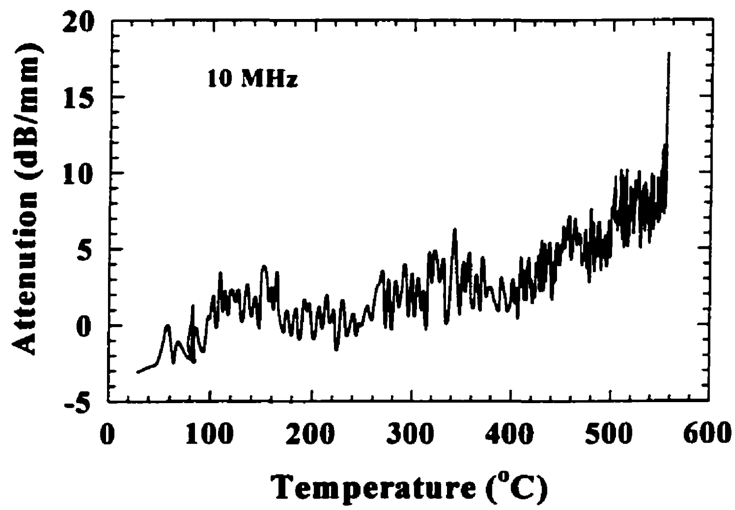

Figure 4-9: Attenuation measurements of the MMC Gra-Ni® 6S:3G at 10 MHz.

Figure 4-9 indicates that the ultrasonic attenuation in the MMC alloy is about the same as in the Al, at the beginning; but it reaches the limit point that we can measure, at about 550°C compared to the straight attenuation for the Al up to its own solidus point. After this melting temperature, the attenuation of the MMC quickly goes up as for the Al sample. As mentioned above, that could be caused by the scattering loss.

4.4 Summary

Laser-ultrasonic is a non-contact and non-destructive method that can be used to measure the ultrasonic properties of materials at elevated temperatures. In this chapter, the ultrasonic properties measured are the ultrasonic velocities and the attenuations for the thixotropic A356, A357, 86S, dendritic A356, dendritic AZ91 and the dendritic MMC Gra-Ni® 6S:3G from room temperature up to temperatures of about 575 °C. The samples were heated by a Gleeble thermal simulator. It was found that the ultrasonic attenuation at 10 MHz in the A356 thixotropic billets is 0.8 dB/mm less than that obtained with a dendritic one up to 500 °C. This difference increases above 500 °C. The velocities and attenuations of the thixotropic billets A356 and A357 have an abrupt change at around 565 °C whereas those of thixotropic 86S and dendritic alloy (A356) have a gentle variation at around 480 and 500 °C, respectively. For the dendritic AZ91 alloy, it was found that the ultrasonic attenuation at 10 MHz can reach values up to 50 dB/mm at high temperature due to the high porosity level in the sample. The velocities and attenuations of this dendritic Mg alloy sample have smooth changes at around 380 °C and a variation in the slope curve at around 450°C which need DSC curves and micrographs to explain. For the dendritic MMC, the ultrasonic attenuation starts at 3 dB/mm less than the thixotropic A356 around room temperature and gradually increases up to 550 °C and by the same time surpassing the A356. The velocity of the dendritic MMC starts at about 100 m/s over the thixotropic A356 at room temperature and gradually decreases up to 550°C, the limit of the measurement. Furthermore, the results are more scattered than for the others Al and Mg alloys due to the presence of scattering agents (6% SiC, 3% graphite).

It is concluded that velocity and the attenuation can vary for three different conditions: the microstructure, the porosity level and the composition of the material. We can see that the thixotropic (86S) samples have the same velocity and attenuation values when they are cast or taken from the billet. Therefore, ultrasonics can provide us with a mean to determine whether the processed part has the desired thixotropic structure or not. Furthermore, with the help of ultrasonic velocity curve made by the Gleeble heating system and laser-ultrasonic, the solid fraction, in thixotropic material, may possibly be determined. These ultrasonic properties provide a mean to monitor the evolution of the microstructure of the part during SS process.

Chapter 5: Ultrasonic monitoring of Semi-solid die-casting

As mentioned in the first chapter, the quality of Semi-Solid (SS) cast parts is dependent on the slurry rheology and die filling characteristics. Since this process involves high pressure and high temperature as well as the corrosive nature of the molten metals, there are practically no sensors available to perform in-line monitoring of the properties of cast parts. The objective of this investigation is to introduce ultrasonic sensors and techniques for monitoring such a semi-solid die-casting process. End of filling of the die, average temperature variation in the thickness of the die and cast part, part detachment or gap formation and solidification of the melt will be studied. The ultrasonic reflection coefficient at the interface between the clad buffer rod (CBR) and the part, velocity and attenuation in the part and time delay in the CBR will be used for this study. At present, all die cast processes use machine control. Furthermore, as mentioned before, the die is filled-up with pressure and temperature sensors. It is our other objective to monitor the ultrasonic properties such as velocity and attenuation of the cast part for possible process control.

In this section of our research, different types of billet materials having different microstructures were tested: aluminum (Al) alloys for SS processing (A356 and A357), magnesium (Mg) alloys AZ91 and dendritic Metal Matrix Composite (MMC) Gra-Ni® 6S:3G. As far as the Mg AZ91 is concerned, three different microstructures were used: (1) a dendritic AZ91 as mentioned in Chapter 4 produced by Performag; (2) a thixotropic billet (primary phase is made up of rounded rosette particles) of Mg made by CANMET; and (3) another Mg billet from CANMET but with a finer thixotropic microstructure (smaller grain size).

5.1 Experimental Set-up

Experiments were carried on with a 600-ton Buhler die-casting machine as shown in Figure 5-1. The CBR sensor shown in Figure 5-2, and described in chapter 2 of this thesis, was used to perform in-line ultrasonic monitoring. To sum up briefly what was presented before, the CBR consisted of a steel core and a stainless steel cladding and was inserted into the die wall as shown in Figure 5-2. The probing end of this sensor was flushed with the cavity of the die (see Figure 5-3). It is flushed because the hole was drilled at an angle of 2° which mould the cavity surface that is at an angle of 2° to facilitate the retrieval of the cast part. The ultrasonic transducer (UT) side of the probe was water cooled to less than 50°C. This UT served as transmitter as well as receiver during the pulse-echo measurements. Furthermore, the commercial UT used in our experiments was a 10 MHz broadband made by Panametric and it will always be the case except when mentioned otherwise.

In the experiments, the billets which were used as feedstock for SS die-casting, were cast after reaching a temperature of about 585°C inside an induction heater. The billets were then injected into the die, of which the temperature was maintained as close as possible to 250°C, by the plunger of the die-casting machine to produce a part. The external and internal views of a cast part are shown in Figure 5-4 and Figure 5-5 respectively. The location of the ultrasonic probe, the location of conventional temperature and pressure sensors, as well as the position of the biscuit are also indicated.

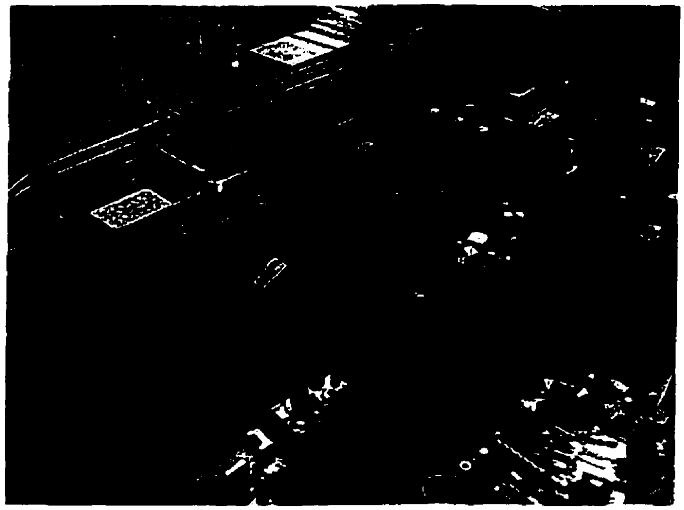

Figure 5-1: Photo of the 600-ton Buhler die-casting machine.

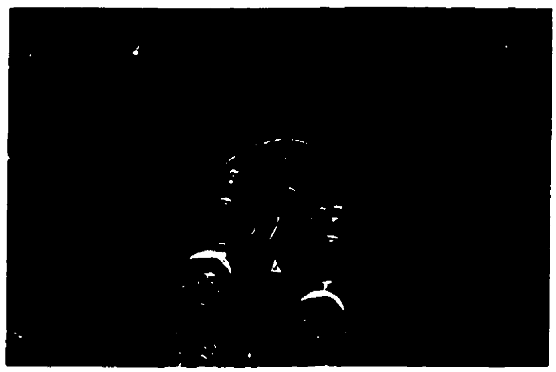

Figure 5-2: Insertion of the CBR in the in-mobile mold.

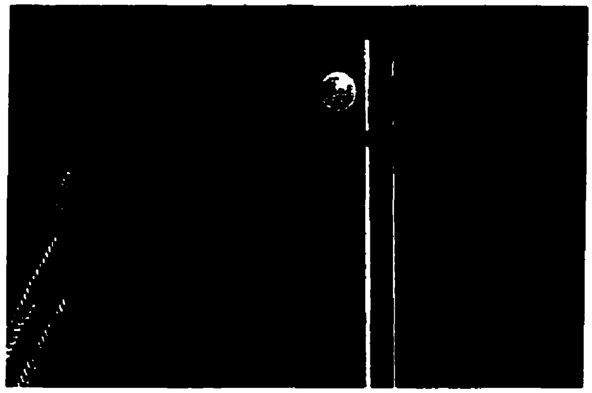

Figure 5-3: Sensor is flushed to the cavity when the insertion is completed.

Figure 5-4: External view of the cast part with sensors.

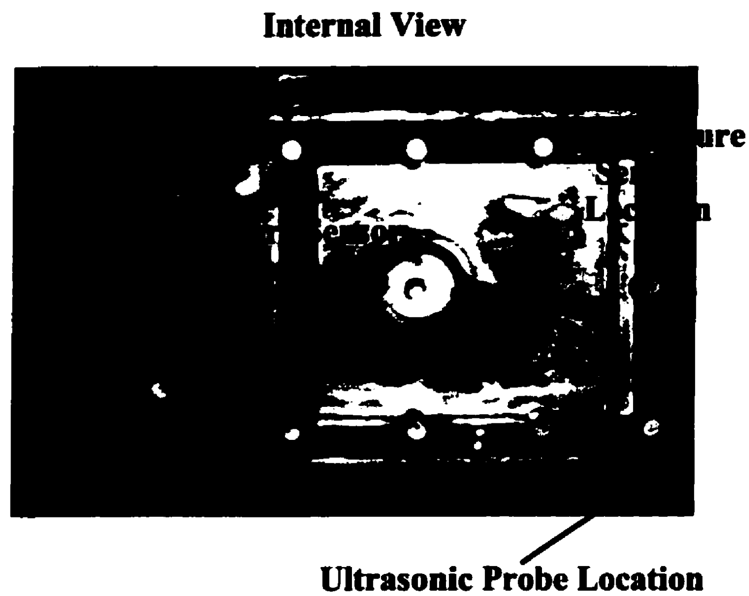

Figure 5-5: Internal view of the cast part with sensors.

The results presented here are typical information retrieved from the analysis of more than 50 casting experiments over many days. In fact, no more than six experiments a day could be achieved due to the difficulty of the induction heating of the billets, the time required to heat the die and problems encountered during casting such as sticking and frozen material in the gate. The majority of the experiments were performed with Al A356 and A357, and a few with the MMC and the Mg.

5.2 Aluminum alloys

In this section, we show the results of the aluminum alloy A356 and A357. However, due to their similar composition and microstructure as shown in Table 4-1 and Figure 4-4; there is no difference in the signals and analysis between these two alloys and the results of our research are similar whether they come from the A356 or the A357 aluminum alloy. As a consequence, only the results of the A356 will be presented in the following paragraphs.

Figure 5-6 and Figure 5-7 show the snap shots of recorded ultrasonic echoes in the probe and cast part during the first second and the entire injection period of one cast cycle respectively. In Figure 5-6 the recording was achieved at every 0.027 second. However, for a time window of 8 μs in the desired ultrasonic signal, the fastest acquisition speed that we could achieve was 0.003 second per trace at a sampling rate of 50 MHz and a for a recording time of 30 seconds. We clearly see in Figure 5-6 the solidification of the cast part as the time delay between L^1 and $L^1{}_2$ decreases.

Even if it is hard to see in Figure 5-6 and Figure 5-7 due to the size of the figures, the following relationship can be derived; the attenuation is nearly proportional to the square of the operating frequency. This is because of the natural ultrasonic attenuation in the 103.66 mm long steel CBR and the 4.7752 mm thick cast part. We can see that the number of cycles within a fixed time frame such as 1 μs is gradually decreasing in the waveforms of L^1, $L^1{}_2$ and $L^1{}_4$. This means the center frequency of the waveform is shifting to a frequency less than and away from 10 MHz, which is the center frequency of the broadband generating and receiving UT.

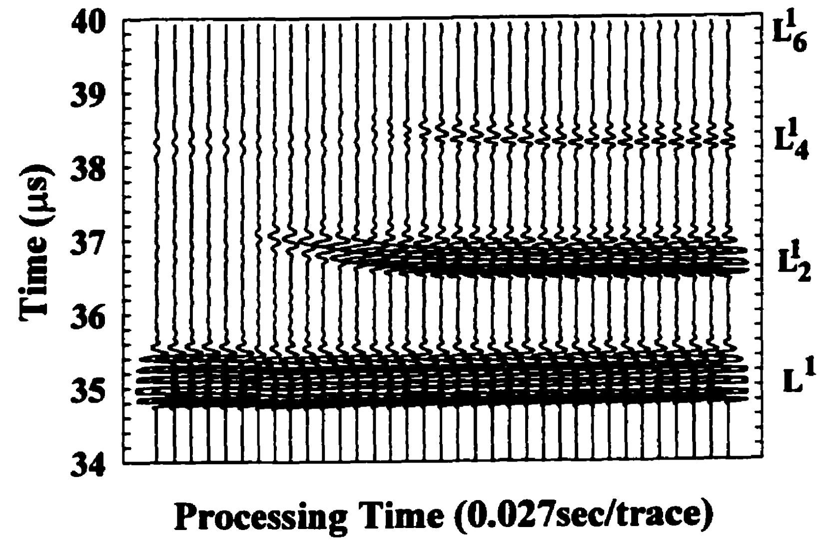

Figure 5-6: Recorded ultrasonic echoes in the probe and cast part during the first second of injection.

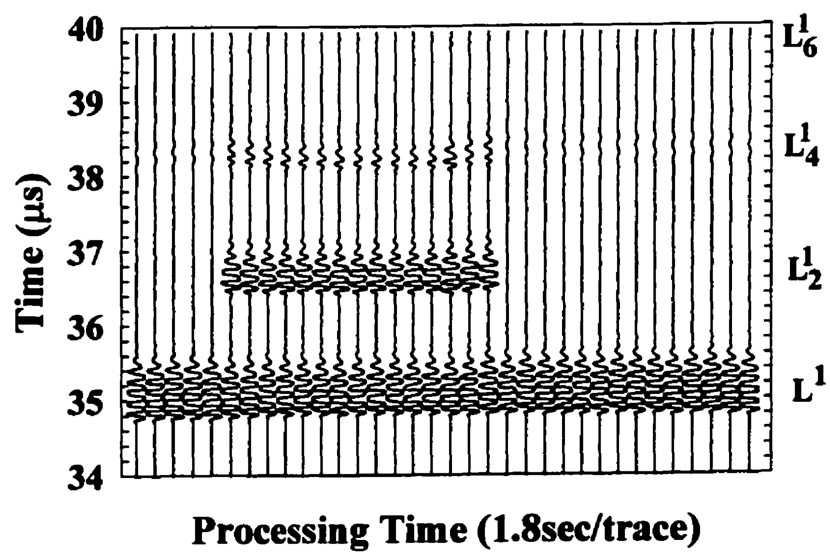

Figure 5-7: Recorded ultrasonic echoes in the probe and cast part during one injection cycle.

The locations of the cavity pressure and temperature sensors in the die are shown in Figure 5-4 and Figure 5-5 respectively. These conventional sensors were not used in [24,62]. It has to be noted that die-casting process is under high pressure and the molten aluminum is corrosive. The cavity pressure sensor was installed behind the ejection pin of the die. Situations such as the bending of the ejection pin may often cause difficulties in obtaining reliable pressure readings. Therefore, in Figure 5-8, the relative change of the pressure rather than the absolute value is used. Since no rugged temperature sensor was available, the sensor head of a K-type thermocouple (TC) was installed (embedded) 1.27 mm away from the cavity surface in order to avoid erosion and damage to the temperature sensor. However, such a distance causes a slower temperature sensing response. The measured result was recorded and is shown in Figure 5-9. In Figure 5-8 and Figure 5-9 the time A indicates the completion of the fast filling stage under high pressure. At time C, the biscuit end, which contains oxides, was cut off as part of the demolding process and the pressure was released as seen in Figure 5-8; however, the cast part was still kept in the die. At time D, the die was opened and the part was ejected.

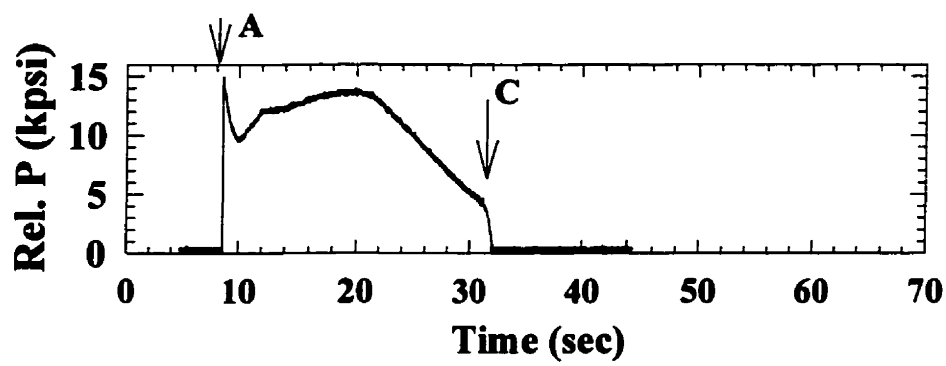

Figure 5-8: Measured cavity pressure profile acquired with a serial recording set-up.

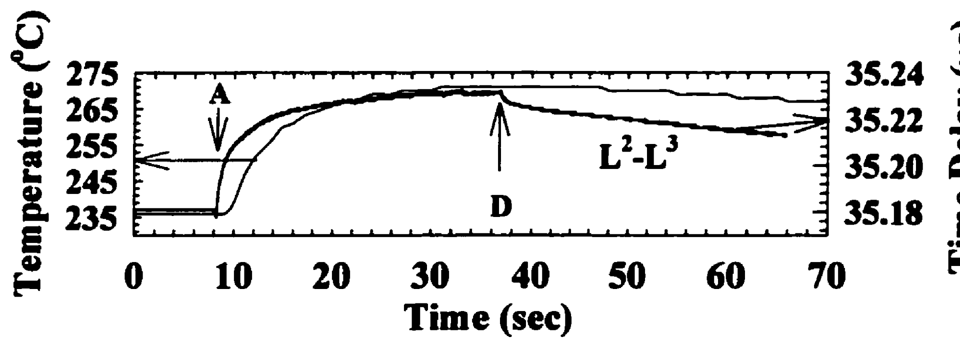

Figure 5-9: Measured die temperature using a thermocouple. The ultrasonic time delay in the CBR is between echoes L^2 and L^3 acquired with the serial recording set-up.

When at time A the cast part reaches the die region where was embedded the conventional temperature sensor, the measured temperature first increases. After the part ejection at time D, the temperature decreases because of the cooling of the die (see Figure 5-9). Similarly, when the alloy enters the cavity and reaches the ultrasonic probe, heat is transferred into the probe made of steel. For solid steel the ultrasonic velocity is lower at higher temperature, resulting in an increase in the time delay. The change of the time delay in the buffer rod (i.e. between the echoes L^2 and L^3 in Figures 2-1) is given in Figure 5-9. In this case, L^1 was not chosen because it was saturated due to large signal amplification at the receiver. We can see that the rise and decay time response of the time delay variation measured by the CBR is faster than that of the temperature measured by the embedded thermocouple which was at 1.27 mm beneath the cavity surface. This is due to the fact that the probing end of the buffer rod was flushed with the cavity wall and directly in contact with the hot viscous semi-solid part. This means that the CBR probe can detect the variation of the temperature of the die with a faster response than that of a conventional thermocouple. The correlation of the time delay in the buffer rod versus the actual temperature of the die is being studied; however, because of the cooling system on the CBR, the measured temperature will be underestimated.

Figure 5-10 and Figure 5-11 show the amplitude variations of the echoes L^2 and L^2_2, respectively, which relate to the reflection coefficient at the BR-cast part interface and the transmitted energy into the cast part. L^1 was not chosen because it was saturated. The general rule for the selection of these echoes such as L^1, L^2 or L^3 is discussed in [67]. As expected, at time A the amplitude of the echo L^2 decreases whereas that of L^2_2 increases because the ultrasonic energy is transmitted into the cast part. It means that the amplitude variation of the echoes L^2 and L^2_2 at the time A in the figures can be used to detect the completion of the fast filling stage under high pressure. As mentioned earlier, at time C, since pressure was released and the part was kept in the die, the ultrasonic coupling between the probing end and the cast part reduces; thus, the amplitude of L^2 (reflection coefficient) increases. At this moment, due to the detachment of the cast part at the interface between the cast part and the mobile die shown in Figure 3-1, no energy was transmitted from the cast part to the mobile die; thus, the amplitude of L^2 increases (more details in chapter 3). It is believed that at time C the ultrasonic probe which was embedded in the in-mobile die and the cast part remained in contact.

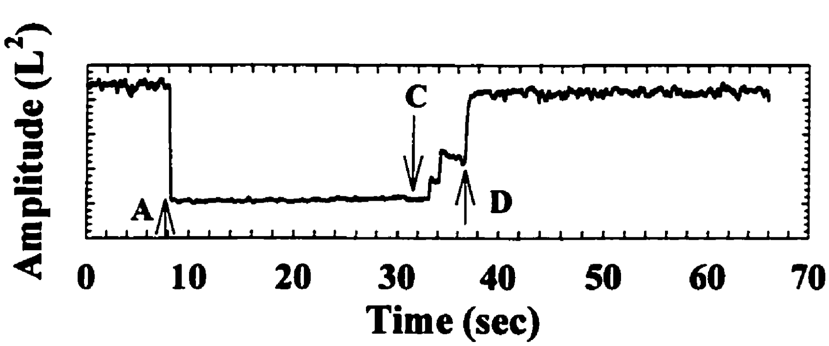

Figure 5-10: Amplitude of signal of L^2 measured with the serial system.

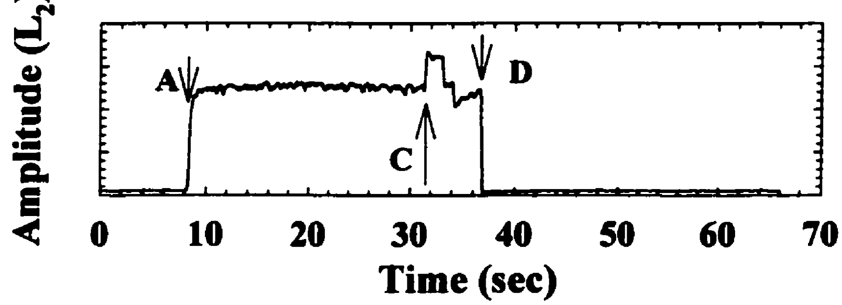

Figure 5-11: Amplitude of signal of L^2_2 measured with serial system.

As the die cast process time evolves from C to D, the ultrasonic coupling at the BR-cast part interface deteriorates; the amplitude of L^2_2 also decreases. In the meantime, the amplitude of L^2 continues to increase. At time D, when the cast part is ejected, the amplitude of L^2_2 decreases to zero and the amplitude of L^2 returns to the amplitude reached before the injection of the viscous semi-solid alloy, but with a little variation due to temperature effects on the rod and the ultrasonic couplant. This means that ultrasonic probe can monitor the completion of the filling, opening for the biscuit cutting, detachment from the die and ejection of the part.

The Figure 5-12 shows the amplitude of L^2 measured with the multiple recording system. At time A, we can draw the same conclusion as for the serial recording (Figure 5-10). In fact, the only difference between the two measured amplitudes is the time span of both recording system acquisitions. In Figure 5-12, we can only see the beginning of the process. The advantages and disadvantages of both recording have been discussed in Chapter 2. The multiple recording will not be shown furthermore because it represents only a small picture of the process compared to the general picture that the serial recording can provide. This decision has been taken to facilitate the reading of the thesis and no important fact was left behind.

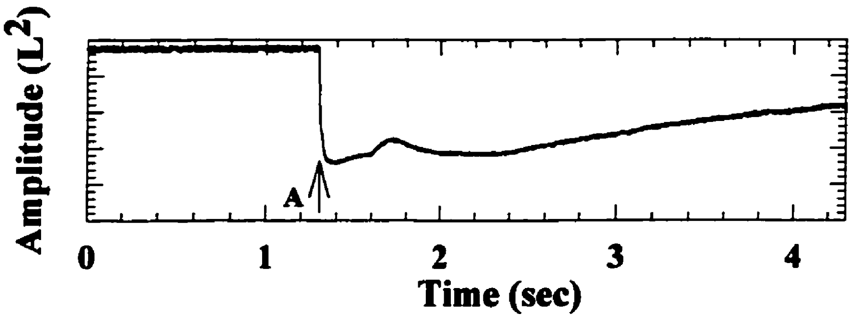

Figure 5-12: Amplitude of signal L^2 measured using the multiple recording system.

At the ultrasonic probe position, the cavity gap or the part thickness, h, was 4.7752 mm. From Figure 5-6 and Figure 5-7 we can obtain the time delay, τ, between echoes L^1 and L^1_2 , that is, the first round trip time in the cast part. Thus, the ultrasonic velocity in the cast part at the probe location can be calculated as in Chapter 3 and is given in Figure 5-13. This velocity change may be related to the average temperature in the cast part, which could be a crucial parameter for process optimization. In Chapter 4, the variations of ultrasonic velocity and attenuation as a function of temperature in a heating process were reported for the same SS A356 and other alloys as used here for casting. Since at time C no pressure was applied to the part, the ultrasonic velocity of 5970 m/s shown in Figure 5-13 can be correlated with the data in Chapter 4 at about 500°C. It must be noted that here the part goes through a solidification process but not a heating process as reported in the previous chapter.

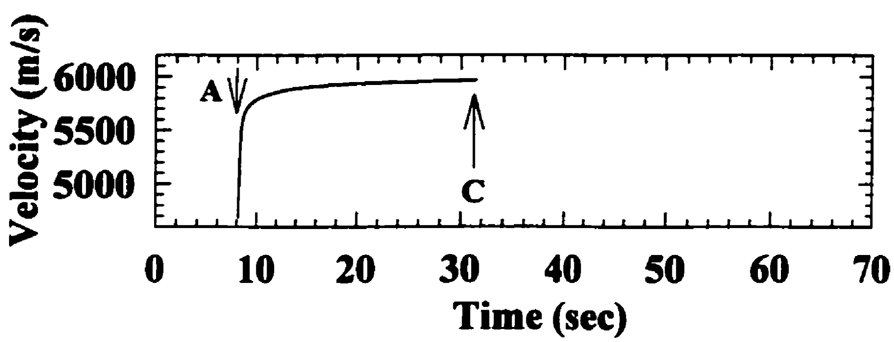

Figure 5-13: Measured ultrasonic velocity of the cast part A356.

As mentioned in the previous chapter, the velocity and the attenuation can vary for three different conditions: the microstructure, the porosity level and the composition of the material. Some investigation needs to be done to confirm these assumptions.

The calculation of ultrasonic attenuation coefficient in the cast part is given in Chapter 3 Section 3.5 and the results are shown in Figure 5-14. In this calculation, the acoustic impedance matching condition at the interface between the probing end and the cast part (steel CBR-cast part interface) was assumed to be identical to that at the interface of the cast part-mobile die made of steel. Planar wave propagation in the cast part was also assumed.

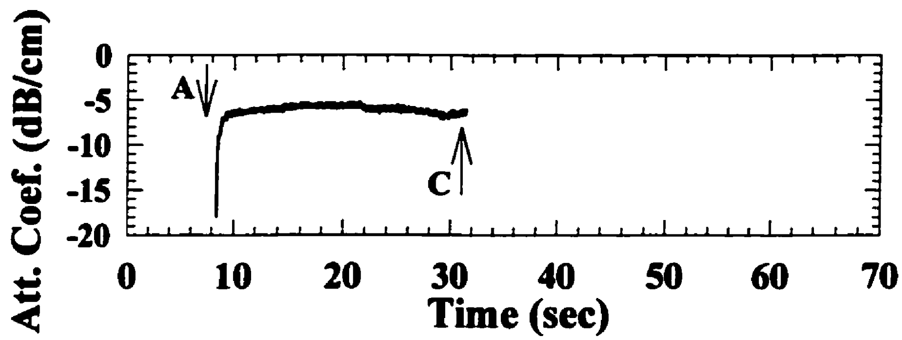

Figure 5-14: Measured ultrasonic attenuation of cast part A356.

Figure 5-15 shows the external view and defects of a cast part in a cold shut situation. Cold shuts are created when two flow fronts solidify before they could impinge together, creating a hole or a surface crack. Even though at the ultrasonic probe location the part was filled, because of the reduction of the pressure caused by the cold shut defects, the measured amplitude variation of the reflected echo from the BR-cast part interface, L^2, shown in Figure 5-16, was quite different than that shown in Figure 5-10 and Figure 5-4, the L^2 and photo of a good part, respectively. This means that the presented ultrasonic method has the ability to monitor the cold shut and incomplete filling of the part (short shots). For the short shots, no signal was acquired because the metal was not reaching the location of the probe (location of the probe is almost at the end of filling of the part).

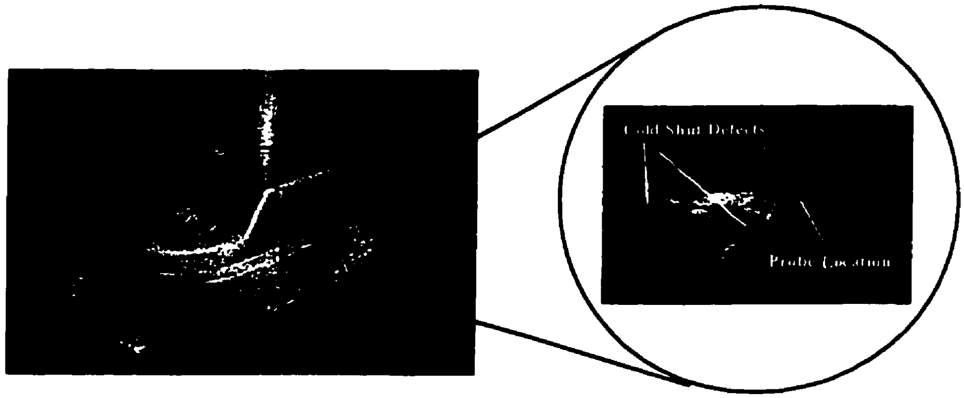

Figure 5-15: External picture of the part with a cold shut defect.

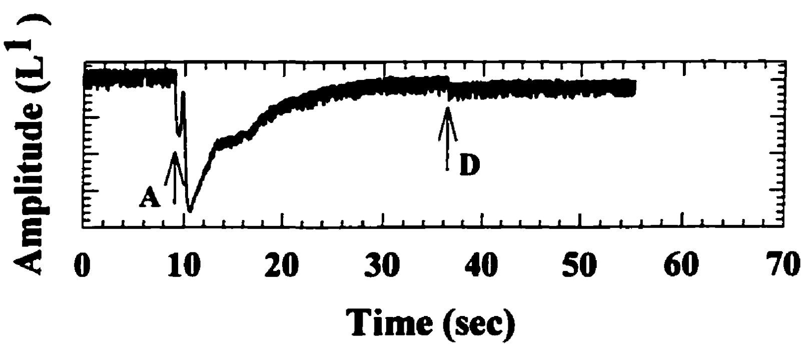

Figure 5-16: Amplitude of the signal of the part with a cold shut.

5.3 Magnesium Alloys

Magnesium alloys are one of the most desirable raw materials in die-casting applications. There are several factors that make Mg alloys an excellent material for manufacturing parts for the automotive, electronics, telecommunications and other industries. Its lightness, about 30% lighter than aluminum, its good EMI shielding, its high stiffness over weight, its abundant quantity and commercial availability and its ability to produce thixotropic structures. One negative aspect of magnesium is the security related to the casting. It is well known that Mg catches fire when air enters in contact with it at elevated temperatures

In this section, we want to demonstrate the CBR's capacity to monitor Mg alloy AZ91 part during casting. The different billets, as mentioned earlier, are cast in the same die with the same embedded ultrasonic probe. The sensing and data acquisition techniques are the same as described previously. However, the billet was heated to 583°C and soaked for a few seconds at this temperature before injection in order to let the entire billet reach a uniform temperature. This soaking is required because Mg has a poorer thermal conductivity than Al. It permits a more uniform temperature throughout the billet when it is injected into the die. In the heating process, some SF_6 gas was distributed on the billet for security reasons. Furthermore, the conclusions are similar to those related to Al alloys presented in the previous section. One can find, in the signals, the same part detachment, die filling, release of pressure and solidification. The only difference between Al and Mg alloys is the quality of the signal as shown in Figure 5-17. The signals for Mg are more noisy than those for Al. This is due to the fact that the condition of wetting, impedance matching, between the steel core of the CBR and the cast part is poorer in magnesium case. The lack of matching created a jittering like graphic as can be seen in Figure 5-18. This Figure is a representation of the amplitude of the signal; but, as we can see, ultrasonic can still monitor the parameters mentioned above, but with reduced sensitivity. In this particular Figure, we can see a gap formation between the point A and C.

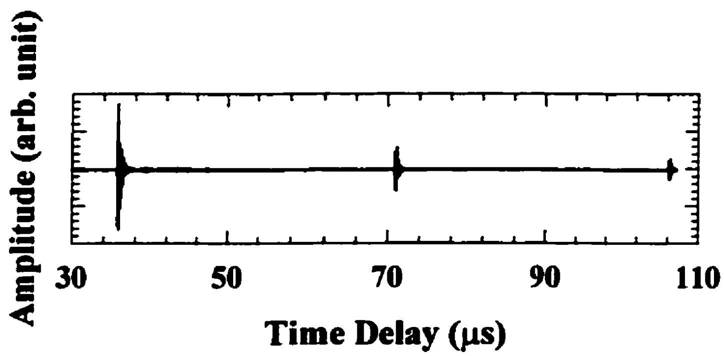

(a)

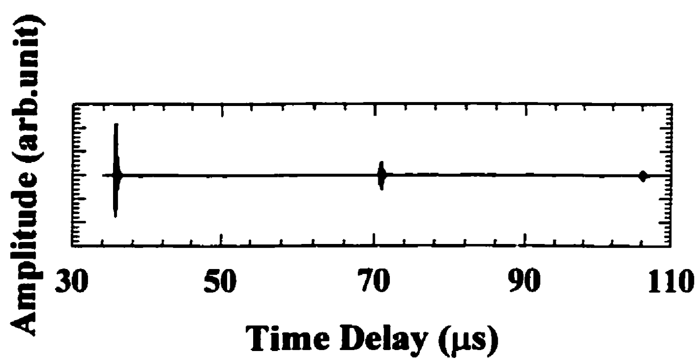

(b)

Figure 5-17: Signal from (a) the magnesium part and (b) aluminum A356.

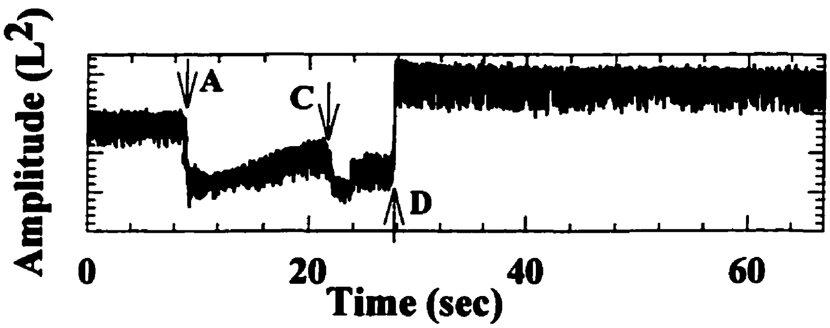

Figure 5-18: Measured amplitude of the signal of L^2 of the globular CANMET billet.

Figure 5-19 to Figure 5-21 show the measured ultrasonic velocities of the cast part of the three kinds of microstructures found in the magnesium billets: dendritic from Performag, globular from CANMET and the rosette from CANMET (smaller grain size). One must note that the velocity profile of the solidifying SS A356 part in Figure 5-13 is different from the velocity profile of the Performag part shown in Figure 5-19. During the solidification process the initial change of velocity in the SS A356 part is an abrupt change and, thereafter, it quickly reaches nearly a constant. However, in the case of the Performag billet, the velocity change is gradual and no sharp change is displayed; but we can see the same phenomenon with the CANMET billets as with the SS A356. This is completely normal because the Performag billet has a dendritic microstructure compared to a SS microstructure for the CANMET ones (thixotropic). Also at time C, where we do not apply any pressure to the three different microstructures, the ultrasonic velocities are 5518 m/s, 5646 m/s and 5708 m/s, as shown in Figure 5-19 to Figure 5-21. We can see that finer are the rosettes the higher is the velocity. Therefore, when we look at the microstructure of the three magnesium cast parts (Figure 5-22) we can say that the CBR can determine the kind of microstructure cast. It can differentiate a dendritic microstructure from a thixotropic one. Furthermore, the CBR can help determine the size of the microstructure; but, for that, it would need good calibration curves of the ultrasonic speed as a function of the temperature and the microstructure used.

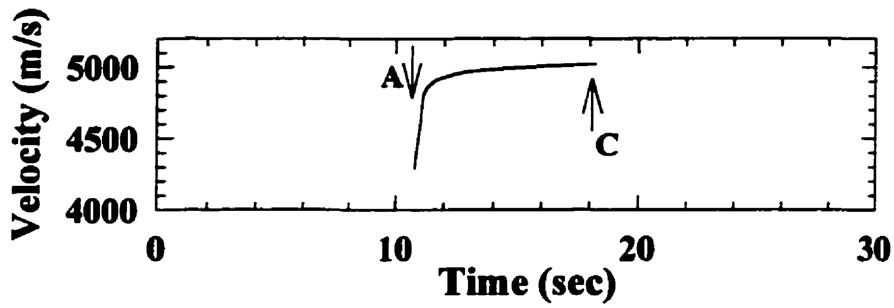

Figure 5-19: Measured ultrasonic velocity of the dendritic AZ91 billet made by Performag.

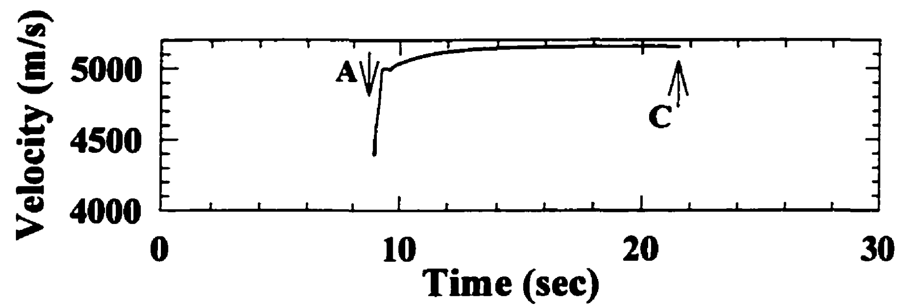

Figure 5-20: Measured ultrasonic velocity of the globular AZ91 billet made by CANMET.

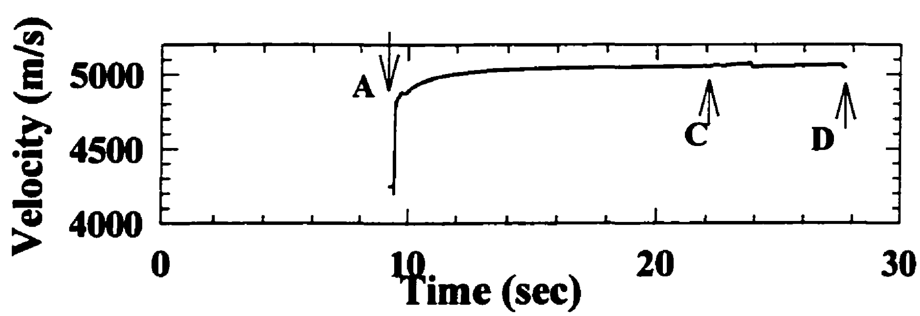

Figure 5-21: Measured ultrasonic velocity of the rosette AZ91 billet made by CANMET.

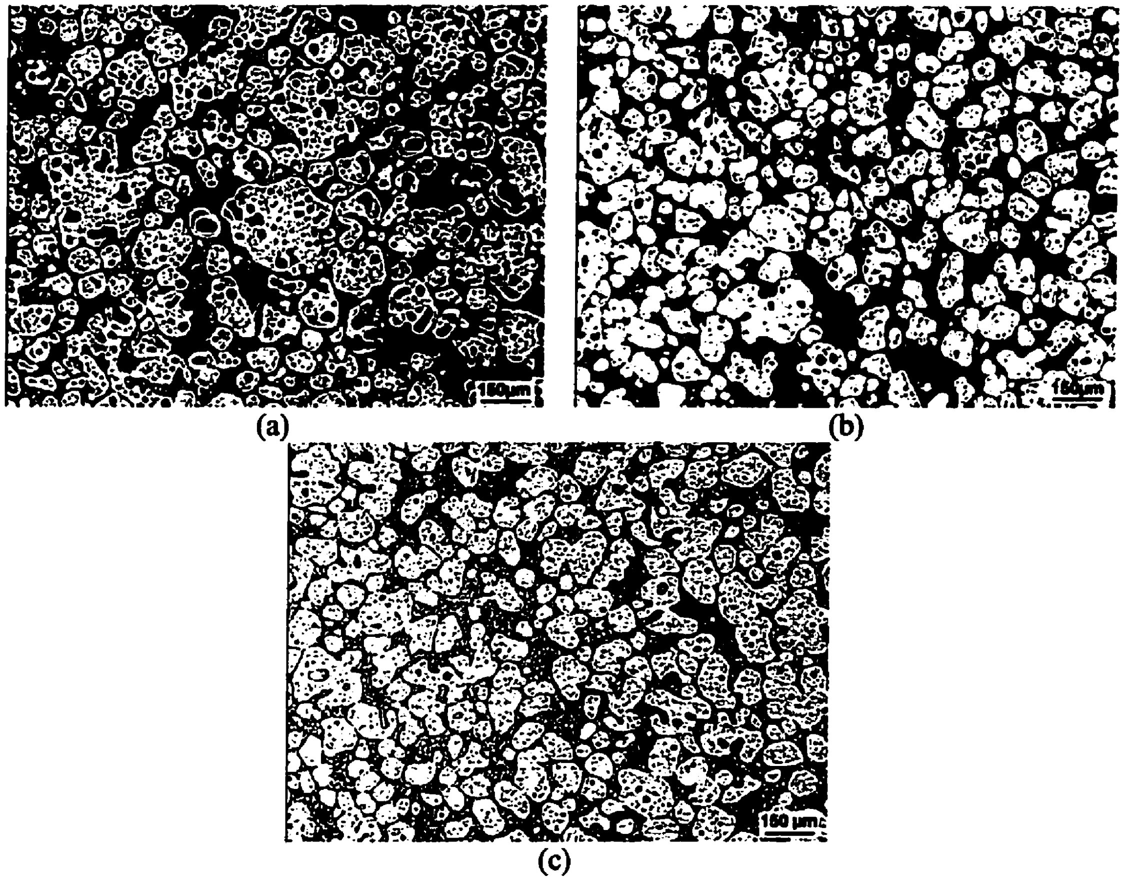

Figure 5-22: Micrograph of the microstructures of (a) Performag, (b) CANMET and (c) finer CANMET.

The measured attenuation coefficient in the cast AZ91 parts is given in Figure 5-23 to Figure 5-25 for different microstructures. It is observed that the attenuation coefficient in this alloy cast part changes depending on the microstructure. As mentioned in the previous section, the velocity and the attenuation can vary for three different conditions: the microstructure, the porosity level and the composition of the material. Since, the composition is the same for all three parts the differences in the curves can be explained only by the microstructure and the porosity. Figure 5-23 to Figure 5-25 can be explained by the high porosity of the parts. The Performag (dentritic) part has the least porosity at the CBR position; this is the reason why its attenuation is so low compared to the two others. Furthermore, Figure 5-24 shows a drop in the attenuation; this is due to the gap formation during the cooling and not due to any other factors. So, only the beginning of the curve should be considered for the comparison (up to about the 23 dB). In Figure 5-25, the attenuation starts at about 60 dB compared to Figure 5-24 which started at 47 dB. This is because the microstructure of Figure 5-25 is rosette form compared to globular form for Figure 5-24.

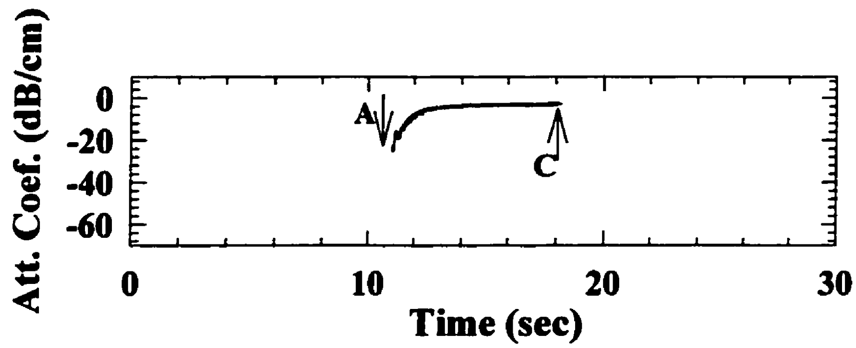

Figure 5-23: Measured ultrasonic attenuation of the dendritic AZ91 billet made by Performag.

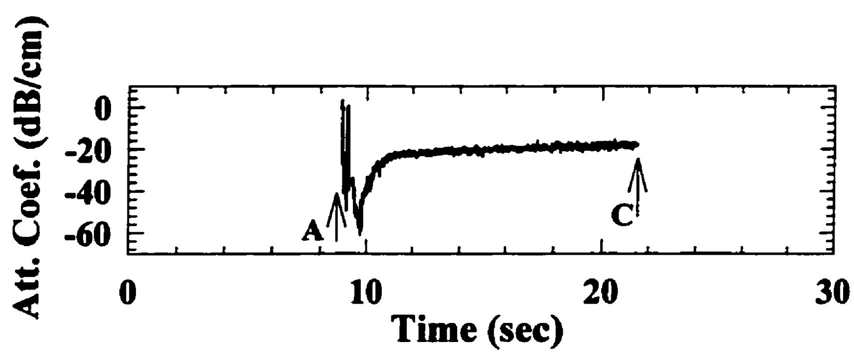

Figure 5-24: Measured ultrasonic attenuation of the globular AZ91 billet made by CANMET.

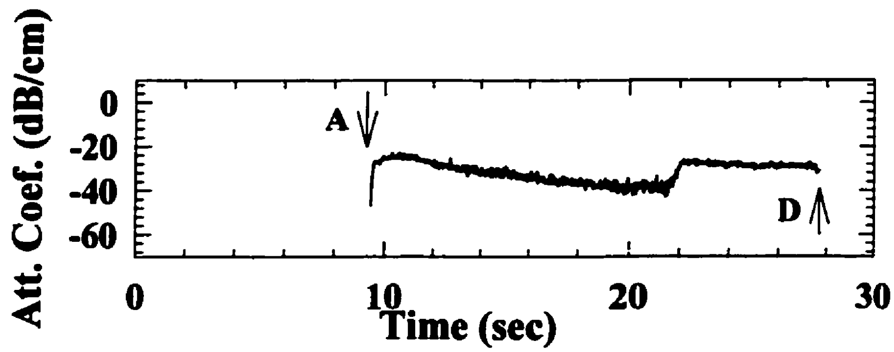

Figure 5-25: Measured ultrasonic attenuation of the rosette AZ91 billet made by CANMET.

5.4 Metal Matrix Composite Alloy

As mentioned earlier, in order to demonstrate that the ultrasound can probe different material properties, dendritic Gra-Ni® 6S:3G MMC billets were cast in the same die in which the same ultrasonic probe was embedded. The sensing and data acquisition techniques and the casting were the same as previously described. However, the billet was heated to 590°C and soaked for a couple minutes at this temperature before injection. The purpose of soaking is to create nucleation sites and the growth of those sites. Depending on the soaking time this procedure creates a microstructure that is less dendritic and more globular, a desired feature for SS die-casting processes. The examination of micrographs (see Figure 5-26) shows that the cast part was mainly dendritic, but contained regions with pockets of spheroidal particles. This indicates that the soaking process used was not able to produce a fully globular thixotropic microstructure as shown in previous Figures (for example Figure 5-22 c). To avoid repetitions, only the different conclusions obtained with this MMC will be covered in the following. It is noted that for the casting of the MMC, the part detachment, completion of the die filling, the release of the metal pressure and the solidification of the part can be in-line monitored as having been demonstrated for the A356, A357 and AZ91 materials.

The quality of the signal obtained, can be assessed in Figure 5-27 in which the time delay between L^2 and L^3 is displayed. This figure shows that the signal received is of good quality and that the wetting between the steel CBR and the cast part is good because there is no jittering as in Figure 5-18.

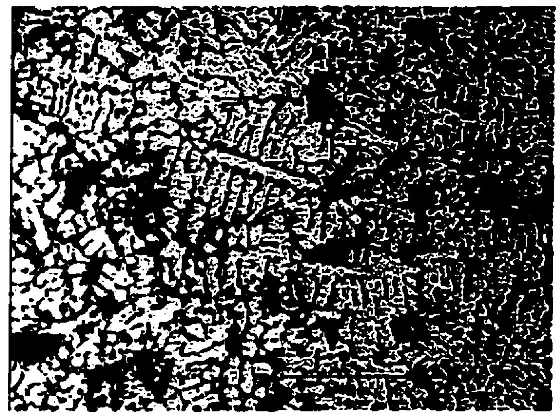

Figure 5-26: Micrograph of the microstructure of the MMC Gra-Ni® 6S:3G.

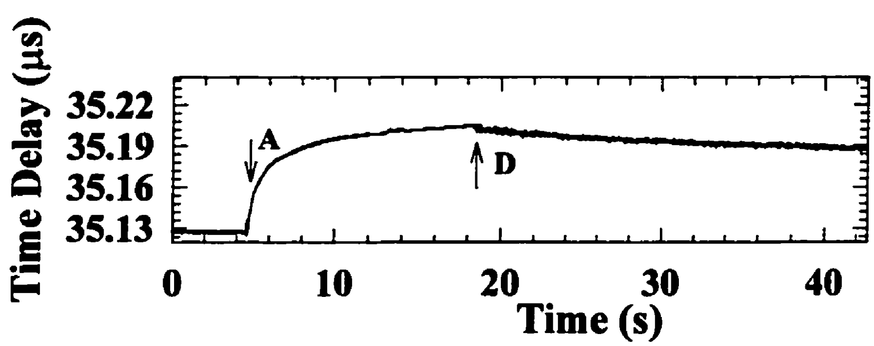

Figure 5-27: Measured time delay of the MMC between L^2 and L^3.

The cycle time in casting was arbitrarily chosen to be shorter than that used in the casting of the thixotropic A356 billets. Figure 5-28 shows the measured ultrasonic velocity in the cast part. It is seen that the velocity profile of the solidifying SS A356 part in Figure 5-13 is different from the Gra-Ni® 6S:3G part shown in Figure 5-28. During the solidification process the initial change of velocity in the SS A356 part is an abrupt change and, then, it quickly reaches nearly a constant. However, in the case of Gra-Ni® 6S:3G, the velocity change is gradual and no sharp change is displayed. A similar difference in the velocity profile as a function of temperature was observed during the heating of a SS A356 and a dendritic A356 sample in chapter 4. Also at time C, no pressure was applied to the Gra-Ni® 6S:3G part, the ultrasonic velocity of 5890 m/s shown in Figure 5-28 can be correlated with the laser-ultrasonic results presented in Figure 4-8 at about 500°C.

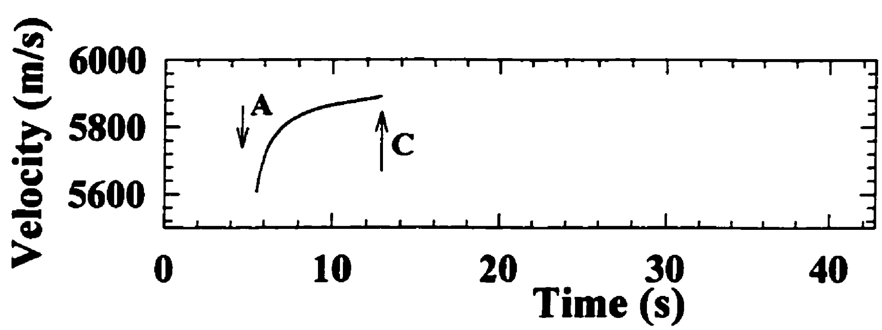

Figure 5-28: Measured ultrasonic velocity of the MMC Gra-Ni® 6S:3G.

The measured ultrasonic attenuation coefficient in the cast Gra-Ni® 6S:3G part is given in Figure 5-29. We can see that the ultrasonic attenuation coefficient in this alloy cast part is 11 dB/cm, which is higher than the 6 dB/cm exhibited in the thixotropic A356 material as shown in Figure 5-14. There are a several reasons that could explain this phenomenon. Firstly, this increased loss could be due to the presence of 6% of silicon carbide and 3% nickel-coated graphite particles which act as ultrasonic scatterers in the

Gra-Ni® alloy. Secondly, dendrites might scatter more ultrasound than globular particles in the thixotropic A356 alloy [66]. And, thirdly, it might be the low level of porosity present in the Gra-Ni® alloy part. As mentioned in Chapter 4 and the previous section, the impact and importance of each of these three reasons need to be further investigated.

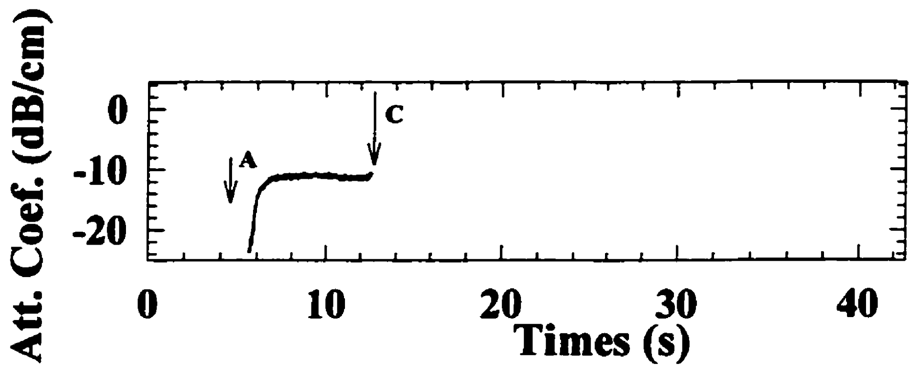

Figure 5-29: Measured ultrasonic attenuation of the MMC Gra-Ni® 6S:3G.

5.5 Summary

In-line ultrasonic monitoring of the die-casting process using billets of different materials such as A356, A357, AZ91 Mg alloys and MMC Gra-Ni® 6S:3G, with thixotropic (globular) and dendritic microstructures for different materials has been presented. Measurements were made by means of a clad steel buffer rod (CBR) sensor embedded in the die and operated in the pulse-echo mode. This single ultrasonic probe monitored the completion of the die filling, the release of the metal pressure, the solidification of the part, the detachment of the metal alloy from the wall cavity and the opening of the die. The variations of average temperatures in the die and part were also monitored through the analysis of the ultrasonic time delay information in the buffer rod and part respectively. The ultrasonic sensor has shown a response time faster than the one displayed by the K-type conventional thermocouple. The measured amplitude profile of the reflected echo at the steel CBR-cast part interface can be used to monitor cold shut defects and incomplete filling. The variations of the attenuation coefficient and the ultrasonic velocity in the cast part may be used to relate to changes in alloy composition, microstructure and porosity. Because ultrasonic sensors can measure in-line the above parameters simultaneously, it may be a good sensor candidate for process control of the die-casting process.

Chapter 6: Conclusion

6.1 Review of the Thesis

In recent years, significant progresses have been made in metal die-casting and metal injection molding processes. The evaluation of part properties inside the die or mold during the production cycle is usually performed onto the part after it has been ejected from the die or mold because of the lack of a proper sensor. But the research has been oriented mainly towards machine control and new processes which are essential to improve the quality and efficiency of the process; little attention has been paid to the part quality inside the cavity for process control. At the present time, sensors limit the advancement of machine and process control. The sensors on the market are limited to conventional pressure, temperature, heat flux and flow detector measurements and have some shortcomings such as slow response, unsteadiness and non-repeatability. These sensors are used for machine control only. As a result, there is a significant demand for the development of cost effective sensors for in-line measurements and for machine and process control. The ability of the ultrasound to interrogate non-invasively, non-destructively and rapidly the regions of the die and cast part is desirable for a modern molding process control and for the development of a new sensor. Ultrasound can be a good sensor candidate for process control of the die-casting process.

The research undertaken for this thesis concentrates its effort on the in-line monitoring, by ultrasound, of a new process which becomes more and more important in the market today. Its potential was first recognized in the early 1970's; but, its growth has just recently begun. This new forming processing technique is called Semi-Solid (SS) forming. This technique uses feeding materials composed of spheroidal particles of solid surrounded by a liquid phase of a lower melting point, rather than the interlocking tree-like dendrites existing in the conventional cast alloy. Furthermore, in this research we used the thixocasting as the forming process, which consists of using conventional die-casting machine with the spheroidal particles as its feedstock material.

In chapter 2, a new design of the Clad Buffer Rod (CBR) was introduced and compared with an old design made up of a Zirconium (Zr) core. The new CBR consists of a double tapered cylindrical shape. The tapered core has a tapered angle of 2°. The maximum diameter (d_L) of the CBR is 11.684 mm and its length ($2l$) is 103.68 mm. The CBR is composed of fine grain steel as the core and a stainless steel cladding made by thermal spray, which is covered with two stainless steel tubes that can be machined. The machined tubes serve to provide the CBR the desired dimensions for the installation into the die and to protect the sprayed coating if it is immersed in liquid metals.

This new CBR has a signal-to-noise ratio (SNR) of more than 30 dB at 250°C, an improvement from the old design that has a SNR of about 20 dB at room temperature. This increase of more than 10 dB near the trailing echo is a significant improvement because it permits us to monitor the signals in the sample such as L_2 and L_4. We also developed an acquisition system, which can achieve a repetition rate up to 3000 Hz with a sampling frequency of 100 MHz. However, high repetition rates cause an important limitation. One can only record for a small period of time at those rates due to limited on-board memory. When high repetition rates are not necessary, serial acquisition with a reduced repetition rate is used. It can achieve hundreds of seconds for the acquisition time but its repetition rate is limited to a maximum of 65 Hz.

In chapter 3, the reflection and transmission coefficient were explained in details. Two equations were used to evaluate the ultrasonic impedance matching between different media. This allows us to calculate the amount of energy that will be transmitted or reflected from the interface between two media. It is demonstrated that it can be used to monitor the end of filling, gap development and solidification during die-casting. The reflection mode was preferred and used because of its simplicity compared to the transmission mode which requires two side access to a specific location in the die. Particular attention was paid to the SNR of the system when using the reflection mode because the ultrasonic signal is traveling twice in the material compared to once for the transmission mode. This double distance is crucial for the SNR because the signal is attenuated twice due to the material attenuation.

In chapter 4, ultrasonic wave velocities and attenuations of the thixotropic A356, A357, and 86S, dendritic A356, AZ91 and MMC Gra-Ni® 6S:3G were obtained by using a laser-ultrasonic method combined with a Gleeble thermal simulation system. The laser-ultrasonic system uses a high power pulsed laser that generates ultrasound on one side of a heated sample and another laser coupled with an optical interferometer to detect ultrasound on the opposite side. The Gleeble thermal system is heating the sample during the acquisition of laser-ultrasonic signals. With this system, we can measure the velocity and/or attenuation in the sample as a function of temperature. The velocity and attenuation can vary due to three different causes: the microstructure, porosity level and composition of the material. It has been demonstrated, by experiments, that the ultrasonic properties of a sample taken from a billet that has not been heated are similar to those of a sample taken from a SS die cast part. Therefore, the ultrasonic monitoring in die-casting can provide us with a mean to determine whether the processed part has the desired thixotropic microstructure or not and the specific microstructure by comparing the results obtained by the laser-ultrasonic method together with the Gleeble thermal simulator system. Furthermore, the ultrasonic method may be used to determine the solid fraction of the material if good calibration curves could be obtained.

In chapter 5, in-line ultrasonic monitoring of the die-casting process using billets such as thixotropic A356 and A357, dendritic Mg alloys AZ91 and dendritic MMC Gra-Ni® 6S:3G was presented. Measurements were made with the CBR sensor embedded in the die operating in the pulse-echo mode. This single ultrasonic probe monitored the completion of the die end of filling, release of the metal pressure, solidification of the part, detachment of the metal alloy from the wall cavity and opening of the die. The variations of average temperatures in the die and part were also monitored through the analysis of the ultrasonic time delay information in the CBR and cast part respectively. The ultrasonic sensor has shown a response time faster than that displayed by the K-type conventional thermocouple. The measured amplitude profile of the reflected echo at the steel CBR-cast part interface can be used to monitor cold shut defects and incomplete filling. The variations of ultrasonic attenuation coefficient and ultrasonic velocity in the cast part may be related to changes in alloy composition, microstructure and porosity. Because ultrasonic sensors can measure in-line the above parameters simultaneously, it may be a good sensor candidate for process control of the die-casting process. Furthermore, it has been proven, by experiments, that the sensors can differentiate different microstructures for magnesium alloy AZ91 by using the ultrasonic velocity in the sample as a parameter

6.2 Originality

The purpose of this research was to improve the understanding of the die-casting process by using the steel CBR as the sensor for in-line ultrasonic monitoring. The laser ultrasonic method is used to obtain the ultrasonic velocity and attenuation of samples as a function of temperature but with no pressure as the reference. This research has brought several major original contributions that are summarized below:

(1) We have designed, fabricated and successfully installed a steel CBR sensor into the die of a semi-solid die caster [27,85]. It has been proven that this sensor can perform in-line monitoring of the die-casting of various aluminum and magnesium alloys mentioned in Chapter 5.

(2) This investigation is the first report concerning in-line ultrasonic monitoring of semi-solid die-casting [27,85]. We used the reflection coefficient, for example, at the probe-part interface, obtained by a simple ultrasonic pulse/echo method, to monitor in-line the die-casting process features such as the end and completion of the filling, part detachment, average temperature of the die and part and the ultrasonic velocity and attenuation of the part. It is observed that the ultrasonic velocity and attenuation in the part can be used to differentiate the thixotropic and dendritic microstructures of the part.

(3) This thesis is also the first study concerning the ultrasonic velocity and attenuation measurement of Mg alloy AZ91 as a function of temperature. We installed the SF_6 supplying system around the sample during laser ultrasonic measurements and the heating process of billets before pouring them into the shot sleeve for injection in order to avoid the burning of the sample. The measurement result shows that the ultrasonic velocity and attenuation as a function of temperature can reveal the microstructure of the billet and the part.

6.3 Future Work

Looking at the purpose of this research, one can say that we improved the understanding of the process; but the research could still be improved. The CBR could be used as a pressure sensor; however, it requires to be calibrated as mentioned by

Nishiwaki and al. [86]. To be able to use the probe for pressure sensing, calibration curves need to be established under high pressure circumstances because the ultrasonic wave velocity depends on both the temperature and the pressure. Another investigation, which could be undertaken in the future, would be to increase the number of CBRs in the die. Sensor array could provide more details throughout the process. This would allow us to retrace, more accurately, the end of filling of the cast part, the solidification and the average temperature in the molten metal and use the results as validation for computer simulations.

Additionaly, the complete theoritical investigation of the CBR, including the relevant modes conversion, could help to grasp the behavior of the CBR in more details. This analysis can provide information helpful in signal processing (noise reduction) and calculation (attenuation in the cast part).

Furthermore, in order to improve accuracy, not only time domain information about reflection coefficients should be considered, as indicated by Drinkwater [87], but also frequency domain information should be included in interpreting reflection coefficients under conditions such as non-uniformly or partially contacted interfaces.

If one wants to understand the solid fraction of semi-solid processes in details, more accurate ultrasonic velocity curves, consisting of the temperature in function of sound velocity, need to be achieved. One way to obtain this result would be to use the Gleeble system by solidifying the sample and not by melting it as we do now.

Appendix A:

2-D Drawings of the Clad Buffer Rod

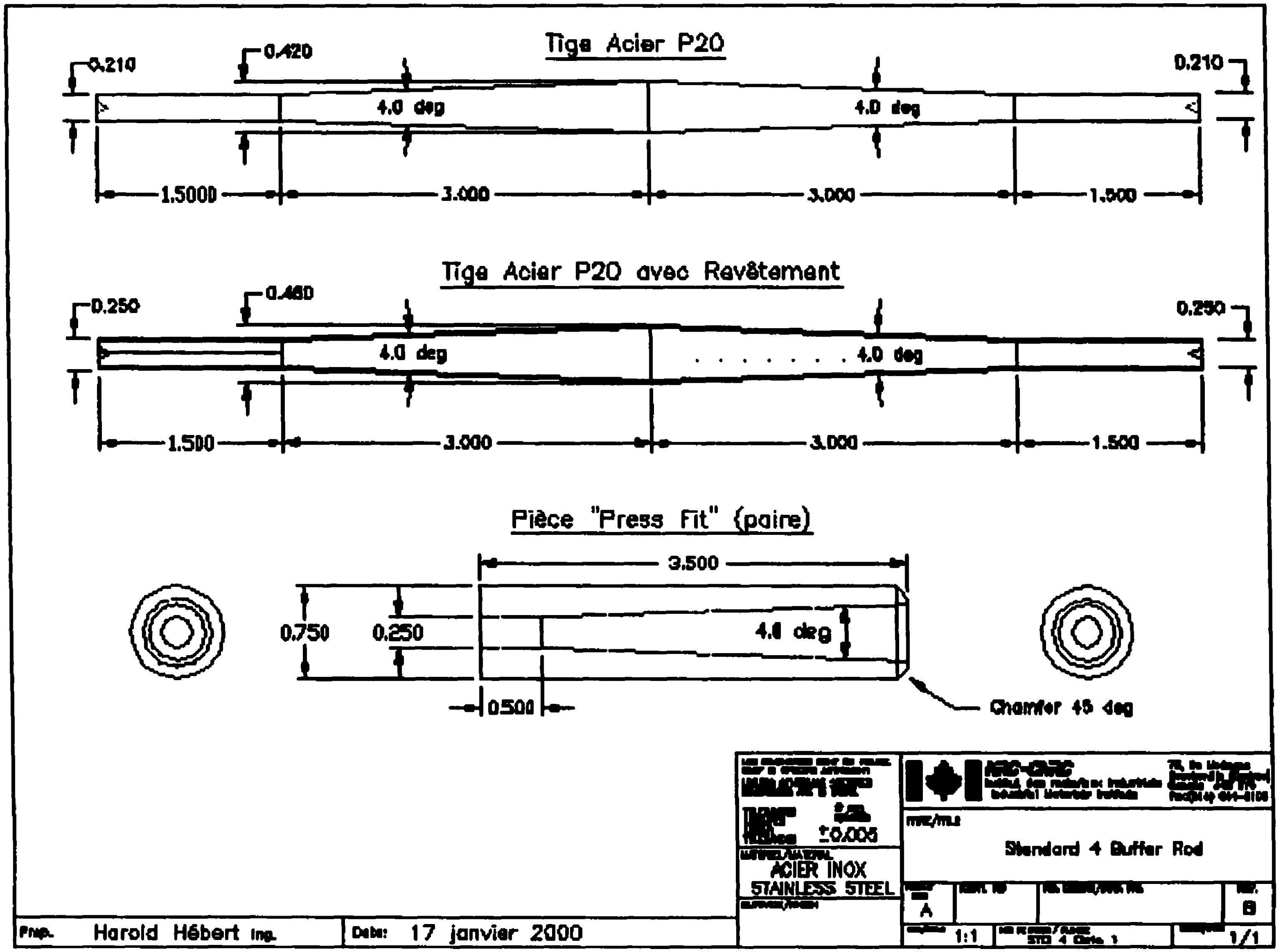

Tige Acier P20
0.210
0.420
4.0 deg
4.0 deg
0.210
1.5000
3.000
3.000
1.500
Tige Acier P20 avec Revêtement
0.250
0.460
4.0 deg
4.0 deg
0.250
1.500
3.000
3.000
1.500
Pièce "Press Fit" (paire)
3.500
0.750
0.250
4.0 deg
0.500
Chamfer 45 deg
±0.005
ACIER INOX
STAINLESS STEEL
Standard 4 Buffer Rod
A
B
1:1
1/1
Prép. Harold Hébert ing.
Date: 17 janvier 2000

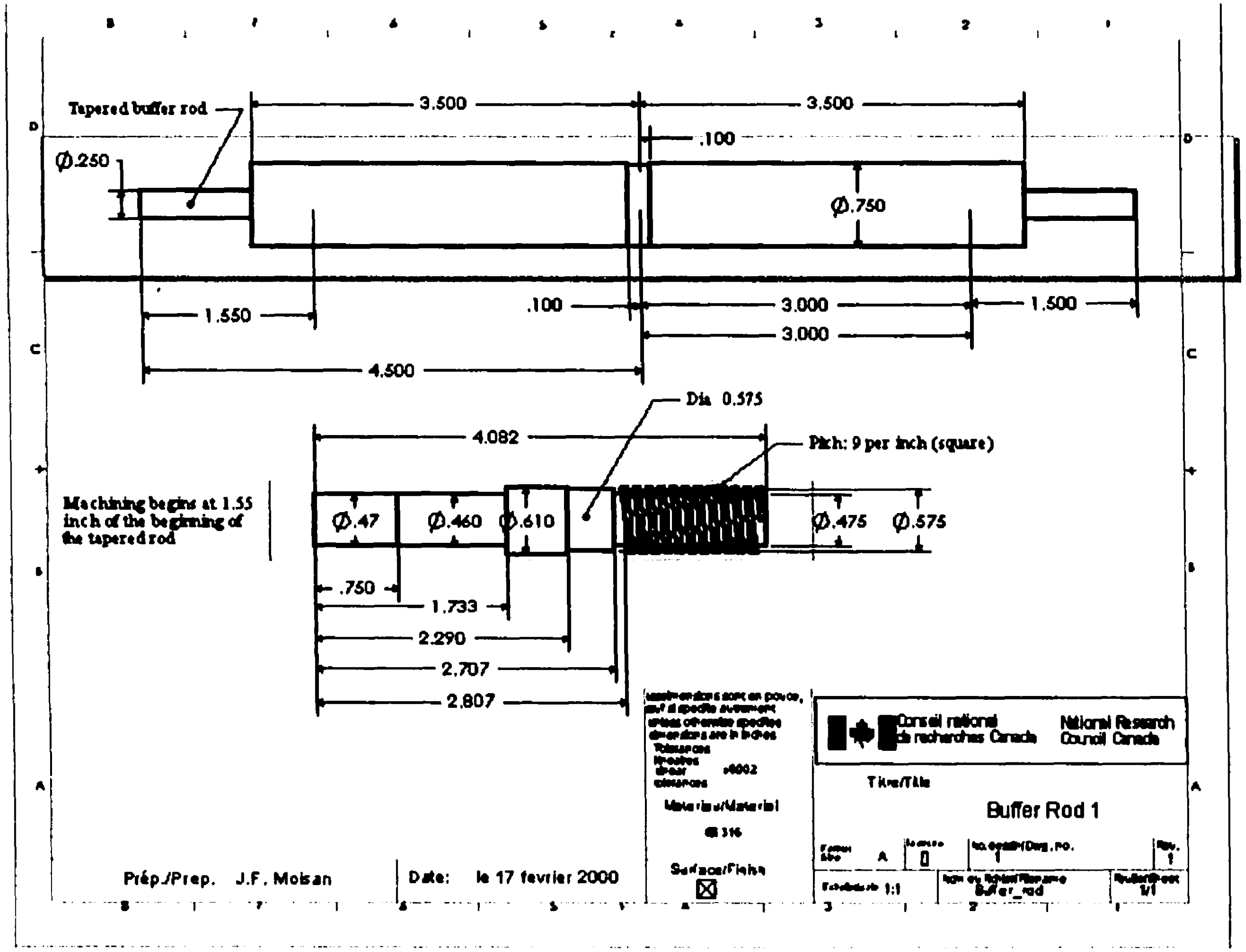

Tapered buffer rod
3.500
3.500
.100
Ø.250
Ø.750
1.550
.100
3.000
1.500
3.000
4.500
Dia 0.575
4.082
Pitch: 9 per inch (square)
Machining begins at 1.55 inch of the beginning of the tapered rod
Ø.47
Ø.460
Ø.610
Ø.475
Ø.575
.750
1.733
2.290
2.707
2.807
Conseil national de recherches Canada
National Research Council Canada
Titre/Title
Buffer Rod 1
Matériel/Material
Surface/Finish
Échelle/Scale 1:1
Buffer_rod
1/1
Prép./Prep. J.F. Moisan
Date: le 17 fevrier 2000

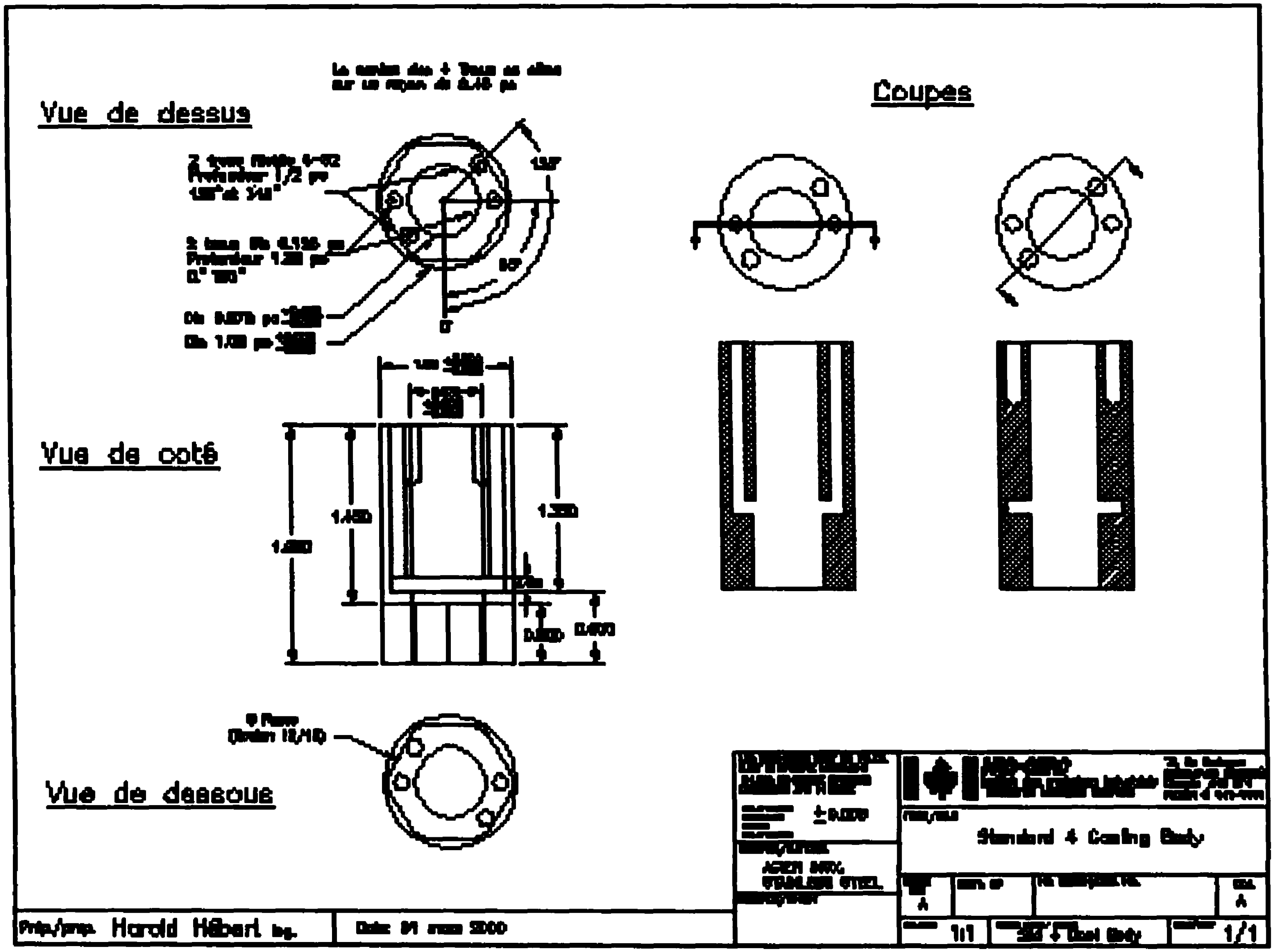

Vue de dessus
Coupes
Vue de coté
Vue de dessous
Standard 4 Cooling Body
1:1
1/1
Harold Hébert ing.

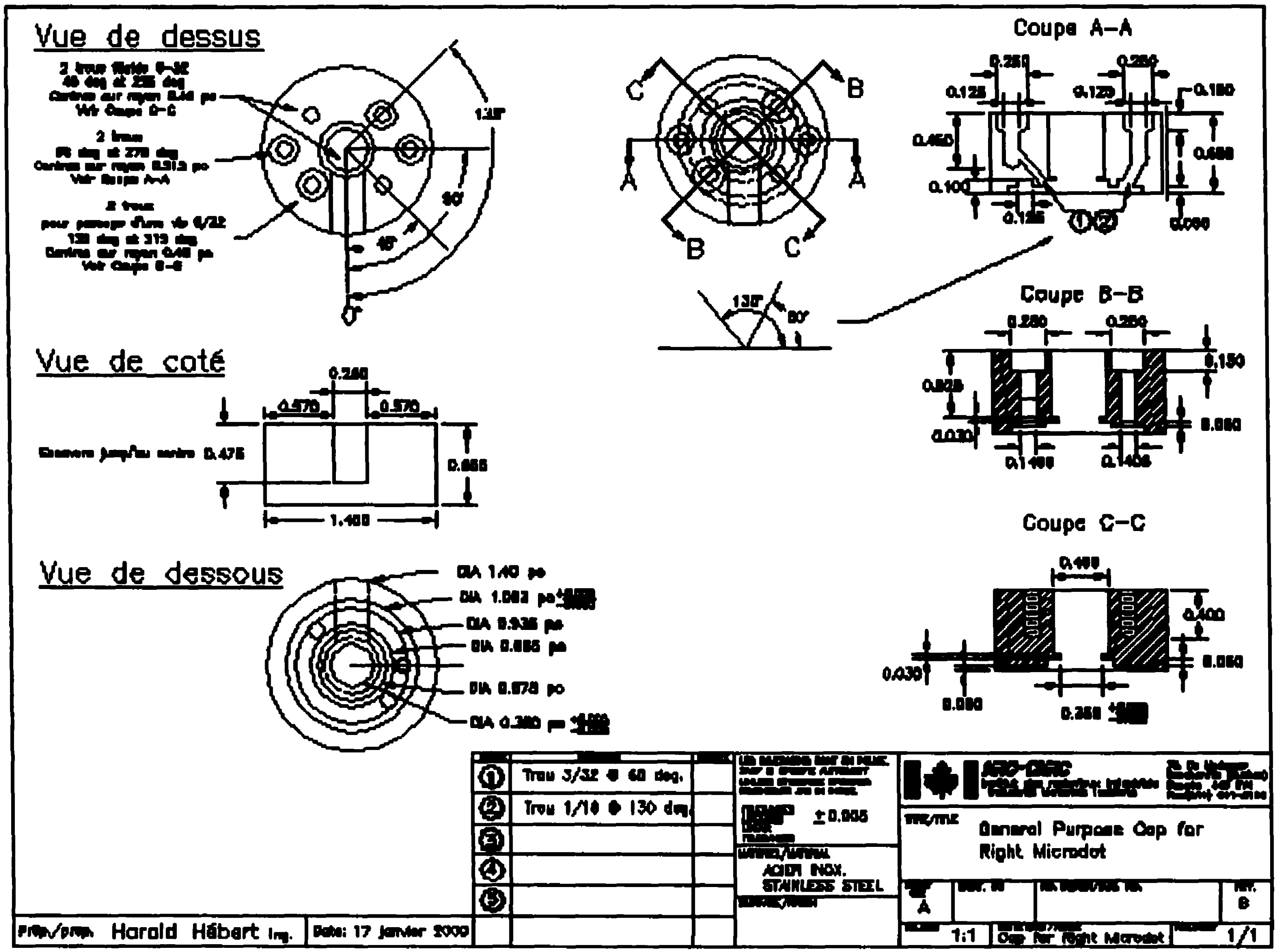
Vue de dessus
Vue de coté
Vue de dessous
Coupe A–A
Coupe B–B
Coupe C–C
B
C
A
130°
60°
90°
45°
0.250
0.570
0.570
0.475
0.688
1.400
DIA 1.40 po
DIA 0.935 po
DIA 0.878 po
0.250
0.125
0.450
0.100
0.150
0.400
0.030
0.050
Trou 3/32 @ 60 deg.
Trou 1/16 @ 130 deg.
± 0.005
ACIER INOX.
STAINLESS STEEL
General Purpose Cap for
Right Microdot
A
B
1:1
Cap for Right Microdot
1/1
Harald Hébert ing.
Date: 17 janvier 2000

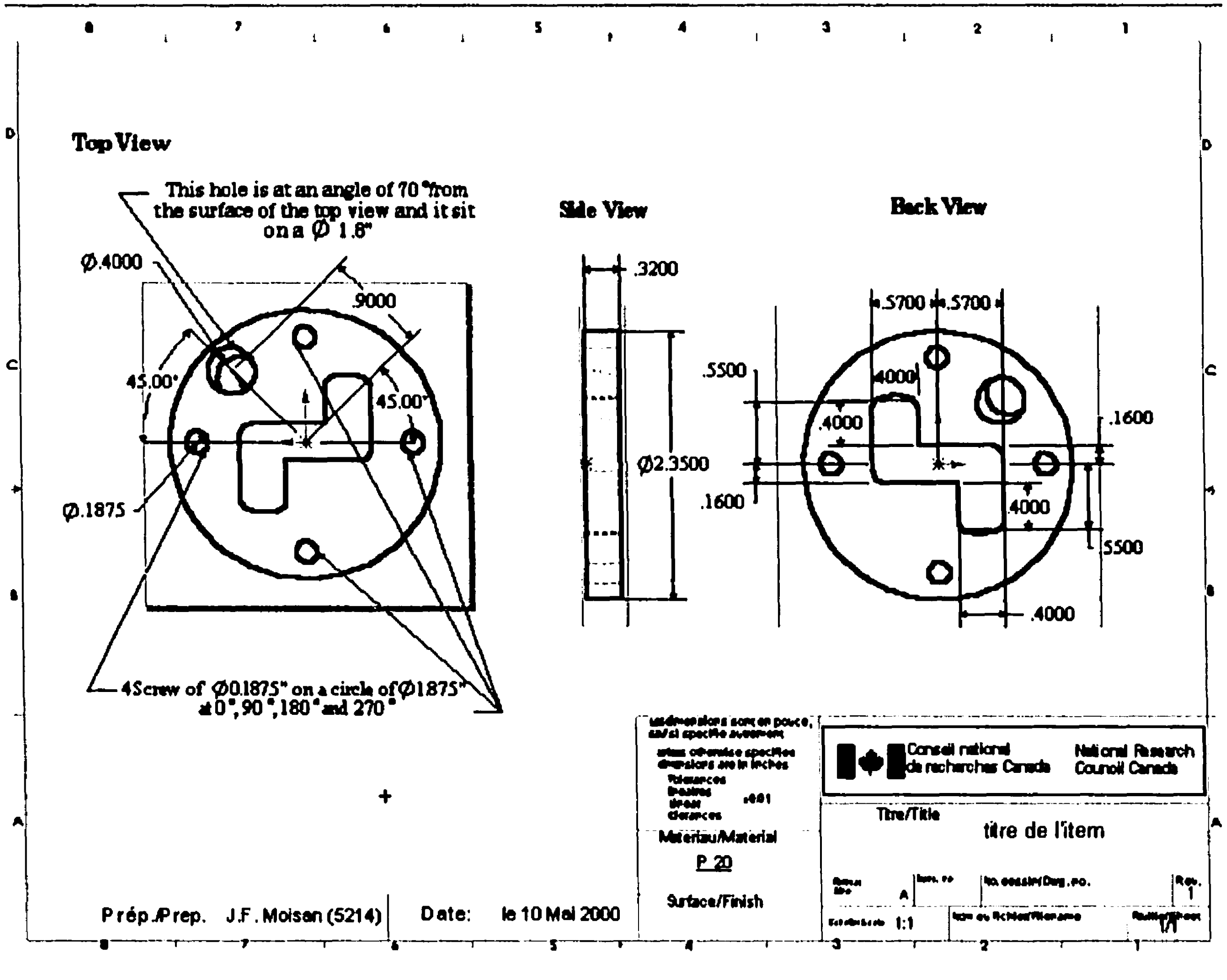

Top View
This hole is at an angle of 70 °from the surface of the top view and it sit on a Ø 1.8"
Ø.4000
.9000
45.00°
45.00°
Ø.1875
4Screw of Ø0.1875" on a circle of Ø1875" at 0°, 90°, 180° and 270°
Side View
.3200
Ø2.3500
Back View
.5700
.5700
.4000
.5500
.4000
.1600
.1600
.4000
.5500
.4000
Conseil national de recherches Canada
National Research Council Canada
Titre/Title
titre de l'item
Matériau/Material
P 20
Surface/Finish
1:1
Prép./Prep. J.F. Moisan (5214)
Date: le 10 Mai 2000

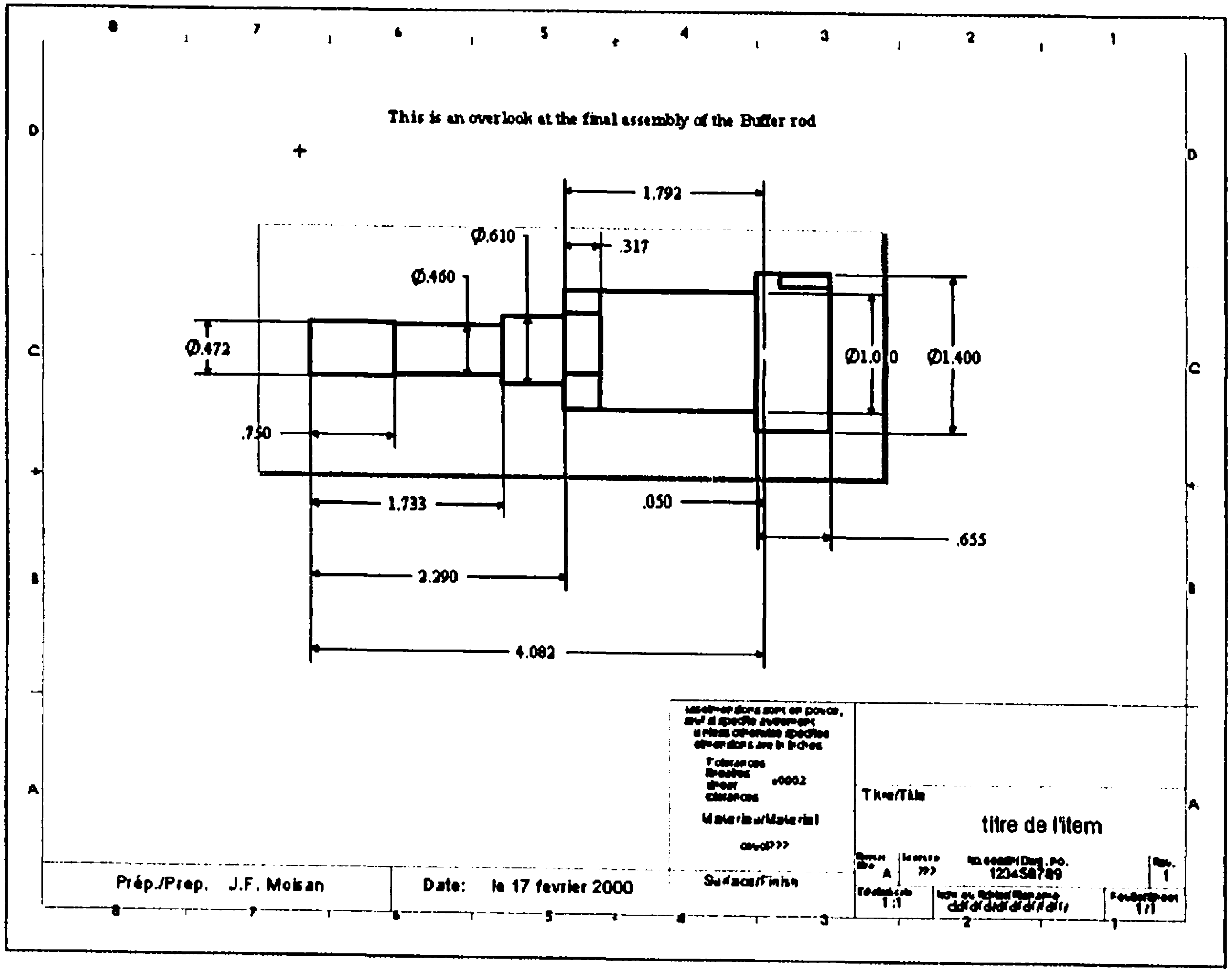

This is an overlook at the final assembly of the Buffer rod
1.792
Ø.610
.317
Ø.460
Ø.472
Ø1.000
Ø1.400
.750
1.733
.050
.655
2.290
4.082
Titre/Title
titre de l'item
Matériau/Material
Surface/Finish
123456789
1:1
1/1
Prép./Prep. J.F. Moisan
Date: le 17 fevrier 2000

References

[1] D. Kazmer, J. Rowland and G. Sherbelis, "The foundation of intelligent process control for injection molding", *J. of Injection Molding Tech.*, Vol. 1, pp. 44-56, 1997.

[2] R.G. Speight, R.M. Rose and P.D. Coates, "Infrared sensor melt temperature measurement technology and benefits for thermoplastic injection molding process control", *J. of Injection Molding Tech.*, Vol. 3, pp. 159-180, 1999.

[3] R. Gendron and L.A. Utracki, "Material characteristics oriented computer control of extrusion - Part1", *Proceding SPE ANTEC*, pp. 958-963, 1991.

[4] J. Cann and Y. Shen, "Computer integrated information and control systems for improved quality and profit", *Trans. the NADCA 15th Int'l Die-Casting Congress and Expos.*, G-T89-021, 1989.

[5] P. Kennedy, *Flow Analysis of Injection Molds*, Hanser Publishers, Munich, Vienna, New York, 1995.

[6] M. Rafizadeh, W.I. Patterson, M.R. Kamal, "Physically-based model of thermoplastics injection molding for control applications", *Int'l Polymer Processes*, Vol. 11, No. 4, pp. 353-362, 1996.

[7] A.N. Alexandrou, G.R. Burgos, V.M. Entov, "Modeling thixotropy and its effects in semi-solid casting", *6thInt'l Conf. on Semi-solid Processing of Alloys and Composites*, pp. 553-558, 2000.

[8] B.Binnet and F.Pineau, "A mixture approach to the mumerical modeling of thixocasting", *6thInt'l Conf. on Semi-solid Processing of Alloys and Composites*, pp. 539-544, 2000.

[9] G. Engelstein, "Virtual molding: a challenge to the analysis industry", *Proc. SPE ANTEC*, pp. 768-771, 1995.

[10] D.M. Gao, K.T. Nguyen, P. Girard, S. Salloum, "Numerical simulation of the sequential filling in injection molding process", *Proc. SPE ANTEC*, pp. 546-550, 1995.

[11] P. Ehret, A. Davidoff, F. Jacques, H. Bung, "Simulation of the complete injection cycle", *Proc. SPE ANTEC*, pp. 542-546, 1994.

[12] D. Frayce, J.F. Hetu, C.A. Loong, "Numerical modeling of filling and solidification in die-casting", *Trans. from the NADCA 17th Int'l Die-Casting Congress and Expos.*, pp. 13-17, 1993.

[13] Y. Iwata, Y. Yamamoto, K. Yonekura, Y. Kagami, "Computer simulation of molten metal flow in thin plate die-casting", *Trans. from the NADCA 16th Int'l Die-Casting Congress and Expos.*, pp. 311-320, 1991.

[14] M.P. Schwarz, A.R. Musgrove, L.D. Hooper, P. Dang, "Validation of numerical simulation of gas bath circulation by LDV measurement", *Proc. of 10th PTD Conf.*, pp. 123-132, 1992.

[15] L.J. Chien, C.L. Thomas, D.R. Lawson, "Sensor/model fusion for improved process understanding and control in injection molding", *CAE and intelligent procedure of polymer material*, MD-79, pp. 189-197, 1997.

[16] C.L. Thomas, Ph.D. dissertation, Dept. of Mech. Eng., Drexel Univ., Philadelphia, 1993.

[17] F. Johannaber, "*Injection molding machines- a user's guide*", Hanser Publishers, Munich, Vienna, New York, 1994.

[18] A.R. Agrawal, I.O. Pandelis, M. Perch, "Injection-molding process control- a review", *Polymer Engineering and Science*, Vol. 27, pp. 1345-1357, 1987.

[19] J.Can, Y.Shen, " Computer integrated information and control system for improved quality and profit", *Trans. from NADCA 15th Int'l Die-Casting Congress and Expos.*, G-T89-021, 1989.

[20] B.Souder, S. Woll, D. Cooper, "Advanced method for monitoring injection molding processes", *Proc. SPE ANTEC*, pp. 644-650, 1994.

[21] Y. Mochiku, Y. Hatamura, K. Shirahige, " Intelligent die-casting and seven sensors", *Trans. from NADCA 15th Int'l Die-Casting Congress and Expos.*, G-T89-024, 1989.

[22] K.K. Wang, "CAE for injection molding: What's Next?", *CAE and Related Innovation for Polymer Process*, ASME, Vol. 90, pp. 299-307, 2000.

[23] I. Catic, A. Abadzic and M.R. Sokele, "Determining the optimum position of temperature sensors in mold for injection molding of polymer", *J. of Injection Molding Tech.*, Vol. 3, No. 4, pp. 194-200, December 1999.

[24] B.Cao, " *On-line Ultrasonic Monitoring of Injection Molding and Die-casting Processes*", Master Thesis, Departement of Electrical Engineering, McGill University, Montréal, 1996.

[25] N. Nishiwaki, A. Cui, M. Konno, S. Hori, "Observation of solidified resin behavior in a cavity by ultrasonic waves", *Procedure, Seiki-Kabou*, Vol. 5, No. 12, pp. 870-874. 1993.

[26] C.J. Yu, J.E. Sunderland, C. Poli, "Thermal contact resistance in injection molding", *Polymer Engineering Science*, Vol. 30, No. 24, pp. 1599-1606, 1990.

[27] J.F. Moisan, C.-K. Jen, J.-W. Liaw, T.-F. Chen, Z. Sun, C.A. Loong, "Ultrasonic sensors and techniques for semi-solid die-casting process", *IEEE Conf. in Puerto Rico (UFFC)*, pp. 483-487, 2000.

[28] B. Cao, H. Wang, C.K. Jen, K.T. Nguyen, J.-G. Legoux, C.A. Loong, M. Viens, " Ultrasonic monitoring of injection molding and die-casting", *NDE for Process Control in Manufacturing Proc. SPIE*, Vol. 2948, pp. 173-186, 1996.

[29] H. Wang B. Cao, C.-K. Jen, K.T. Nguyen, M. Viens, "On-line ultrasonic monitoring of the injection molding process", *Polym. Eng. Sci.*, Vol. 37, No. 2, pp. 363-376, 1997

[30] N. Nishiwaki, S. Hori, K. Shimazaki, T. Arai, "Visualization of plastics material characteristic by ultrasonic wave", *Proc. of the 1st Pacific Symposium on Flow Visualization and Image Proceeding*, Vol. 1, pp. 225-230, 1997.

[31] M. Fleming, " SSM: some thoughts on past milestone and on the path ahead", *6thInt'l Conf. on Semi-solid Processing of Alloys and Composites*, pp. 11-14, 2000.

[32] D.B. Spencer, Ph.D. Thesis, Massachusetts Institute of Technology, Cambridge, MA, 1971.

[33] S.P. Midson, R.B. Minkler, H.G. Brucher, "Gating of semi-solid aluminum castings", *6thInt'l Conf. on Semi-solid Processing of Alloys and Composites*, pp. 67-71, 2000.

[34] A. Lowe, K. Ridgway, H. Atkinson, "The pros and cons of semi-solid processing", *Materials World*, Vol. 7, No. 9, pp. 541-543, 1999.

[35] K.K. Wang, H. Peng, N. Wang, S.-P. Wang, "Method and apparatus for injection molding of semi-solid metals", US Patent 5,501,266, 1996.

[36] D. Apelian, "A roadmap for semi-solid processing", *6thInt'l Conf. on Semi-solid Processing of Alloys and Composites*, pp. 47-54, 2000.

[37] Z. Fan, S. Ji, M.J. Bevis, "Twin-screw rheomolding- a new semi-solid processing technology", *6thInt'l Conf. on Semi-solid Processing of Alloys and Composites*, pp. 61-66, 2000.

[38] D. Walukas, S. LeBeau, N. Prewitt, R. Decker, "Thixomolding® - Technology opportunities and practical uses", *6thInt'l Conf. on Semi-solid Processing of Alloys and Composites*, pp. 109-114., 2000.

[39] J. Cui, G. Lu, J. Dong, K. Xia, "Microstructure after casting and reheating in a continuously cast aluminum alloy 7075", *6thInt'l Conf. on Semi-solid Processing of Alloys and Composites*, pp. 701-704, 2000.

[40] S.H. Juang, S.-M. Wu, C.-Y. Ma, H. Peng, "Study on mechanical properties of an A356 aluminum alloy with thixotropic Properties", *6thInt'l Conf. on Semi-solid Processing of Alloys and Composites*, pp. 705-710, 2000.

[41] M. Rosso, M. Cordini, P. Giordano, "Mechanical properties and microstructure investigations on a MMC thixoforming Brake Drum", *6thInt'l Conf. on Semi-solid Processing of Alloys and Composites*, pp. 711-716, 2000.

[42] Y.S. Yang, and C.-Y. A. Tsao, "Formability of semi-solid formed A356 alloys with dendrictic and non-dendritic structures", *6thInt'l Conf. on Semi-solid Processing of Alloys and Composites*, pp. 717-722, 2000.

[43] P. Kapranos, P.J. Ward, H. V. Atkinson, D. H. Kirkwood, "Near net shaping by semi-solid metal processing", *Materials and Design*, Vol. 21, pp. 387-394, 2000.

[44] B. Nohn, U. Morjan, D. Hartmann, "Thixoforming of steel", *6thInt'l Conf. on Semi-solid Processing of Alloys and Composites*, pp. 265-272, 2000.

[45] K. Miwa, S. Kawamura, "Semi-solid extrusion forming process of stainless steel", *6thInt'l Conf. on Semi-solid Processing of Alloys and Composites*, pp. 279-281, 2000.

[46] S. Abdelfattak, M. Robelet, A. Rassili, M. Bobadilla, "Thixoforming of steels inductive reheating and basic investigation", *6thInt'l Conf. on Semi-solid Processing of Alloys and Composites*, pp. 283-288, 2000.

[47] H.K. Junk, C.G. Kang, " Reheating process of cast and wrought aluminum alloys for thixoforging and their globularization mechanism", *Journal of Materials Processing Technology*, Vol. 104, pp. 244-253, 2000.

[48] F. Manero, W.I. Patterson, M.R. Kamal, "Cavity temperature profile measurement during injection moulding", *SPE ANTEC Technical Papers*, pp. 577-581, 1997.

[49] G.C. Peischl, I. Bruker, "Melt homogeneity in injection molding: application of a ring-bar device", *Polymer Engineering Science*, Vol. 29, No. 3, pp. 202-208, 1989.

[50] J. Shen, R. Edwards, C.L. Thomas, A.J. Bur, "Ultrasonic melt temperature measurement during extrusion", *Proc. SPE ANTEC*, pp. 2076-2079, 1998.

[51] K. B. Migerl, A.J.Bur, "Measurement of temperature profiles during polymer processing", *Proc. SPE ANTEC*, pp. 2278-2282, 1997.

[52] R.G. Speight, P. D'Agostino, J.S. Hermann, "Melt and mould temperature measurements for polymer injection moulding", *Proc. SPE ANTEC*, pp. 568-572, 1997.

[53] C. Maier, "Infrared temperature measurement of polymer", *Polymer Engineering Science*, Vol. 36, No. 11, pp. 1502-1512, June 1996.

[54] S. Quillet, PH. Le Bot, D. Delaunay, Y. Jarny, "Heat transfer at the polymer-metal interface. A method of analysis and its application to injection molding", *ASME Proceeding of the 32th National Heat Transfer Conf.*, Vol. 2, pp. 9-16, 1997.

[55] A.J. Bur, F.W. Wang, C.L. Thomas, J.L. Rose, "In-line optical monitoring of polymer injection molding", *Polymer Engineering Science*, Vol. 34, No. 8, pp. 671-679, 1994.

[56] A.J. Bur, C.L. Thomas, "A multi-functional optical sensor for monitoring polymer injection molding", *Proc. SPE ANTEC*, pp. 2798-2804, 1995.

[57] J.P. Monchalin, "Progress towards the application of laser-ultrasonic in industry", *Progress in QNDE*, Vol. 12a, pp. 495-506, 1993.

[58] R.C Addison Jr., A.D.W. McKie, T.-L.T. Liao, H.-S. Ryang, " In situ monitoring of molding processes using laser-based ultrasound", *Proc. Of Review of Progress in QNDE*, Vol. 13, pp. 2237-2244, 1994.

[59] P.T. Cole, "The generation and reception of ultrasonic surface waves in mild steel at high temperatures", *Ultrasonics*, Vol. 16, pp. 151-155, 1978.

[60] B.W. Maxfield, A. Kuramoto, J.-K. Hulbert, "Evaluating EMAT designs for selected applications", *Materials Evaluation*, Vol. 45, pp. 1166-1183, 1987.

[61] T. Arakawa, K. Yoshikawa, S. Chiba, K. Muto and Y. Atsuta., "Applications of brazed-type ultrasonic probes for high and low temperatures uses", *Nondestr. Test. Eval.*, Vol. 7, pp. 263-72, 1992.

[62] S.-S.L. Wen , C.K. Jen, K.T. Nguyen, "Advance in on-line monitoring of the injection molding process using ultrasonic techniques", *Int'l Polymer Processing XIV*, pp. 1-8, 1999.

[63] C.K. Jen, J.G. Legoux, "High performance clad metallic buffer rods", *IEEE Ultrasonics Symposium*, pp. 771-776, 1996.

[64] C.K. Jen, K,T, Nguyen, "Novel clad ultrasonic buffer rods for the monitoring of industrial materials processing", *Proceeding of the 1st American Conf. on NDT*, pp. 99-106, 1998.

[65] I. Ihara, C.K. Jen, D.R. Franca, " Materials evaluation using long clad buffer rods", *IEEE Sendai*, Miyagi, Japan, pp. 803-807, 1998.

[66] C.-K. Jen, J.-W. Liaw, T.F. Chen, A. Moreau, J.P. Monchalin, C.C. Yang, "Ultrasonic technique for monitoring of semi-solid metal processing", *6thInt'l Conf. on Semi-solid Processing of Alloys and Composites*, pp. 247-251, 2000.

[67] C.K. Jen, B. Cao, K. T. Nguyen, C. A. Loong, J. -G. Legoux, "On line ultrasonic monitoring of a die-casting process using buffer rods", *Ultrasonics*, pp. 335-344, 1997.

[68] C.K. Jen, A. Safaai-Jazi, J.F. Bussière, G.W. Farnell, "Longitudinal mode fiber acoustic waveguide with solid core and solid cladding", U.S. Patent no. 4,743,870, May 10th, 1988.

[69] C.K. Jen, J.G. Legoux, "Clad ultrasonic waveguides with reduced trailing echoes", U.S. Patent no. 5,828,274, May 28th, 1996.

[70] J.-D. Aussel, J.-P. Monchalin, "Precision laser-ultrasonic velocity measurement and elastic constant determination", *Ultrasonics*, Vol. 35, No. 5, pp. 335-344, 1997

[71] A. Moreau, F. Taheri, "Elastic moduli measurements of composite ceramics at high temperatures using laser ultrasonics", *Proc. Int'l Polymer Processing*, Vol. XIV, pp. 175-182, 1999.

[72] J.-F. Bussière, M. Dubois, A. Moreau, J.-P. Monchalin, "Characterizing materials with laser-ultrasonics", *Nondestructive Characterization of Materials IX*, pp. 131-141, 1999.

[73] L. Piché, A. Hamel, R. Gendron, M. Dumoulin, J. Tatibouet, "Ultrasonic characterization of polymer melts under processing conditions", US Patent 5,133,112, July 18th, 1995.

[74] L. Piché, F. Massines, A. Hamel, C. Neron, "Ultrasonic characterization of polymer under simulated processing conditions", US Patent 4,754,645, July 5th, 1988.

[75] C.K. Jen, J.G. Legoux, L. Parent, "Experimental evaluation of clad metallic buffer rods for high temperature ultrasonic measurements", *NDT&E International*, pp. 145-153, 2000.

[76] I. Ihara, H. Aso, H. Koguchi, C.-K. Jen, "Development of ultrasonic sensors for high temperature measurements- utilization of a wave propagation simulation technique for designing an ultrasonic buffer rod", *Proc. 21st Symp. On Ultrasonic Electronics*, Sendai, Japan, pp. 133-134, Nov.6-8, 2000.

[77] L.C. Lynnworth, "*Ultrasonic measurements for process control, theory, Techniques, Applications*", Academic Press Inc., San Diego, 1989.

[78] L. Wu, S.J. Chen, R. Malloy, "Development of an on-line cavity pressure based expert system for injection molding process", *Proc. SPE ANTEC*, pp. 444-449, 1991

[79] R.G. Speight, E.P. Yazbak, P.D. Coates, "In-line pressure and infrared temperature measurements for injection moulding process control", *Proc. SPE ANTEC*, pp. 642-646, 1995.

[80] M.G. Hansen, A. Khettry, "In-line monitoring of molten polymers: near infrared spectroscopy, robust probes, and rapid data analysis", *Polymer Engineering and Science*, Vol. 34, No. 23, pp. 1758-1766, 1994.

[81] D.W. Yu, M. Esseghir, C.G. Gogos, "The use of on-line optical microscopy for monitoring compounding and other polymer processing operation", *Proc. SPE ANTEC*, pp. 136-144, 1995.

[82] S.-S. Wen, "*Advances in On-line Ultrasonic Monitoring of Injection Molding Process*", Master Thesis, Department of Electrical Engineering, McGill University, Montréal, 1998.

[83] B.A. Auld, *Acoustic Fields and Waves in Solids*, John Wiley & Son, United State of America, 1973.

[84] J.-P. Monchalin, C. Néron, J.-F. Buissière, P. Bouchard, C. Padioleau, R. Héon, M. Choquet, J.-D. Aussel, C. Carnois, P. Roy, G. Durou, J.-A. Nilson, "Laser-ultrasonics: from the laboratory to the shop floor", *Advanced Performance Materials*, 5, pp. 7-23, 1998.

[85] J.-F. Moisan, C.-K. Jen, J.-W. Liaw, C.-Q, Zheng, T.-F. Chen, Z. Sun, C.A. Loong, "Ultrasonic Sensor and Technique for In-line Monitoring of Die Casting Process", to be submitted to Measurement Science and Technology.

[86] N. Nishiwaki, M. Konno, A. Cui, S. Hori, "Pressure measurement in molding process by ultrasonic wave", *Proc. Seikei-Kakou*, Vol. 5, No. 11, pp. 779-785, 1993.

[87] B. Drinkwater, P. Cawler," Measurement of the frequency dependence of the ultrasonic reflection coefficient form thin interface layers an partially contacting interfaces", *Ultrasonics*, Vol. 35, pp. 479-788, 1997.